
Supporting Information

Synthesis, Structures, and Chiroptical Properties of NBN-doped Helicenes with Boron Atoms in the Inner Rims

Weiwen Zhuang^{a‡}, Yujian Liu^{b‡}, Ziqi Deng^a, Yu Guo^c, Philip C.Y. Chow^c, David Lee Phillips^a, Wei Jiang^b, Zhaojun Wang^{b*}, and Junzhi Liu^{a*}

^a Department of Chemistry and State Key Laboratory of Synthetic Chemistry, The University of Hong Kong, Pokfulam Road, Hong Kong, China

^b Key Laboratory of Organic Optoelectronics and Molecular Engineering, Department of Chemistry, Tsinghua University, Beijing, China

^c Department of Mechanical Engineering, The University of Hong Kong, Pokfulam Road, Hong Kong, China

E-mail: wangzhaojun@mail.tsinghua.edu.cn; juliu@hku.hk

Contents

1. Materials and measurements	S2
2. Experimental procedures	S3
3. X-ray crystallography	S11
4. Optical and electrochemical properties	S18
5. Chiral resolution and chiroptical properties	S22
6. Theoretical calculations.....	S27
7. NMR spectra and high-resolution mass spectrometry.....	S40
8. References.....	S64

1. Materials and measurements

All chemicals were purchased from Dieckmann (Hong Kong) or Energy-Chemical (China). Pd₂(dba)₃, tris(dibenzylideneacetone)dipalladium(0); dppf, 1,1'-bis(diphenylphosphino)ferrocene; *t*-BuONa, sodium *tert*-butoxide; *n*-BuLi, *n*-butyllithium; EtOAc, ethyl acetate; DMSO, dimethyl sulfoxide.

¹H NMR (400 or 600 MHz) and ¹³C NMR (100 or 151 MHz) spectra were recorded on a Bruker the Avance DRX Bruker 400 or 600 MHz FTNMR Spectrometer using DMSO-*d*₆, CDCl₃ or CD₂Cl₂ as deuterated solvents. Chemical shifts (δ) are reported in ppm. High resolution mass spectra were obtained on a Bruker Q-Tof Maxis II mass spectrometer, a DFS high resolution magnetic sector mass spectrometer or a Bruker Autoflex Speed MALDI TOF MS.

The borylative reaction mixture of compound **8** or **9b** was quenched by cold water and passed through a pad of celite, then concentrated under vacuo. The reside was purified by LaboACE LC-5060 (JAL, Japan) recycling preparative gel permeation chromatography (GPC) assembled with JAIGEL-2.5HR column.

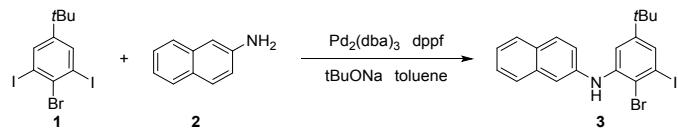
Absorption spectra were measured with Agilent Technologies Cary 60 UV-Vis spectrophotometer in a 1-cm quartz cell. Fluorescence measurements were measured with Agilent Technologies Cary Eclipse fluorescence spectrophotometer at room temperature. Photoluminescence quantum yields (Φ_{PL}) were determined by HAMAMATSU Quantaurus-QY instrument at room temperature. Time-resolved photoluminescence decays were measured with PicoHarp 300 in a 1-mm quartz cuvette. Femtosecond transient absorption spectra were measured with a femtosecond Ti/Sapphire regenerative amplifier laser system (Spitfire-Pro, Spectra-Physics Company), and an automated data acquisition transient absorption spectrometer (Ultrafast, Helios) was used to record the transient absorption spectra in a 1-mm quartz cuvette.

Cyclic Voltammetry (CV) measurements were carried out on a CHI660E potentiostat (CH Instruments, USA) in a three-electrode cell in an anhydrous dichloromethane solution of Bu₄NPF₆ (0.1 M) with a scan rate of 100 mV/s at room temperature. All potentials were further calibrated against ferrocene/ferrocenium (Fc/Fc⁺) by selecting decamethylferrocene (DMFc) as a reference.

Circular dichroism (CD) spectra were collected on JASCO J-1700 circular dichroism spectrometer in toluene. Circularly polarized luminescence (CPL) spectra were collected on JASCO CPL-300 circularly polarized luminescence spectrometer in toluene.

2. Experimental procedures

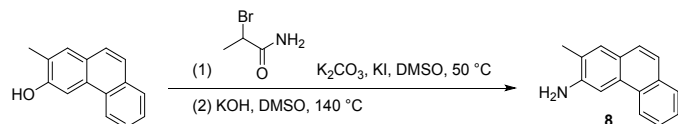
Synthesis of *N*-(2-bromo-5-(*tert*-butyl)-3-iodophenyl)naphthalen-2-amine (**3**):



A mixture of **1**^[S1] (2.44 g, 5.20 mmol, 1.5 equiv.), naphthalen-2-amine **2** (500 mg, 3.50 mmol, 1.0 equiv.), $\text{Pd}_2(\text{dba})_3$ (140 mg, 0.16 mmol), dppf (170 mg, 0.32 mmol) and *t*BuONa (500 mg, 5.20 mmol, 1.5 equiv.) were dissolved in toluene (70 mL). The mixture was stirred at 60 °C for 16 h under nitrogen atmosphere. After cooling to room temperature, water was added to quench the reaction. The aqueous solution was extracted with EtOAc (3 x 50 mL). The combined organic layers were washed with brine, dried over anhydrous Na_2SO_4 , filtered, and concentrated in vacuo. The residue was subjected to column chromatography with hexane/dichloromethane (*V/V* = 5:1) as the eluent to afford **3** (970 mg, 2.03 mmol, 58% yield) as a white solid.

¹H NMR (400 MHz, CDCl_3) δ 7.82 (d, *J* = 8.0 Hz, 1H), 7.80 (d, *J* = 8.0 Hz, 1H), 7.70 (d, *J* = 8.0 Hz, 1H), 7.52 (d, *J* = 2.3 Hz, 1H), 7.48-7.44 (m, 2H), 7.41-7.36 (m, 2H), 7.31 (dd, *J* = 8.0, 2.3 Hz, 1H), 6.36 (br, 1H), 1.25 (s, 9H). ¹³C NMR (101 MHz, CDCl_3) δ 152.95, 141.96, 139.50, 134.58, 130.18, 129.53, 129.31, 127.88, 126.97, 126.81, 124.58, 121.32, 116.59, 115.41, 113.56, 102.44, 34.88, 31.18. HRMS (ESI) m/z [M+H]⁺ Calcd for $\text{C}_{20}\text{H}_{20}\text{BrIN}^+$ 479.9818; Found 479.9817.

Synthesis of 2-methylphenanthren-3-amine (**8**):



Compound **8** was prepared by the reported Smiles rearrangement reaction^[S2] with modifications: a 100 mL Schlenk flask was charged with 2-methylphenanthren-3-ol^[S3] (750 mg, 3.60 mmol, 1.0 equiv.), 2-bromopropanamide (820 mg, 5.40 mmol, 1.5 equiv.), K_2CO_3 (750 mg, 5.40 mmol, 1.5 equiv.) and KI (60 mg, 0.36 mmol, 10 mol%). DMSO (18 mL) was then added. The resultant suspension was stirred at 50 °C for 24 hours. The mixture was allowed to cool down to room temperature, KOH (1.21 g, 21.61 mmol, 6.0 equiv.) was finally added, and stirring was continued at 140 °C for 8 hours. The mixture was then cooled to room temperature and saturated NH_4Cl solution (50 mL) was added to quench the reaction. The aqueous solution was extracted with EtOAc (3 x 50 mL). The combined organic layers were washed with brine, dried over anhydrous Na_2SO_4 , filtered, and concentrated in vacuo. The residue was subjected

to column chromatography with hexane/EtOAc ($V/V = 10:1$) as the eluent to afford **8** (590 mg, 2.85 mmol, 79% yield) as a brown solid.

^1H NMR (400 MHz, DMSO-*d*₆) δ 8.45 (d, $J = 8.0$ Hz, 1H), 7.84-7.82 (m, 2H), 7.59-7.49 (m, 4H), 7.42 (d, $J = 8.0$ Hz, 1H), 5.33 (br, 2H), 2.27 (s, 3H). ^{13}C NMR (101 MHz, DMSO-*d*₆) δ 146.64, 131.75, 129.73, 129.24, 128.80, 128.22, 126.60, 125.86, 125.68, 124.17, 123.62, 122.25, 121.43, 104.06, 17.68. HRMS (ESI) m/z [M+H]⁺ Calcd for C₁₅H₁₄N⁺ 208.1121; Found 208.1119.

General procedure for the Buchwald-Hartwig amination and methylation sequence (**GPA**):

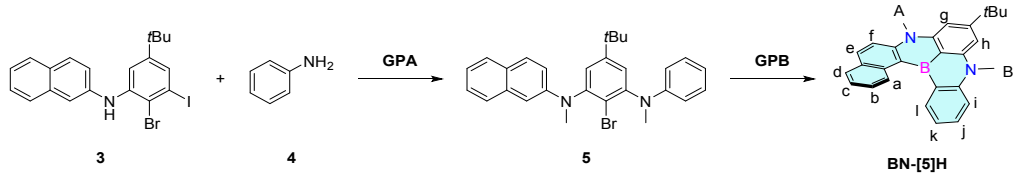
A mixture of aryl iodine, aniline derivatives (1.05 equiv. for one iodine atom), Pd₂(dba)₃ (10 mol%), dppf (20 mol%) and *t*BuONa (1.05 equiv. for one iodine atom) were dissolved in toluene. The mixture was stirred at 100 °C under nitrogen atmosphere. After completion, the mixture was cooled to room temperature, passed through a pad of celite and rinsed with EtOAc. The obtained organic phase was concentrated in vacuo.

The residue was dissolved in THF. NaH (2.0 equiv. for each -NH) was added under nitrogen flow and stirred for 30 minutes at room temperature. MeI (2.0 equiv. for each -NH) was finally injected via syringe and the mixture was heated to 65 °C. After completion, water was added to quench the reaction. The aqueous solution was extracted with EtOAc. The combined organic layers were washed with brine, dried over anhydrous Na₂SO₄, filtered, and concentrated in vacuo. The residue was subjected to column chromatography with hexane/dichloromethane ($V/V =$ from 10:1 to 5:1) as the eluent to afford the linear precursors (Compounds **5**, **6**, **9a**, **9b**, and **10**).

General procedure for the fold-in borylation (**GPB**):

A solution of *n*-butyllithium in pentane (1.6 M, 2.0 equiv.) was added slowly to a solution of **5**, **6**, **9a**, **9b**, or **10** (1.0 equiv.) in *o*-xylene (0.1 M) at room temperature under a nitrogen atmosphere. After stirring at 50 °C for 30 minutes, the mixture was cooled with ice/water bath (0 °C) and boron tribromide (3.0 equiv.) was slowly injected via a micro syringe. The reaction mixture was stirred at room temperature for 2 h. *N,N*-Diisopropylethylamine (Hunig's base, 6.0 equiv.) was added at 0 °C and then the reaction mixture was moved to a 130 °C oil bath and stirred for 12 h. The reaction mixture was cooled to room temperature and saturated NH₄Cl solution was added to quench the reaction. The aqueous solution was extracted with EtOAc. The combined organic layers were washed with brine, dried over anhydrous Na₂SO₄, filtered, and concentrated in vacuo. The residue was subjected to column chromatography with hexane/dichloromethane ($V/V =$ from 80:1 to 9:1) as the eluent to afford **BN-[5]H**, **BN-[6]H**, **BN-[7]H**, **E[6]H**, and **E[4]H**, respectively, in racemic forms.

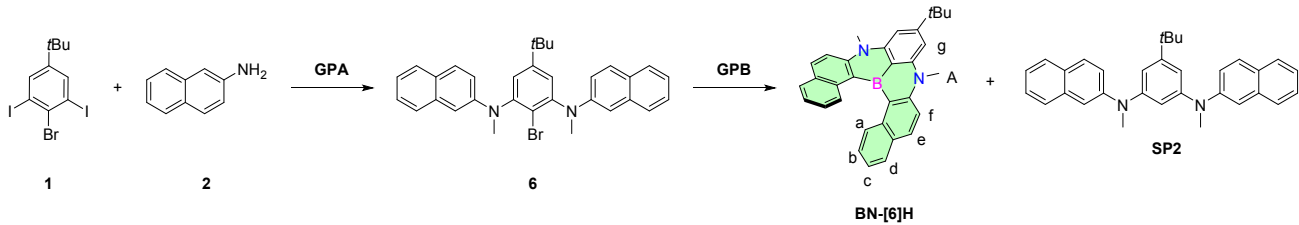
Synthesis of 5-(*tert*-butyl)-3,7-dimethyl-3,7-dihydro-3,7-diaza-11b-boranaphtho[3,2,1-*no*]tetraphene (**BN-[5]H**):



Compound **5** (565 mg, 1.20 mmol, 82% yield, white solid) was prepared by **GPA** using compound **3** (700 mg, 1.46 mmol). ¹H NMR (400 MHz, CDCl₃) δ 7.68 (d, *J* = 8.4 Hz, 2H), 7.60 (d, *J* = 9.0 Hz, 1H), 7.38 (t, *J* = 8.4 Hz, 1H), 7.26-7.20 (m, 5H), 6.99 (d, *J* = 2.5 Hz, 1H), 6.80-6.74 (m, 2H), 6.61 (d, *J* = 8.0 Hz, 2H), 3.38 (s, 3H), 3.30 (s, 3H), 1.27 (s, 9H). ¹³C NMR (101 MHz, CDCl₃) δ 153.74, 148.60, 148.48, 148.34, 146.54, 135.09, 129.19, 128.67, 127.70, 127.57, 126.48, 125.92, 125.69, 123.05, 122.56, 117.58, 117.43, 113.07, 106.64, 39.69, 39.35, 35.07, 31.34. HRMS (ESI) m/z [M+H]⁺ Calcd for C₂₈H₃₀BrN₂⁺ 473.1592; Found 473.1580.

BN-[5]H (40.3 mg, 0.10 mmol, 19% yield, light yellow solid) was prepared by **GPB** using compound **5** (250 mg, 0.53 mmol). ¹H NMR (600 MHz, CD₂Cl₂) δ 8.87 (d, *J* = 8.5 Hz, 1H, *l*), 8.31 (dd, *J* = 7.5, 1.7 Hz, 1H, *a*), 8.08 (d, *J* = 9.2 Hz, 1H, *e*), 7.88-7.83 (m, 2H, *f, j*), 7.58-7.61 (m, 1H, *c*), 7.55 (d, *J* = 8.5 Hz, 1H, *d*), 7.42-7.38 (m, 1H, *i*), 7.38-7.34 (m, 1H, *k*), 7.13 (s, 1H, *g*), 7.09 (s, 1H, *h*), 7.05 (m, 1H, *b*), 4.05 (s, 3H, *A*), 3.95 (s, 3H, *B*), 1.52 (s, 9H, *tBu*). ¹³C NMR (151 MHz, CD₂Cl₂) δ 156.52, 147.81, 146.39, 145.75, 137.33, 135.83, 132.90, 131.50, 129.72, 128.96, 128.18, 126.02, 124.39, 119.19, 116.91, 115.63, 101.82, 101.34, 37.85, 36.87, 36.50, 32.00. HRMS (ESI) m/z [M]⁺ Calcd for C₂₈H₂₇BN₂⁺ 402.2262; Found 402.2269.

Synthesis of 9-(*tert*-butyl)-7,11-dimethyl-7,11-dihydro-7,11-diaza-17c-boraphenanthro[2,3,4-*no*]tetraphene (**BN-[6]H**):



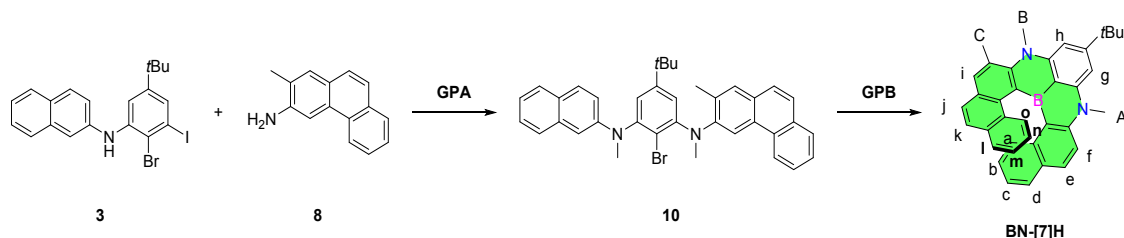
Compound **6** (2.20 g, 4.20 mmol, 84% yield, white solid) was prepared by **GPA** using compound **1** (2.32 g, 5.00 mmol). ¹H NMR (400 MHz, CDCl₃) δ 7.68 (d, *J* = 8.3 Hz, 4H), 7.62 (d, *J* = 9.0 Hz, 2H), 7.38 (m, 2H), 7.27-7.19 (m, 4H), 7.01 (s, 2H), 6.80 (dd, *J* = 9.0, 2.5 Hz, 2H), 3.39 (s, 6H), 1.26 (s, 9H). ¹³C NMR (101 MHz, CDCl₃) δ 153.74, 148.54, 146.53, 135.10, 128.69, 127.72, 127.61, 126.50, 125.70,

122.87, 122.59, 117.44, 106.72, 39.72, 35.07, 31.32. HRMS (MALDI-TOF) m/z Calcd for C₃₂H₃₁BrN₂ 522.1665; Found 522.1670.

BN-[6]H. (119.4 mg, 0.26 mmol, 22% yield, light yellow solid) was prepared by **GPB** using compound **6** (630 mg, 1.20 mmol). ¹H NMR (600 MHz, CD₂Cl₂) δ 8.11 (d, *J* = 9.2 Hz, 2H, *e*), 7.91 (d, *J* = 9.2 Hz, 2H, *f*), 7.89 (d, *J* = 8.3 Hz, 2H, *a*), 7.83 (d, *J* = 8.0 Hz, 2H, *d*), 7.27-7.24 (m, 2H, *c*), 7.21 (s, 2H, *g*), 6.91-6.87 (m, 2H, *b*), 4.11 (s, 6H, *A*), 1.54 (s, 9H, *tBu*). ¹³C NMR (151 MHz, CD₂Cl₂) δ 155.59, 145.86, 144.61, 136.21, 132.78, 129.89, 128.70, 127.92, 126.14, 123.94, 117.06, 101.86, 37.86, 36.48, 32.08. HRMS (MALDI-TOF) m/z Calcd for C₃₂H₂₉BN₂ 452.2418; Found 452.2439.

SP2. ¹H NMR (400 MHz, CDCl₃) δ 7.72-7.64 (m, 6H), 7.42-7.38 (m, 2H), 7.31-7.24 (m, 6H), 6.86 (d, *J* = 8.4 Hz, 2H), 6.72 (t, *J* = 8.4 Hz, 1H), 3.41 (s, 6H), 1.26 (s, 9H). ¹³C NMR (101 MHz, CDCl₃) δ 153.48, 149.66, 146.73, 134.87, 128.91, 128.47, 127.64, 126.76, 126.34, 123.55, 121.47, 113.91, 113.41, 113.16, 40.85, 35.12, 31.43. HRMS (ESI) m/z [M+H]⁺ Calcd for C₃₂H₃₃N₂⁺ 445.2638; Found 445.2650.

Synthesis of 9-(*tert*-butyl)-7,11,12-trimethyl-7,11-dihydro-7,11-diaza-19d-borabeno[*a*]phenanthro[2,3,4-*no*]tetraphene (**BN-[7]H**):

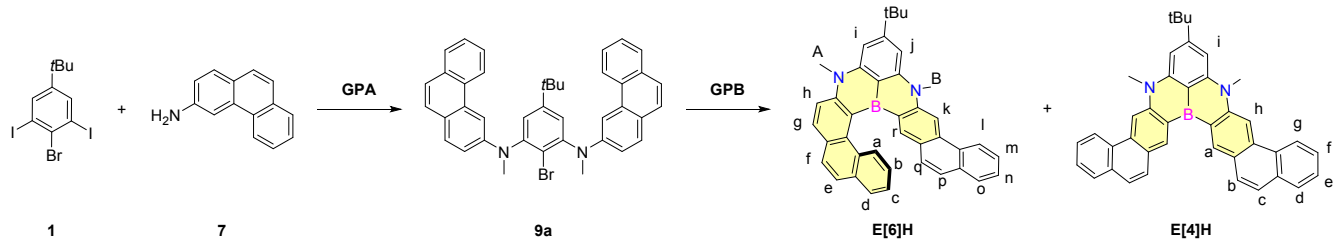


Compound **10** (670 mg, 1.14 mmol, 76% yield, light brown solid) was prepared by **GPA** using compound **3** (720 mg, 1.50 mmol). ¹H NMR (400 MHz, CDCl₃) δ 8.65 (d, *J* = 8.2 Hz, 1H), 8.33 (s, 1H), 7.90 (dd, *J* = 7.8, 1.5 Hz, 1H), 7.73-7.52 (m, 8H), 7.42-7.32 (m, 1H), 7.21 (t, *J* = 7.4 Hz, 1H), 7.09 (d, *J* = 2.3 Hz, 1H), 6.96 (d, *J* = 2.5 Hz, 1H), 6.91 (d, *J* = 2.4 Hz, 1H), 6.76 (dd, *J* = 9.0, 2.5 Hz, 1H), 3.46 (s, 3H), 3.38 (s, 3H), 2.13 (s, 3H), 1.15 (s, 9H). ¹³C NMR (101 MHz, CDCl₃) δ 153.13, 151.44, 148.54, 148.21, 146.63, 135.11, 132.31, 132.23, 131.21, 130.10, 129.53, 128.85, 128.66, 128.34, 127.69, 127.43, 126.47, 126.42, 126.34, 126.31, 125.29, 123.08, 122.57, 122.41, 121.52, 120.23, 117.17, 112.25, 106.34, 41.86, 39.59, 34.98, 31.25, 19.40. HRMS (MALDI-TOF) m/z Calcd for C₃₇H₃₅BrN₂ 586.1978; Found 586.2008.

BN-[7]H (124.4 mg, 0.24 mmol, 24% yield, light yellow solid) was prepared by **GPB** using compound **10** (590 mg, 1.00 mmol). ¹H NMR (600 MHz, CD₂Cl₂) δ 7.97 (s, 1H, *i*), 7.84-7.79 (m, 2H, *e*, *f*), 7.75 (d, *J* = 8.5 Hz, 1H, *j*), 7.73 (d, *J* = 8.4 Hz, 1H, *o*), 7.59 (d, *J* = 8.5 Hz, 1H, *k*), 7.44 (dd, *J* = 8.0,

1.3 Hz, 1H, *l*), 7.40 (dd, *J* = 7.9, 1.3 Hz, 1H, *d*), 7.28 (s, 1H, *h*), 7.27 (s, 1H, *g*), 7.12 (d, *J* = 8.5 Hz, 1H, *a*), 6.95-6.89 (m, 1H, *m*), 6.89-6.82 (m, 1H, *c*), 6.39 (ddd, *J* = 8.3, 6.8, 1.4 Hz, 1H, *n*), 6.33 (ddd, *J* = 8.3, 6.7, 1.4 Hz, 1H, *b*), 4.18 (s, 3H, *B*), 4.00 (s, 3H, *A*), 2.91 (s, 3H, *C*), 1.57 (s, 9H, *tBu*). ^{13}C NMR (151 MHz, CD_2Cl_2) δ 155.98, 150.89, 148.83, 145.28, 144.86, 135.83, 135.12, 135.08, 132.99, 132.21, 131.47, 129.30, 128.05, 127.60, 127.25, 127.17, 127.01, 126.93, 125.99, 125.76, 125.34, 124.93, 123.33, 123.07, 116.59, 104.09, 102.45, 46.04, 37.66, 36.44, 32.07, 23.92. HRMS (EI) m/z [M] $^+$ Calcd for $\text{C}_{37}\text{H}_{33}\text{BN}_2^+$ 516.2731; Found 516.2734.

Synthesis of 5-(*tert*-butyl)-3,7-dimethyl-3,7-dihydro-3,7-diaza-15b-borabeno[*a*]benzo[5,6]phenanthro[4,3,2-*hi*]tetracene (**E[6]H**) and 8-(*tert*-butyl)-6,10-dimethyl-6,10-dihydro-6,10-diaza-18b-borabeno[8,9,10-*hi*]tetracene (**E[4]H**):



Compound **9a** (770 mg, 1.23 mmol, 72% yield, white solid) was prepared by **GPA** using compound **1** (800 mg, 1.72 mmol). ^1H NMR (400 MHz, CDCl_3) δ 8.56-8.54 (m, 2H), 7.87-7.84 (m, 4H), 7.71 (d, *J* = 8.0 Hz, 2H), 7.64-7.51 (m, 8H), 7.40 (s, 2H), 6.92 (dd, *J* = 8.0, 4.0 Hz, 2H), 3.54 (s, 6H), 1.32 (s, 9H). ^{13}C NMR (101 MHz, CDCl_3) δ 154.13, 148.56, 147.41, 132.91, 131.74, 129.88, 129.51, 128.73, 126.89, 126.50, 126.08, 125.93, 124.93, 123.39, 123.11, 122.71, 115.79, 103.72, 39.76, 35.20, 31.38. HRMS (ESI) m/z [M+H] $^+$ $\text{C}_{40}\text{H}_{36}\text{BrN}_2^+$ 623.2056; Found 623.2041.

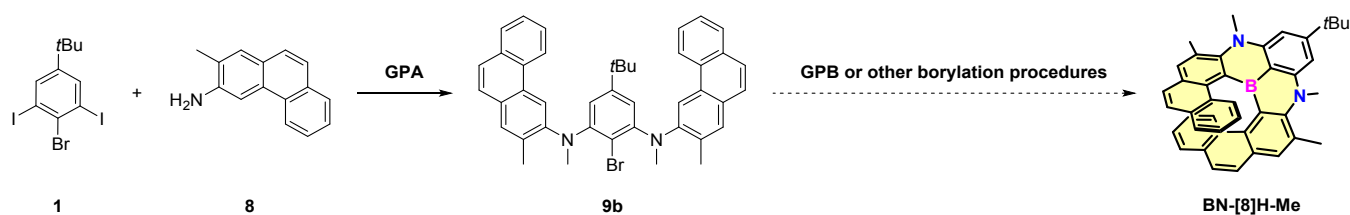
E[6]H (156.2 mg, 0.28 mmol, 22% yield) and **E[4]H** (15.1 mg, 0.02 mmol, 2% yield) were prepared by **GPB** using compound **9a** (800 mg, 1.28 mmol). No **BN-[8]H** was observed in this reaction. The reaction mixture was first purified by column chromatography with hexane/dichloromethane (*V/V* = from 100:1 to 15:1), then further purified by GPC.

E[6]H ^1H NMR (600 MHz, CD_2Cl_2) δ 8.78 (d, *J* = 8.3 Hz, 1H, *l*), 8.56 (s, 1H, *k*), 8.20 (dd, *J* = 8.7, 4.2 Hz, 2H, *g*, *a*), 7.98 (d, *J* = 9.0 Hz, 1H, *h*), 7.92 (d, *J* = 8.5 Hz, 1H, *f*), 7.89-7.84 (m, 2H, *d*, *e*), 7.76 (dd, *J* = 7.7, 1.4 Hz, 1H, *o*), 7.64 (ddd, *J* = 8.3, 6.9, 1.4 Hz, 1H, *n*), 7.56 (td, *J* = 7.4, 1.2 Hz, 1H, *m*), 7.49 (s, 1H, *r*), 7.33-7.23 (m, 3H, *i*, *p*, *j*), 7.20 (ddd, *J* = 8.0, 6.8, 1.2 Hz, 1H, *c*), 6.86 (d, *J* = 8.8 Hz, 1H, *q*), 6.72 (ddd, *J* = 8.3, 6.8, 1.4 Hz, 1H, *b*), 4.22 (s, 3H, *B*), 4.17 (s, 3H, *A*), 1.60 (s, 9H, *tBu*). ^{13}C NMR (151 MHz, CD_2Cl_2) δ 157.25, 147.44, 146.71, 146.24, 145.97, 136.52, 136.37, 133.62, 133.44, 133.27, 132.89, 132.14, 131.14, 130.33, 128.97, 127.66, 127.63, 127.33, 126.86, 126.58, 126.50, 126.49, 125.68, 125.47,

124.19, 123.94, 123.27, 116.40, 106.71, 102.44, 101.96, 37.63, 37.30, 36.66, 32.05. HRMS (MALDI-TOF) m/z Calcd for C₄₀H₃₃BN₂ 552.2731; Found 552.2740.

E[4]H ¹H NMR (600 MHz, CD₂Cl₂) δ 9.40 (s, 2H, *a*), 8.91 (d, *J* = 8.1 Hz, 2H, *g*), 8.79 (s, 2H, *h*), 8.04 (d, *J* = 8.7 Hz, 2H, *b*), 7.96 (dd, *J* = 7.8, 1.4 Hz, 2H, *d*), 7.77-7.67 (m, 6H, *f*, *e*, *c*), 7.21 (s, 2H, *i*), 4.20 (s, 6H, *Me*), 1.58 (s, 9H, *tBu*). ¹³C NMR (151 MHz, CD₂Cl₂) δ 158.27, 147.45, 146.75, 136.85, 133.66, 133.32, 130.55, 129.25, 128.16, 127.83, 126.78, 126.43, 124.89, 123.58, 107.35, 102.02, 37.62, 36.76, 31.99. HRMS (MALDI-TOF) m/z Calcd for C₄₀H₃₃BN₂ 552.2731; Found 552.2751.

Synthesis of 2-bromo-5-(*tert*-butyl)-N¹,N³-dimethyl-N¹,N³-bis(2-methylphenanthren-3-yl)benzene-1,3-diamine (**9b**) and attempts towards 11-(*tert*-butyl)-8,9,13,14-tetramethyl-9,13-dihydro-9,13-diaza-21d-borabenzo[*a*]benzo[5,6]phenanthro[2,3,4-*no*]tetraphene (**BN-[8]H-Me**):



Compound **9b** (440 mg, 0.68 mmol, 63% yield, white solid) was prepared by **GPA** using compound **1** (500 mg, 1.08 mmol). ¹H NMR (400 MHz, CDCl₃) δ 8.64 (d, *J* = 8.2 Hz, 2H), 8.33 (s, 2H), 7.89 (dd, *J* = 7.9, 1.5 Hz, 2H), 7.69-7.56 (m, 8H), 6.68 (s, 2H), 3.46 (s, 6H), 2.07 (s, 6H), 0.97 (s, 9H). ¹³C NMR (151 MHz, CDCl₃) δ 152.39, 151.28, 148.54, 132.26, 132.23, 131.12, 130.11, 129.52, 128.83, 128.16, 126.47, 126.28, 125.14, 122.60, 119.23, 117.42, 111.87, 41.96, 34.85, 31.13, 19.51. HRMS (ESI) m/z [M+H]⁺ C₄₂H₄₀BrN₂⁺ 651.2369; Found 651.2345.

Although we tried to modified **GPB** (adjusted the amount of different reagents, reaction temperature, or time) and applied several other borylation conditions to synthesize **BN-[8]H-Me**, no desired product was obtained.

Other borylation procedures:

(a). A solution of *n*-butyllithium in pentane (1.6 M, 2.0 equiv.) was added slowly to a solution of **9b** (1.0 equiv.) in *o*-xylene or *tert*-butylbenzene (0.1 M) at room temperature under a nitrogen atmosphere. After stirring at 50 °C for 30 minutes, the mixture was cooled with ice/water bath (0 °C) and boron tribromide (3.0 equiv.) was slowly injected via a micro syringe. The reaction mixture was stirred at room temperature for 2 h. Pempidine (6.0 equiv.) was added at 0 °C and then the reaction mixture was moved to a 130 °C oil bath and stirred for 12 h. The reaction mixture was cooled to room temperature and saturated NH₄Cl solution was added to quench the reaction. The aqueous solution was extracted with EtOAc. The combined organic layers were washed with brine, dried over anhydrous Na₂SO₄, filtered, and

concentrated in vacuo. Passed through a pad of celite. The residue was analyzed by GPC and MS (MALDI-TOF).

(b). A solution of *n*-butyllithium in pentane (1.6 M, 2.0 equiv.) was added slowly to a solution of **9b** (1.0 equiv.) in 1,2-dichlorobenzene (0.1 M) at room temperature under a nitrogen atmosphere. After stirring at rt for 12 hours, the mixture was cooled with ice/water bath (0 °C) and boron tribromide (3.0 equiv.) was slowly injected via a micro syringe. The reaction mixture was stirred at room temperature for 2 h. Pempidine or Hunig's base (6.0 equiv.) was added at 0 °C and then the reaction mixture was moved to a 180 °C oil bath and stirred for 12 h. The reaction mixture was cooled to room temperature and saturated NH₄Cl solution was added to quench the reaction. The aqueous solution was extracted with EtOAc. The combined organic layers were washed with brine, dried over anhydrous Na₂SO₄, filtered, and concentrated in vacuo. Passed through a pad of celite. The residue was analyzed by GPC and MS (MALDI-TOF).

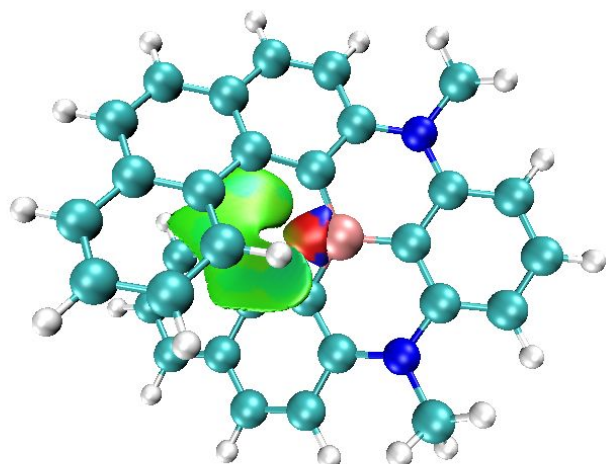


Figure S1 The independent gradient model analysis based on Hirshfeld partition (IGMH) isosurface (green color) of δg^{inter} (isovalue=0.005) for **BN-[7]H**. Isosurface color code: red—repulsions, green—van der Waals interactions, blue—strong attraction.

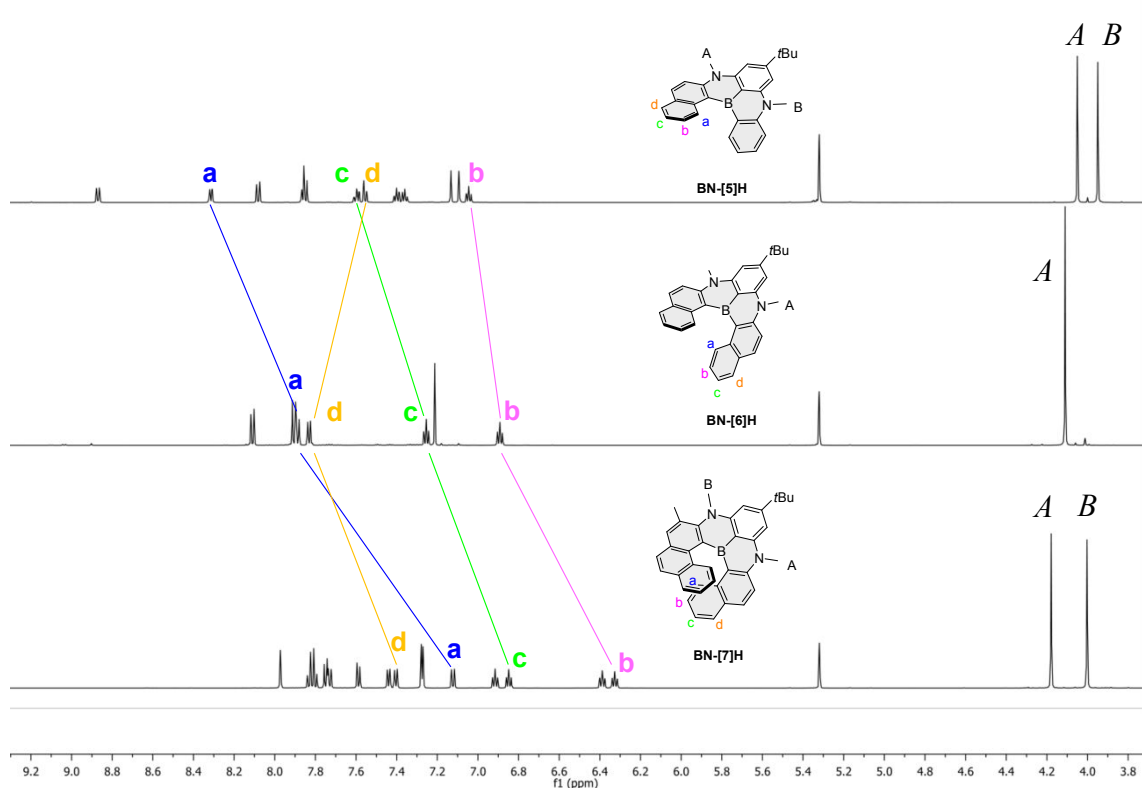


Figure S2 ^1H NMR spectra of **BN-[n]H** (top: n=5; middle: n=6; bottom: n=7) in CD_2Cl_2 at 298 K (600 MHz).

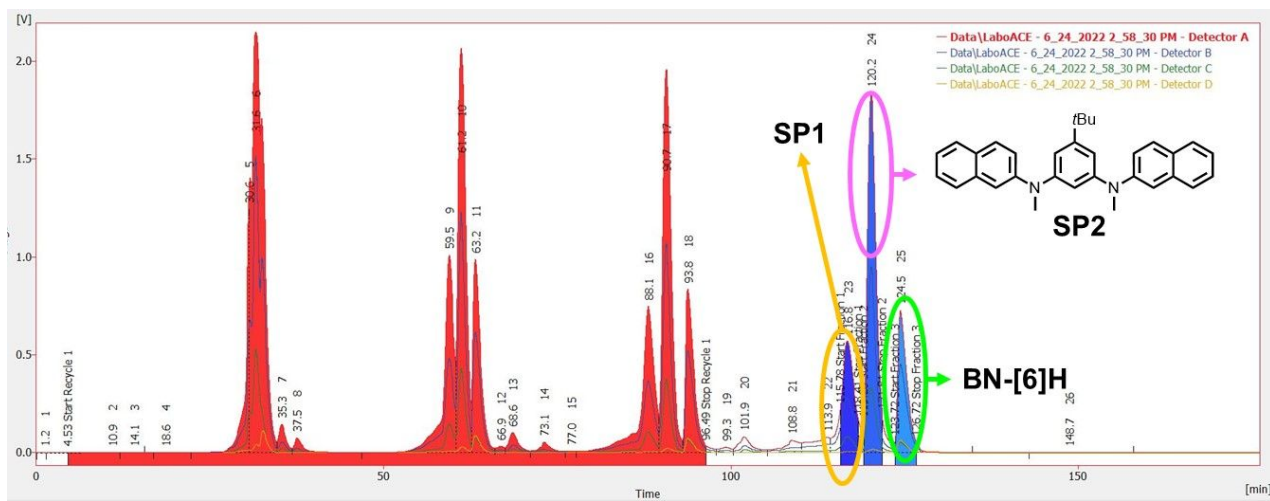


Figure S3 Recycling-GPC trace of the borylative reaction affording BN-[6]H.

3. X-ray crystallography

Single crystals of **BN-[5]H**, **BN-[6]H**, **BN-[7]H**, **E[6]H**, and **E[4]H** were obtained by slow diffusion of methanol into toluene solutions. XtaLAB Synergy, Dualflex, HyPix diffractometer; Bruker APEX-II CCD diffractometer; and XtaLAB AFC12 (RINC): Kappa single diffractometer were used for crystal screening, unit cell determination, and data collection for the X-ray crystal structure of **BN-[5]H**; **BN-[6]H**; **BN-[7]H**, **E[6]H**, and **E[4]H**, respectively. The X-ray crystallographic coordinates for structures reported in this article have been deposited at Cambridge Crystallographic Data Centre (CCDC), under deposition number, CCDC 2235573 for **BN-[5]H**, CCDC 2235575 for **BN-[6]H**, CCDC 2235579 for **BN-[7]H**, CCDC 2239651 for **E[6]H**, CCDC 2239653 for **E[4]H**. These data can be obtained free of charge from CCDC via <https://www.ccdc.cam.ac.uk/structures/>.

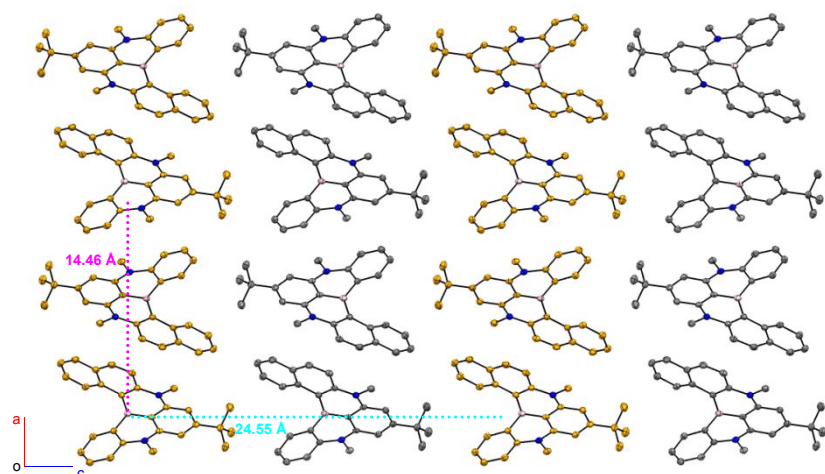


Figure S4 Molecular packing of **BN-[5]H**. All the hydrogen atoms are omitted for clarity.

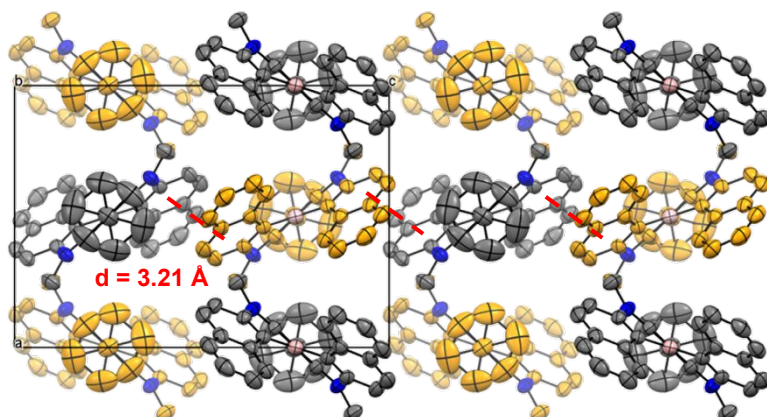


Figure S5 Molecular packing of **BN-[6]H**. All the hydrogen atoms are omitted for clarity. Disorder of *tert*-butyl groups was observed.

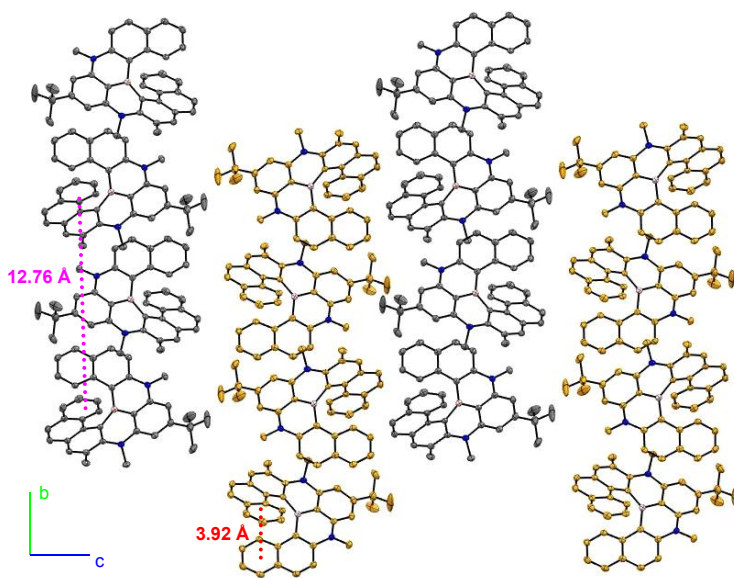


Figure S6 Molecular packing of **BN-[7]H**. All the hydrogen atoms are omitted for clarity.

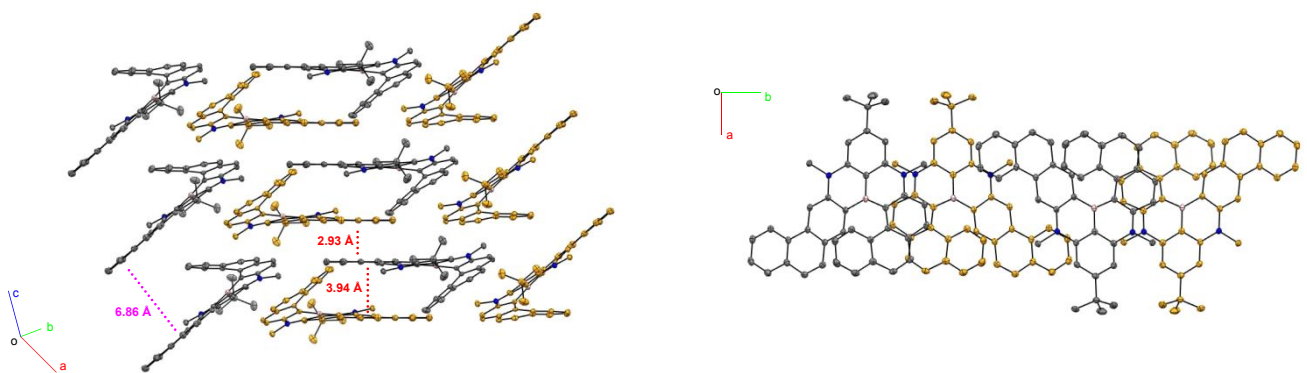


Figure S7 Molecular packing of **E[6]H**. All the hydrogen atoms are omitted for clarity.

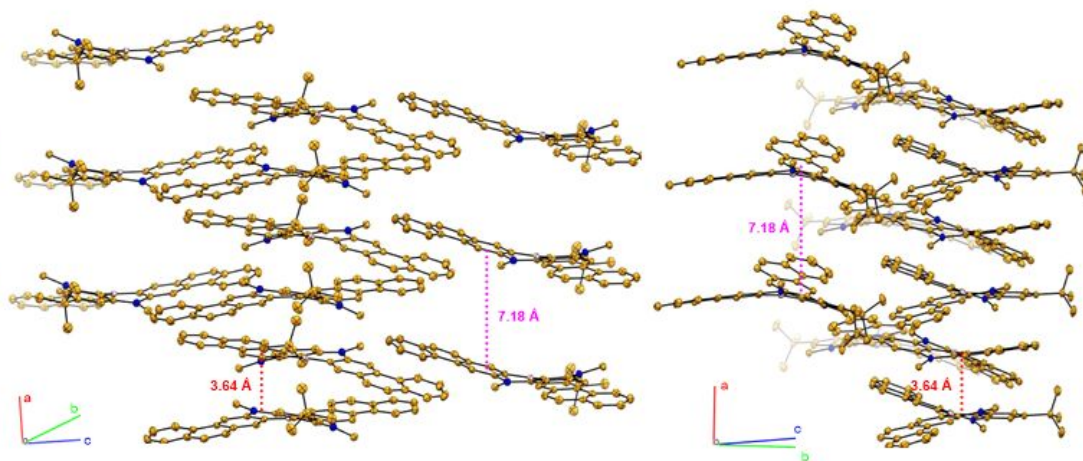


Figure S8 Molecular packing of **E[4]H**. All the hydrogen atoms are omitted for clarity.

Table S1. Crystallographic data and details of the structural refinements of **BN-[5]H**.

Compound name	BN-[5]H
CCDC number	2235573
Empirical formula	C ₂₈ H ₂₇ BN ₂
Formula weight	406.23
Temperature/K	100.00(10)
Crystal system	monoclinic
Space group	<i>P</i> 2 ₁ /c
<i>a</i> /Å	14.4557(3)
<i>b</i> /Å	6.00320(10)
<i>c</i> /Å	24.5572(5)
$\alpha/^\circ$	90
$\beta/^\circ$	90.757(2)
$\gamma/^\circ$	90
Volume/Å ³	2130.90(7)
Z	4
$\rho_{\text{calc}}/\text{g/cm}^3$	1.266
μ/mm^{-1}	0.560
F(000)	865.0
Crystal size/mm ³	0.1 × 0.04 × 0.04
Radiation	CuKα ($\lambda = 1.54184$)
2θ range for data collection/°	6.114 to 143.358
Index ranges	-17 ≤ <i>h</i> ≤ 17, -2 ≤ <i>k</i> ≤ 7, -30 ≤ <i>l</i> ≤ 29
Reflections collected	12832
Independent reflections	3950 [$R_{\text{int}} = 0.0383$, $R_{\text{sigma}} = 0.0409$]
Data/restraints/parameters	3950/0/285
Goodness-of-fit on F ²	1.053
Final R indexes [I>=2σ (I)]	$R_1 = 0.0428$, $wR_2 = 0.1105$
Final R indexes [all data]	$R_1 = 0.0510$, $wR_2 = 0.1167$
Largest diff. peak/hole / e Å ⁻³	0.36/-0.22

Table S2. Crystallographic data and details of the structural refinements of **BN-[6]H**.

Compound name	BN-[6]H
CCDC number	2235575
Empirical formula	C ₃₂ H ₂₉ BN ₂
Formula weight	452.38
Temperature/K	301.00
Crystal system	orthorhombic
Space group	<i>Pbcn</i>
<i>a</i> /Å	10.9917(4)
<i>b</i> /Å	14.1697(5)
<i>c</i> /Å	15.7360(6)
$\alpha/^\circ$	90
$\beta/^\circ$	90
$\gamma/^\circ$	90
Volume/Å ³	2450.87(16)
Z	4
$\rho_{\text{calc}}/\text{g/cm}^3$	1.226
μ/mm^{-1}	0.070
F(000)	960.0
Crystal size/mm ³	0.4 × 0.1 × 0.1
Radiation	MoK α ($\lambda = 0.71073$)
2 Θ range for data collection/°	4.69 to 56.576
Index ranges	-14 ≤ <i>h</i> ≤ 14, -18 ≤ <i>k</i> ≤ 18, -20 ≤ <i>l</i> ≤ 20
Reflections collected	22940
Independent reflections	3048 [$R_{\text{int}} = 0.0531$, $R_{\text{sigma}} = 0.0282$]
Data/restraints/parameters	3048/10/178
Goodness-of-fit on F ²	1.055
Final R indexes [I>=2σ (I)]	$R_1 = 0.0463$, $wR_2 = 0.1201$
Final R indexes [all data]	$R_1 = 0.0730$, $wR_2 = 0.1444$
Largest diff. peak/hole / e Å ⁻³	0.15/-0.18

Table S3. Crystallographic data and details of the structural refinements of **BN-[7]H**.

Compound name	BN-[7]H
CCDC number	2235579
Empirical formula	C ₃₇ H ₃₃ BN ₂
Formula weight	516.46
Temperature/K	99.98(11)
Crystal system	monoclinic
Space group	<i>P</i> 2 ₁ /n
<i>a</i> /Å	7.97733(6)
<i>b</i> /Å	14.84806(11)
<i>c</i> /Å	23.76860(16)
$\alpha/^\circ$	90
$\beta/^\circ$	92.2615(7)
$\gamma/^\circ$	90
Volume/Å ³	2813.15(3)
Z	4
$\rho_{\text{calc}}/\text{g/cm}^3$	1.219
μ/mm^{-1}	0.531
F(000)	1096.0
Crystal size/mm ³	0.02 × 0.014 × 0.01
Radiation	Cu K α ($\lambda = 1.54184$)
2 Θ range for data collection/°	9.536 to 155.338
Index ranges	-10 ≤ <i>h</i> ≤ 7, -16 ≤ <i>k</i> ≤ 18, -30 ≤ <i>l</i> ≤ 27
Reflections collected	14611
Independent reflections	5722 [$R_{\text{int}} = 0.0167$, $R_{\text{sigma}} = 0.0179$]
Data/restraints/parameters	5722/1032/367
Goodness-of-fit on F ²	1.037
Final R indexes [I>=2σ (I)]	$R_1 = 0.0428$, $wR_2 = 0.1080$
Final R indexes [all data]	$R_1 = 0.0448$, $wR_2 = 0.1093$
Largest diff. peak/hole / e Å ⁻³	0.27/-0.32

Table S4. Crystallographic data and details of the structural refinements of **E[6]H**.

Compound name	E[6]H
CCDC number	2239651
Empirical formula	C ₄₀ H ₃₃ BN ₂
Formula weight	552.49
Temperature/K	293(2)
Crystal system	monoclinic
Space group	<i>P</i> 2 ₁ /c
<i>a</i> /Å	13.6942(2)
<i>b</i> /Å	28.8541(4)
<i>c</i> /Å	7.36970(10)
$\alpha/^\circ$	90
$\beta/^\circ$	91.5540(10)
$\gamma/^\circ$	90
Volume/Å ³	2910.95(7)
Z	4
$\rho_{\text{calc}}/\text{g/cm}^3$	1.261
μ/mm^{-1}	0.550
F(000)	1168.0
Radiation	Cu K α ($\lambda = 1.54178$)
2 Θ range for data collection/°	6.126 to 155.298
Index ranges	-17 ≤ <i>h</i> ≤ 16, -36 ≤ <i>k</i> ≤ 36, -8 ≤ <i>l</i> ≤ 9
Reflections collected	17874
Independent reflections	5947 [$R_{\text{int}} = 0.0360$, $R_{\text{sigma}} = 0.0463$]
Data/restraints/parameters	5947/0/393
Goodness-of-fit on F ²	0.652
Final R indexes [I>=2σ (I)]	$R_1 = 0.0561$, wR ₂ = 0.1800
Final R indexes [all data]	$R_1 = 0.0723$, wR ₂ = 0.1924
Largest diff. peak/hole / e Å ⁻³	0.31/-0.21

Table S5. Crystallographic data and details of the structural refinements of **E[4]H**.

Compound name	E[4]H
CCDC number	2239653
Empirical formula	C ₄₀ H ₃₃ BN ₂
Formula weight	552.49
Temperature/K	293(2)
Crystal system	orthorhombic
Space group	<i>P</i> 2 ₁ 2 ₁ 2 ₁
<i>a</i> /Å	7.18200(10)
<i>b</i> /Å	15.6780(2)
<i>c</i> /Å	25.7919(3)
$\alpha/^\circ$	90
$\beta/^\circ$	90
$\gamma/^\circ$	90
Volume/Å ³	2904.15(6)
<i>Z</i>	4
$\rho_{\text{calc}}/\text{g/cm}^3$	1.264
μ/mm^{-1}	0.552
F(000)	1168.0
Radiation	Cu K α ($\lambda = 1.54178$)
2 Θ range for data collection/°	6.598 to 155.356
Index ranges	-9 ≤ <i>h</i> ≤ 8, -17 ≤ <i>k</i> ≤ 19, -32 ≤ <i>l</i> ≤ 31
Reflections collected	14229
Independent reflections	5507 [$R_{\text{int}} = 0.0680$, $R_{\text{sigma}} = 0.0858$]
Data/restraints/parameters	5507/0/393
Goodness-of-fit on F ²	0.796
Final R indexes [I>=2σ (I)]	$R_1 = 0.0504$, wR ₂ = 0.1378
Final R indexes [all data]	$R_1 = 0.0757$, wR ₂ = 0.1426
Largest diff. peak/hole / e Å ⁻³	0.24/-0.29
Flack parameter	0.9(4)

4. Optical and electrochemical properties

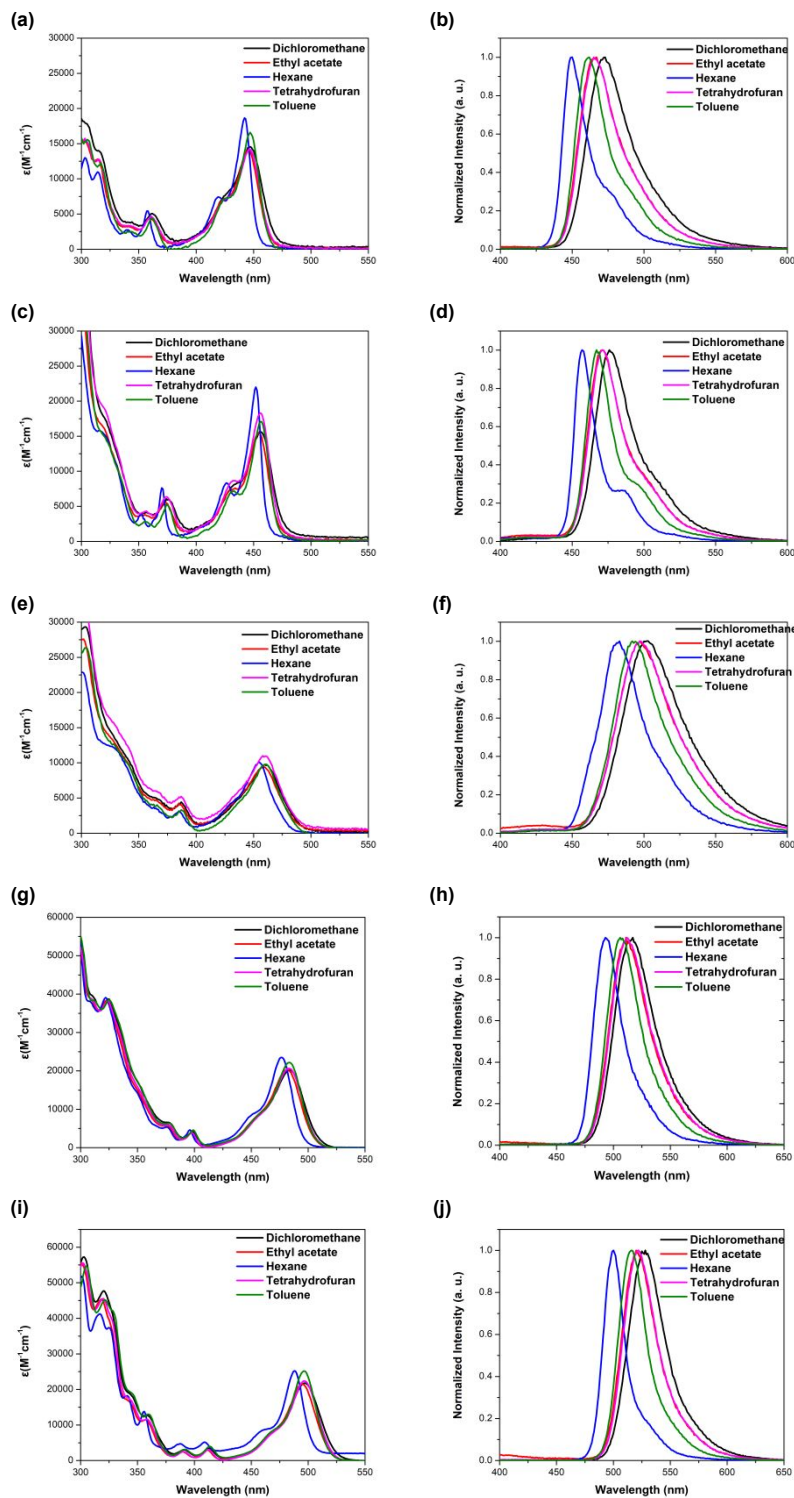


Figure S9 UV-Vis absorption (left) and normalized fluorescence emission (right) spectra of **BN-[5]H** (a and b), **BN-[6]H** (c and d), **BN-[7]H** (e and f), **E[6]H** (g and h), and **E[4]H** (i and j) in different solutions (1×10^{-5} M).

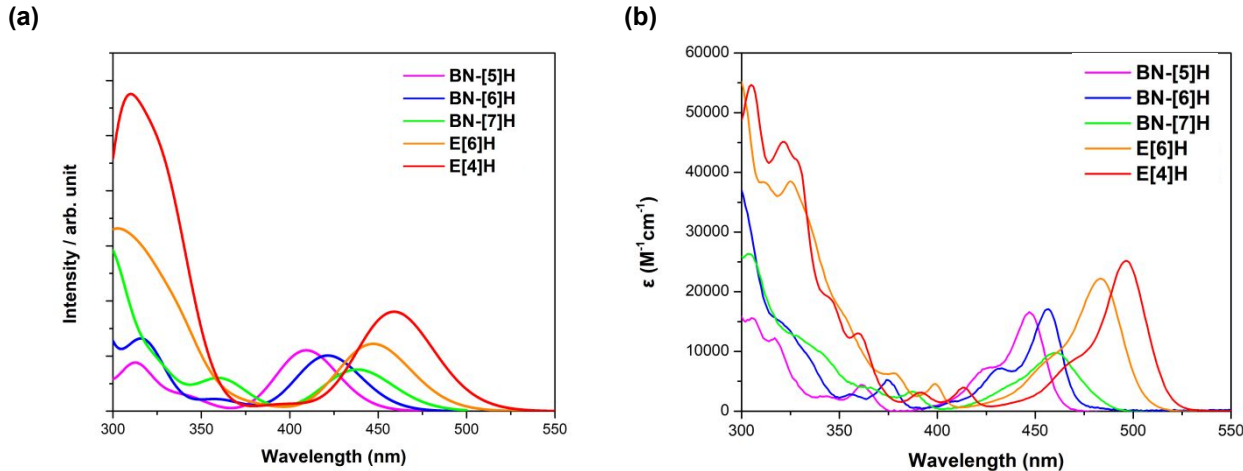


Figure S10 (a) Calculated UV-Vis spectra of NBN-doped helicenes at the PBE0/6-311G(d) level. (b) Measured UV-Vis spectra of NBN-doped helicenes in toluene.

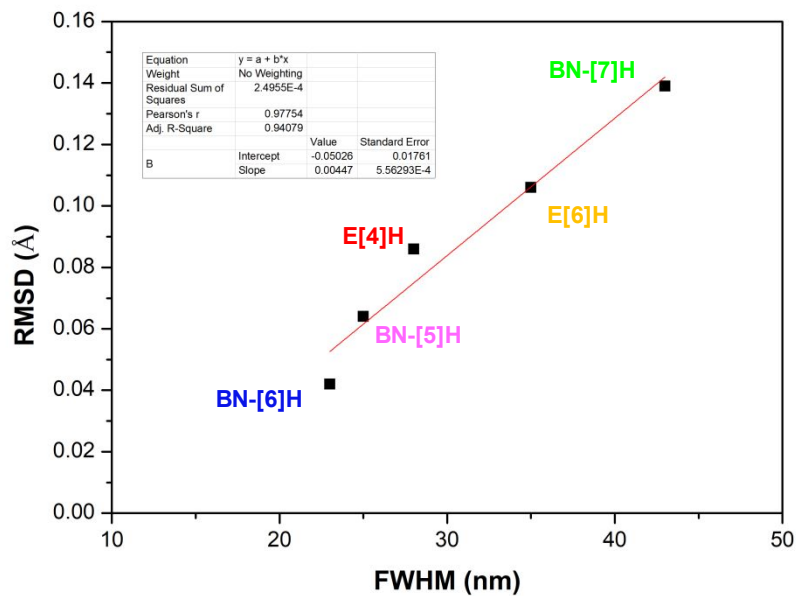


Figure S11 The correlation between full-width at half-maximum (FWHM) and root-mean-square deviation of atomic positions (RMSD) between the ground states (S_0) and the lowest singlet states (S_1) calculated at the (TD)B3LYP/6-31G(d) level.

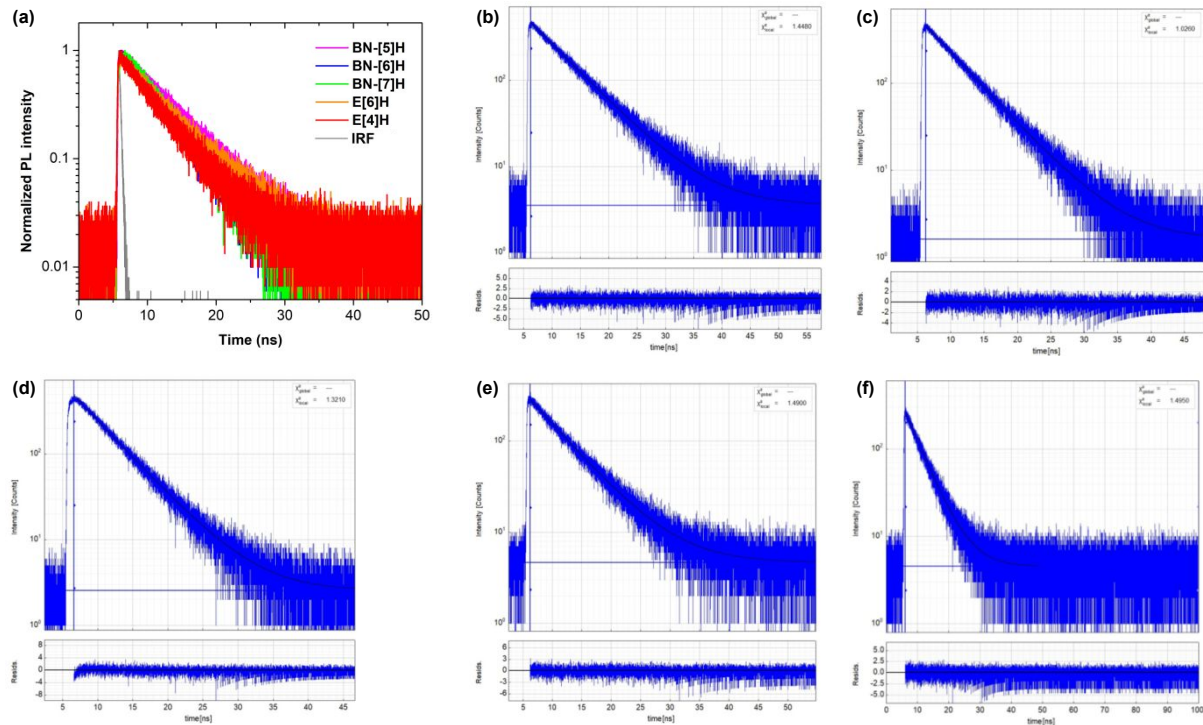


Figure S12 Time-resolved photoluminescence (TRPL) decays of (a) NBN-doped helicenes and IRF, (b) BN-[5]H, (c) BN-[6]H, (d) BN-[7]H, (e) E[6]H, and (f) E[4]H.

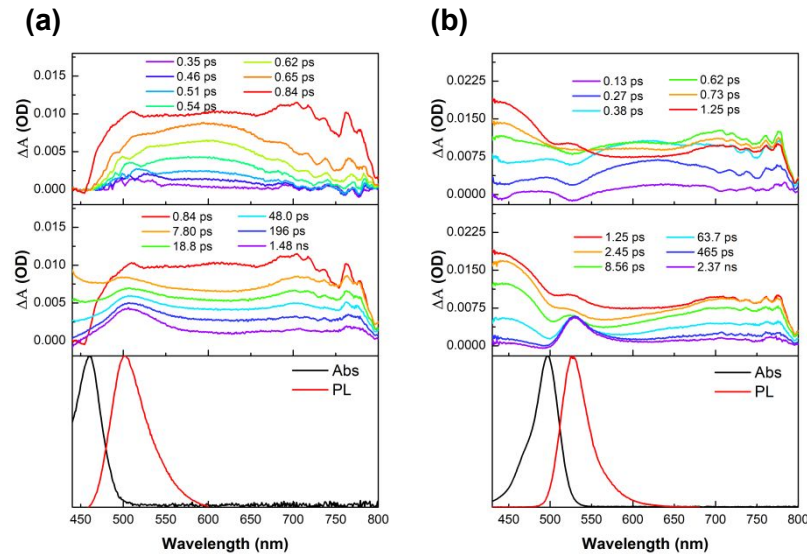


Figure S13 Femtosecond transient absorption spectra (top for early spectral conversion and middle for the late-time process) and steady-state absorption/emission spectra (bottom) in dichloromethane of (a) BN-[7]H and (b) E[4]H.

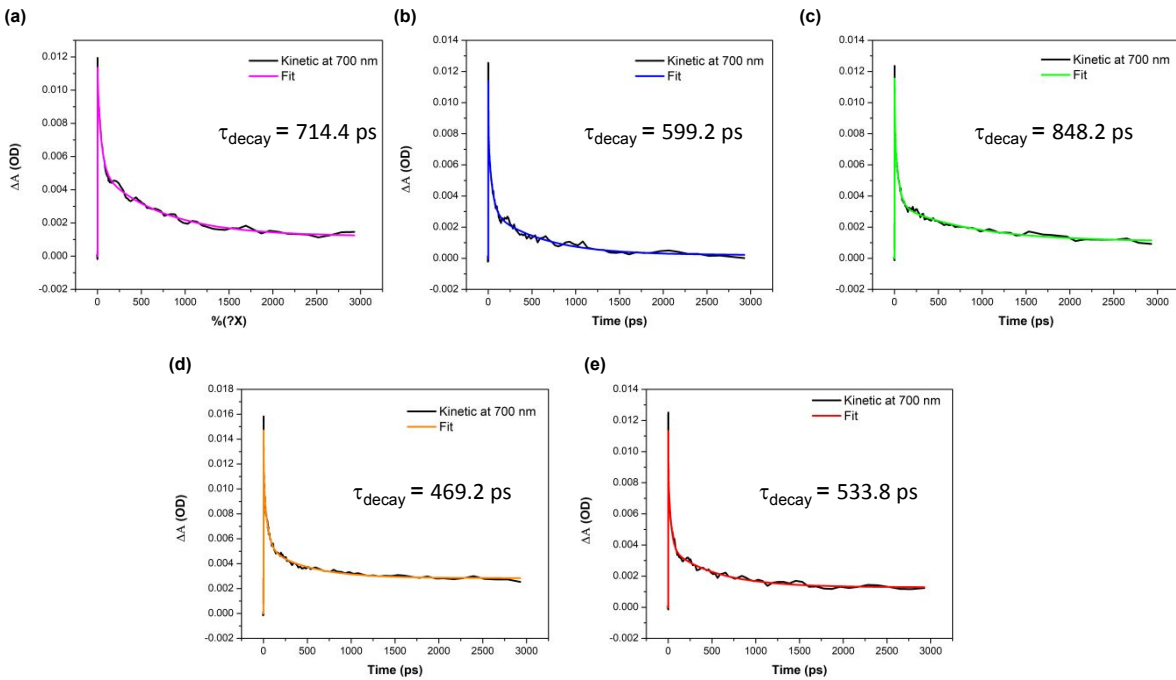


Figure S14 Kinetic profiles at 700 nm of fs-TA spectra of (a) BN-[5]H, (b) BN-[6]H, (c) BN-[7]H, (d) E[6]H, and (e) E[4]H.

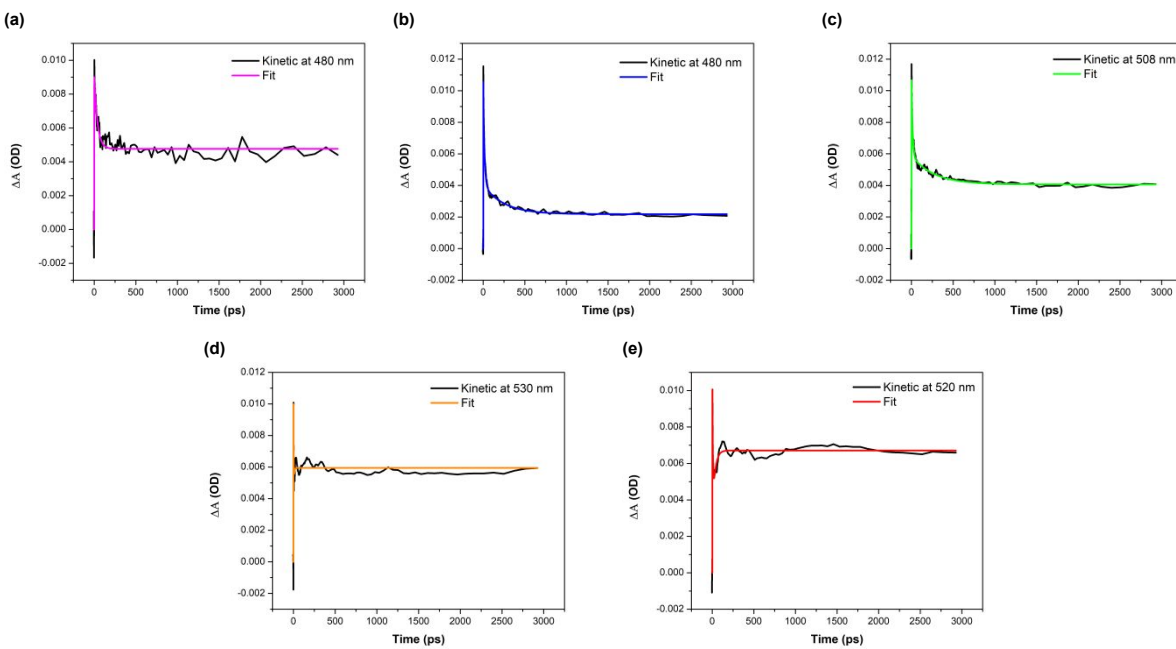


Figure S15 Kinetic profiles at selected wavelengths of fs-TA spectra of (a) BN-[5]H, (b) BN-[6]H, (c) BN-[7]H, and (d) E[6]H. Although the decay times were not obtained by multiexponential decay fitting, owing to the time limit of up to 3 ns, the decay times are longer than their corresponding decay times at 700 nm.

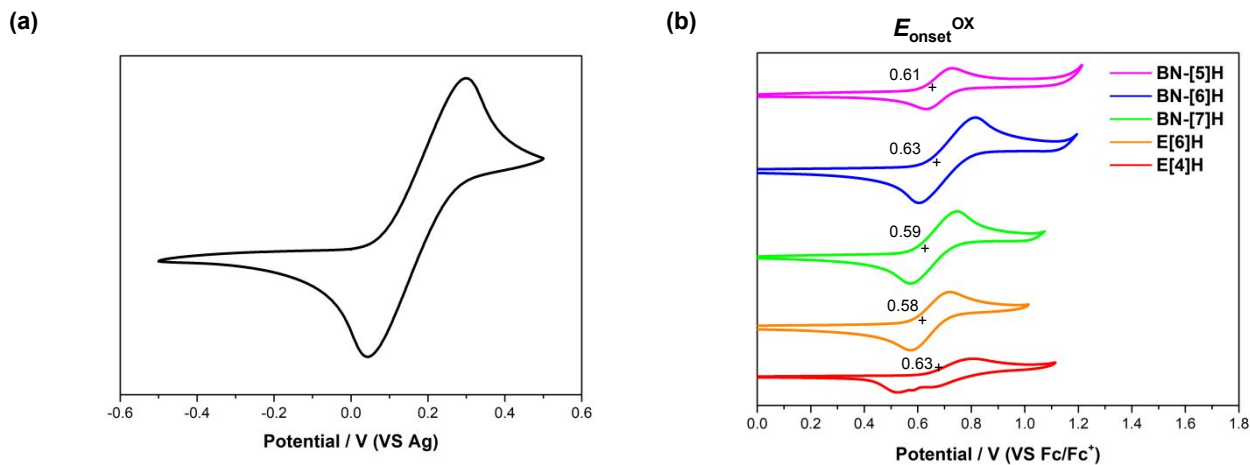


Figure S16 Cyclic voltammetry curves of decamethylferrocene (a) and NBN-doped helicenes in degassed dichloromethane solution containing Bu_4NPF_6 (0.1 M) in a three-electrode cell with a scan rate of 100 mV/s at room temperature.

5. Chiral resolution and chiroptical properties

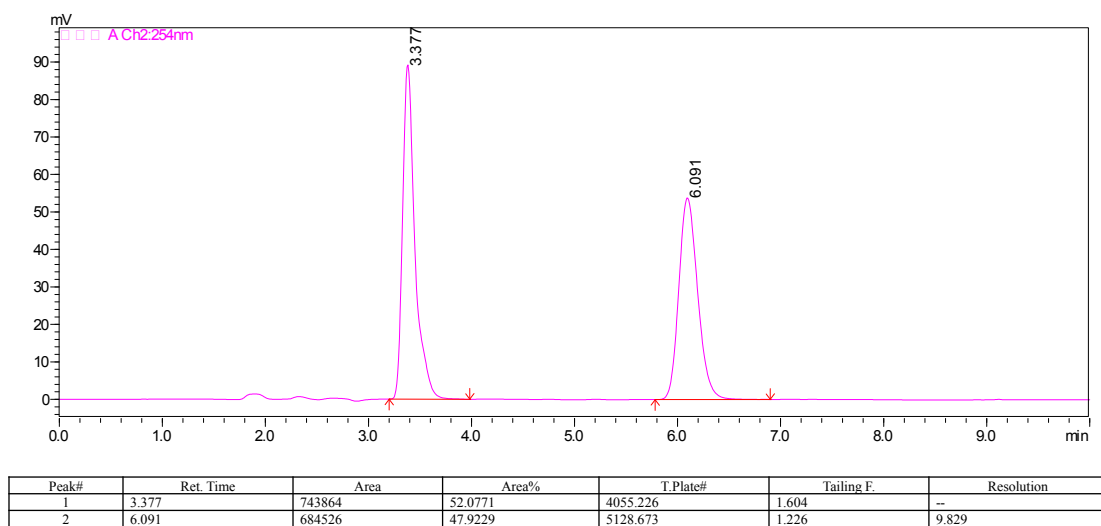
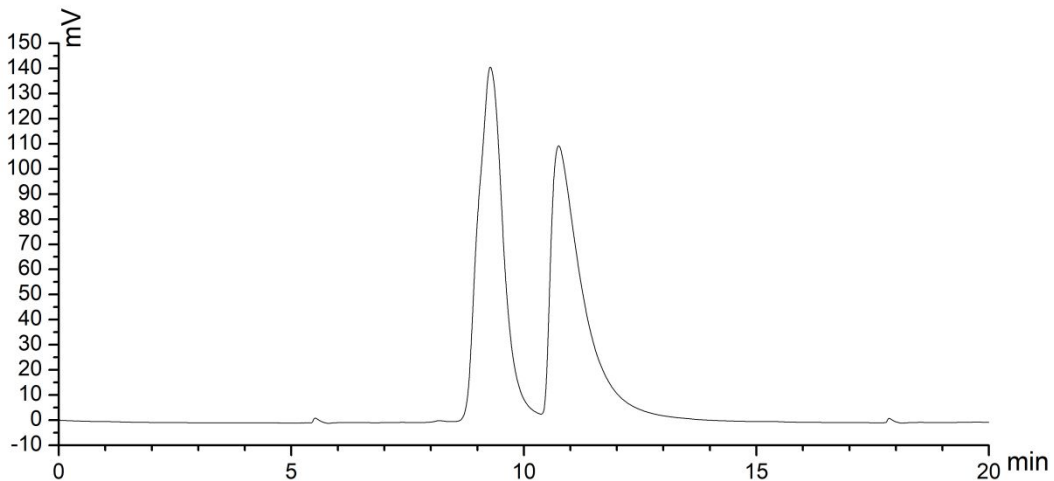


Figure S17 Resolution of **BN-[6]H** by chiral HPLC monitored at 254 nm was performed with a CHIRALPAK IBN column (0.10 cm I.D. \times 25 cm L). Injection volume was 1 μL , and a mixture of *n*-hexane/EtOH = 80/20 (V/V) was used as the eluent with a flow rate of 1.0 mL/min at 25 °C. Comparing the experimental and simulated ECD spectra, the first peak with retention time of 3.377 min is (*M*)-BN-[6]H, and the second peak with retention time of 6.091 min is (*P*)-BN-[6]H.



Peak#	Ret. Time	Area	Area%	Height	T.Plate#	Tailing
1	9.278	5370076	50.5980	141445	1487	1.272
2	10.748	5500077	49.4020	110104	1372	3.220

Figure S18 Resolution of BN-[7]H by chiral HPLC monitored at 254 nm was performed with a CHIRALPAK IC column (1.0 cm I.D.×15 cm L). Injection volume was 40 μ L, and a mixture of *n*-hexane/CH₂Cl₂ = 75/25 (V/V) was used as the eluent with a flow rate of 3.0 mL/min at 25 °C. Comparing the experimental and simulated ECD spectra, the first peak with retention time of 9.278 min is (*P*)-BN-[7]H, and the second peak with retention time of 10.748 min is (*M*)-BN-[7]H.

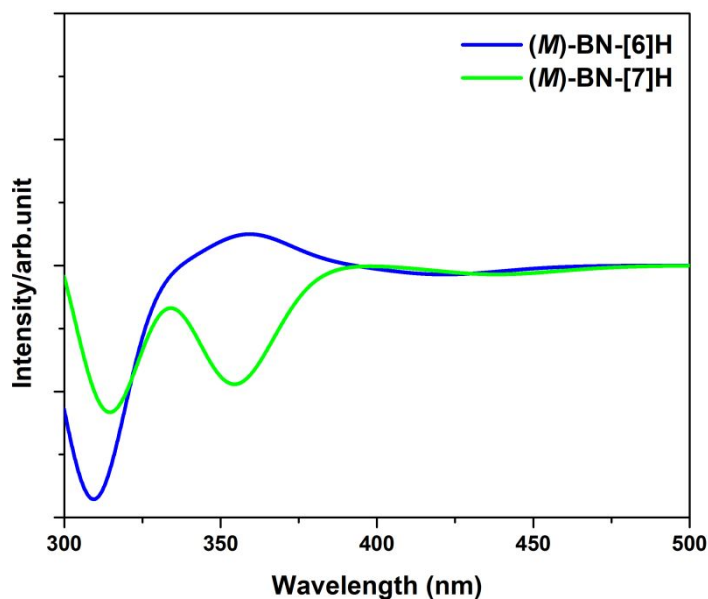


Figure S19 Calculated ECD spectra for model (*M*)-BN-[6]H and (*M*)-BN-[7]H at the PBE0/6-311G(d) level.

CPL spectra

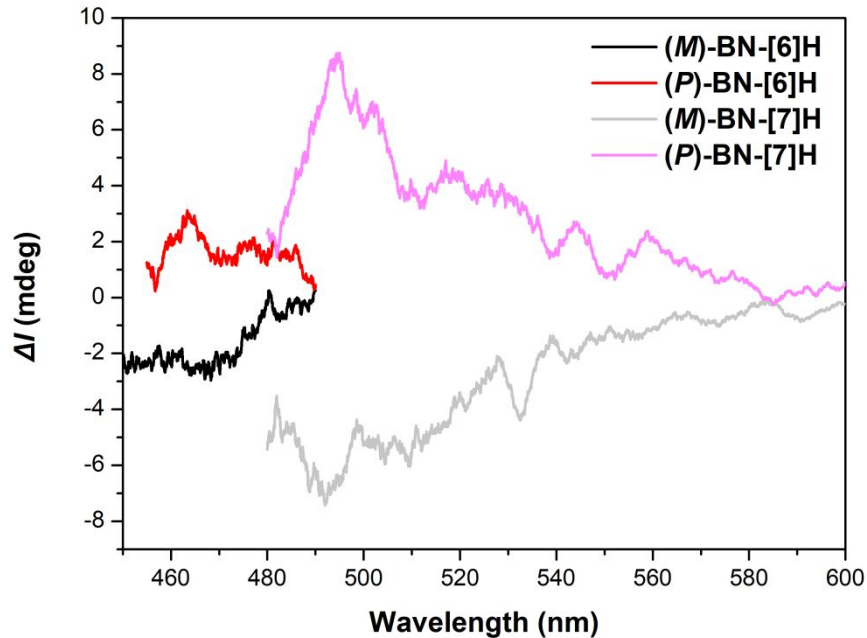


Figure S20 CPL spectra of **BN-[6]H** and **BN-[7]H** in toluene (1×10^{-5} M).

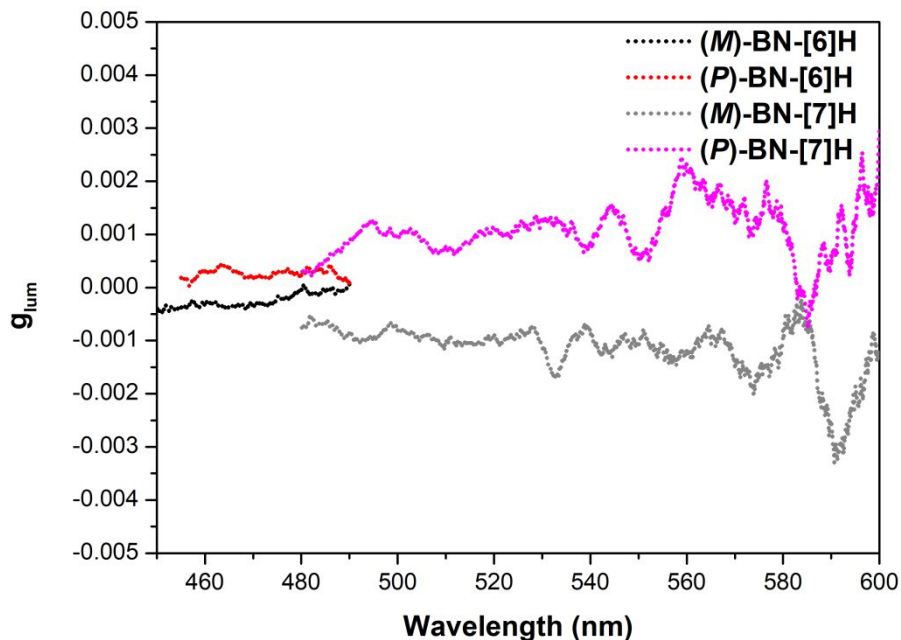
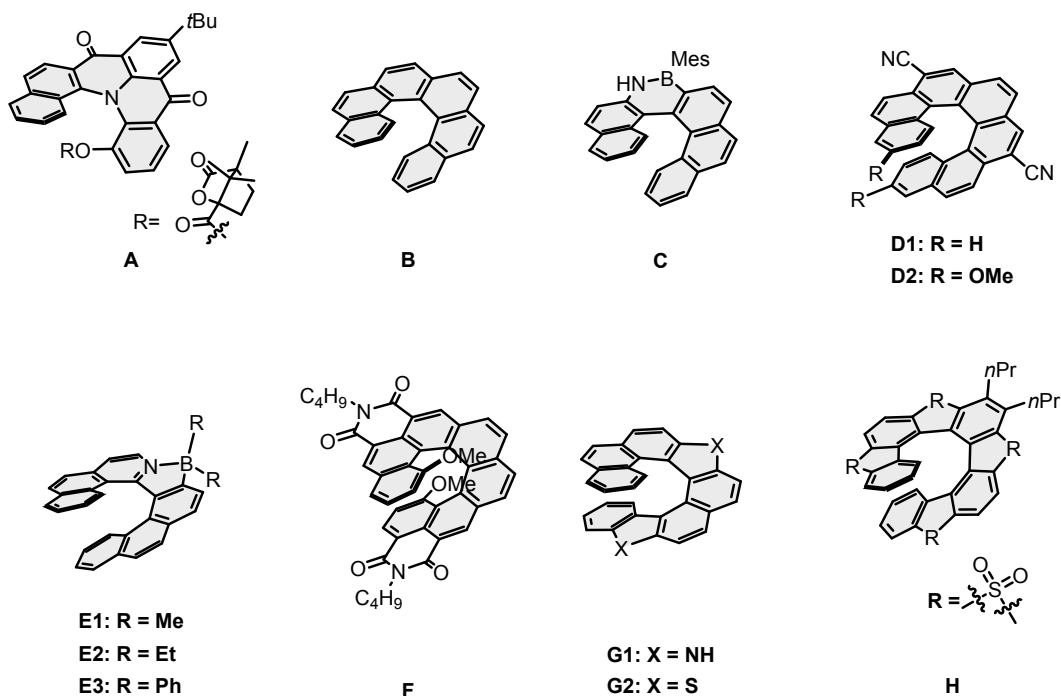


Figure S21 Luminescence dissymmetry factors of **BN-[6]H** and **BN-[7]H** in toluene (1×10^{-5} M), $g_{lum(BN-[6]H)} = 0.4 \times 10^{-3}$ and $g_{lum(BN-[7]H)} = 1.0 \times 10^{-3}$.

Table S6. The $|g_{abs}|_{max}$ values of single-stranded helical molecules.



Compound	$ g_{abs} _{max}$	λ/nm	Solvent	Reference	Year
A	0.001	442	CHCl_3	S4	2003
B	0.009	324	CH_2Cl_2	S5	2018
C	0.005	308	CH_2Cl_2	S6	2022
D1	0.016	421	CHCl_3	S7	2021
D2	0.016	418	CHCl_3	S7	2021
E1	0.0112	323	CH_2Cl_2	S8	2021
E2	0.0091	324	CH_2Cl_2	S8	2021
E3	0.0076	325	CH_2Cl_2	S8	2021
F	0.011	410	CH_2Cl_2	S9	2020
G1	0.019	403	CH_2Cl_2	S10	2021
G2	0.017	404	CH_2Cl_2	S10	2021
H	0.005	300	THF	S11	2016
BN-[6]H	0.021	344	Toluene	This work	2023
BN-[7]H	0.018	358	Toluene	This work	2023

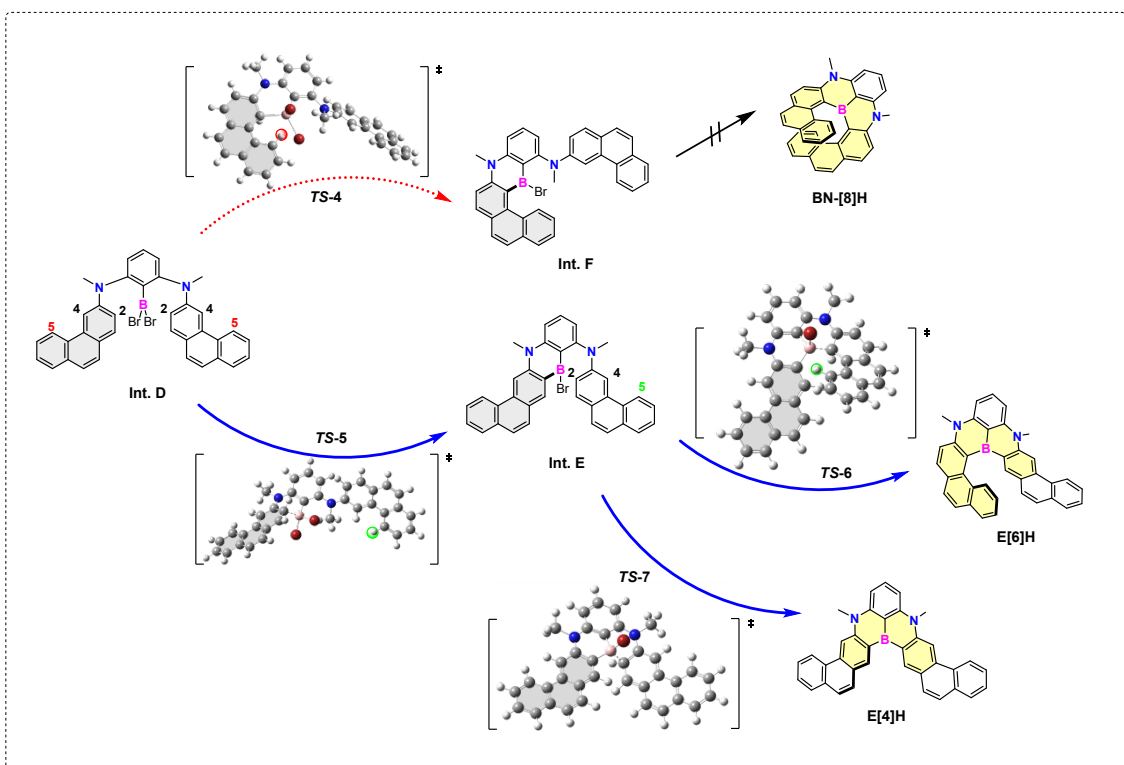
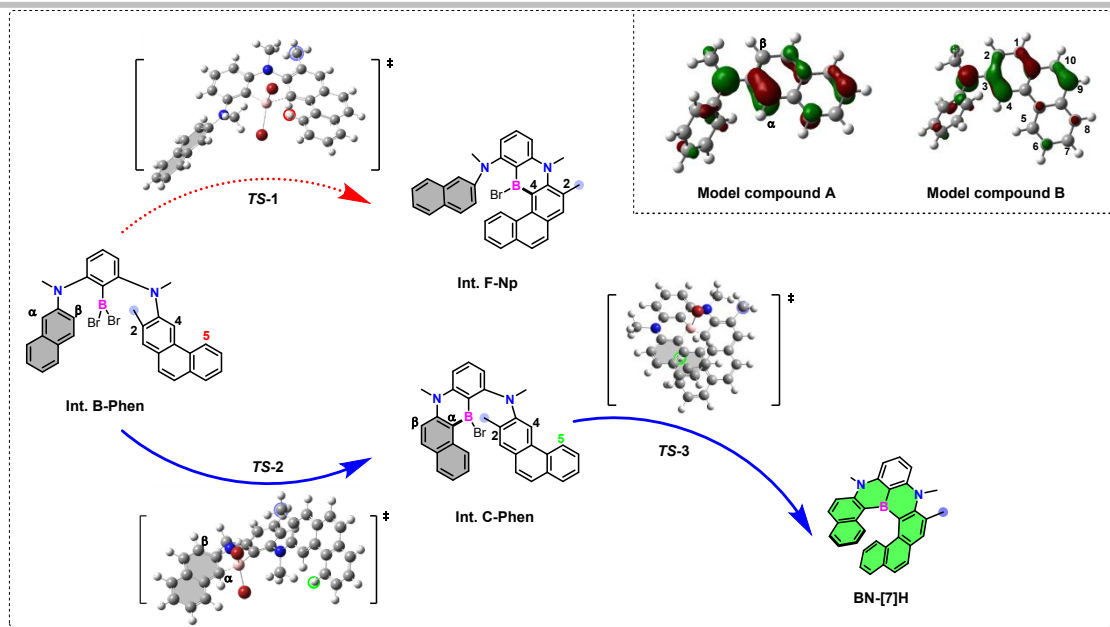


Figure S23 Simplified transition states (TS) analysis of C-H borylation steps in the case of **BN-[8]H**.

6. Theoretical calculations

The density functional theory (DFT) calculations were performed with the Gaussian 16 quantum chemistry package^[S12] employing the PBE0^[S13] or B3LYP^[S14] hybrid functional. The *tert*-butyl groups and the additional methyl group of C ring in **BN-[7]H** were reduced to hydrogen atoms for simplicity. Structures were optimized with the 6-311G(d)^[S15] or Def2-TZVP^[S16] basic set. The time-dependent density functional theory (TD-DFT) calculation^[S17] was conducted after the geometry optimization and considered the solvent used during experiments (toluene) through the self-consistent reaction field (SCRF) method using the polarizable continuum model (PCM)^[S18] with Grimme's D3BJ dispersion correction^[S19]. The optimized structures and transition states (TS) were confirmed by harmonic frequency calculations. Nucleus independent chemical shifts (NICS) values were calculated using the standard gauge invariant atomic orbital (GIAO)^[S20] method using B3LYP functional with the 6-311+G(d,p) basic set. The independent gradient model analysis based on Hirshfeld partition (IGMH) isosurfaces and calculated UV-Vis, ECD spectra were generated using Multiwfn software.^[S21]

Table S7. Calculated photophysical properties data of **BN-[5]H**, **BN-[6]H**, **BN-[7]H**, **E[6]H**, and **E[4]H** at the PBE0/6-311G(d) level.

compd	Excited States	Wavelength [nm]	Oscillator Strength	Transitions
BN-[5]H	S ₁	409	0.246	H -> L 97.2%
	S ₂	341	0.057	H -> L+1 93.3%
	S ₃	323	0.012	H-1 -> L 91.4%
	S ₄	312	0.186	H-2 -> L 85.6% H -> L+2 6.3%
	S ₅	293	0.010	H -> L+3 77.4% H-3 -> L 8.7%
	S ₆	284	0.061	H-1 -> L+1 58.6%, H -> L+2 18.6%, H -> L+3 6.6%, H-2 -> L+1 5.4%
	S ₇	280	0.440	H -> L+2 56.7%, H-1 -> L+1 23.7%, H-2 -> L 6.9%
	S ₈	273	0.090	H-3 -> L 37.4%, H-2 -> L+1 28.6%, H -> L+3 7.8%, H-1 -> L+1 7.3%, H -> L+4 6.8%
	S ₉	265	0.288	H-3 -> L 37.3%, H-2 -> L+1 31.2%, H-1 -> L+3 7.8%, H -> L+2 7.3%, H-4 -> L 7.0%
BN-[6]H	S ₁	422	0.225	H -> L 97.7%

	S ₂	359	0.047	H → L+1 96.3%
	S ₃	330	0.012	H-1 → L 92.0%
	S ₄	323	0.008	H → L+2 76.5% H-3 → L 19.2%
	S ₅	321	0.154	H-2 → L 81.2% H → L+3 10.3%
	S ₆	311	0.154	H-3 → L 77.3% H → L+2 20.1%
	S ₇	302	0.011	H-1 → L+1 70.0% H-2 → L+1 21.1%
	S ₈	287	0.373	H → L+3 72.1%, H-2 → L 11.0%, H-3 → L+1 10.2%
	S ₉	287	0.129	H-2 → L+1 62.9% H-1 → L+1 25.4%
	S ₁	438	0.168	H → L 97.1%
	S ₂	366	0.067	H → L+1 90.1%
	S ₃	362	0.006	H-1 → L 73.8% H → L+2 14.8%
	S ₄	355	0.071	H → L+2 79.3% H-1 → L 15.0%
	S ₅	326	0.098	H-2 → L 83.9% H → L+3 8.1%
BN-[7]H	S ₆	325	0.022	H-3 → L 42.6% H-1 → L+1 42.5%
	S ₇	317	0.085	H-1 → L+1 45.7% H-3 → L 39.9%
	S ₈	305	0.078	H → L+3 55.8%, H-1 → L+2 29.1%, H-3 → L 7.0%
	S ₉	299	0.424	H-1 → L+2 48.2%, H → L+3 19.7%, H-2 → L 8.5%, H-2 → L+1 7.2%, H-3 → L+1 6.0%
	S ₁	447	0.272	H → L 97.1%
	S ₂	379	0.020	H-1 → L 93.2%
	S ₃	358	0.043	H → L+1 87.3%
E[6]H	S ₄	348	0.007	H → L+2 71.5%, H-2 → L 19.7%
	S ₅	340	0.113	H-2 → L 73.7%, H → L+2 16.4%
	S ₆	336	0.150	H → L+3 71.5%, H-3 → L 20.0%

			H-1 -> L+1 32.4%, H-3 -> L 26.2%, H-4 -> L 10.1%, H -> L+3 7.7%, H -> L+1 5.7%, H-2 -> L+1 5.5%
S ₇	326	0.107	H-3 -> L 27.8%, H-1 -> L+2 22.8%, H-4 -> L 16.2%, H -> L+3 11.7%
S ₉	313	0.114	H-4 -> L 42.4%, H-1 -> L+1 41.1%, H-3 -> L 9.7%
S ₁	459	0.402	H -> L 97.9%
S ₂	397	0.028	H-1 -> L 95.2%
S ₃	345	0.116	H -> L+1 73.9%, H-2 -> L 10.0%, H-1 -> L+2 8.9%
S ₄	344	0.042	H -> L+3 36.1%, H -> L+2 32.8%, H-3 -> L 15.0%, H-1 -> L+1 10.7%
E[4]H	S ₅	0.121	H -> L+3 53.1%, H -> L+2 36.1%, H-3 -> L 5.5%
	S ₆	0.420	H-2 -> L 81.0%
S ₇	321	0.261	H-4 -> L 53.7%, H -> L+1 13.3%, H-1 -> L+3 12.5%, H-1 -> L+2 6.1%, H-2 -> L 5.7%
S ₈	317	0.325	H-3 -> L 58.3%, H -> L+2 26.8%, H-1 -> L+1 5.3%
S ₉	307	0.274	H-1 -> L+3 61.5%, H-4 -> L 27.3%

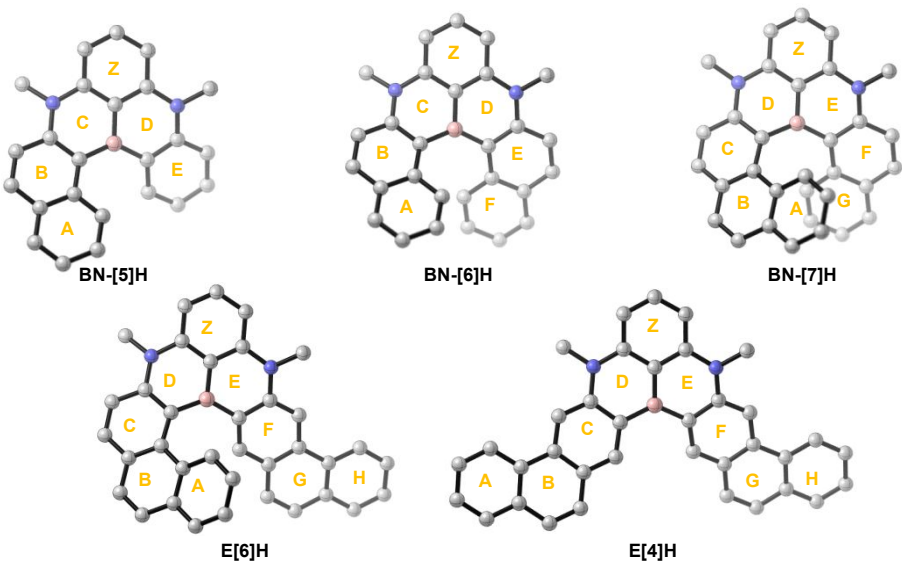
Table S8. Coordinates of electric transition dipole moments (μ) and magnetic transition dipole moments (m) of model (M)-BN-[6]H and (M)-BN-[7]H at the PBE0/6-311G(d) level.

compd	Excited States	μ [a.u.]			m [a.u.]		
		x	y	z	x	y	z
(M)-BN-[6]H	S ₀ →S ₁	0	-1.760	-0.136	0	-0.078	0.325
	S ₀ →S ₂	-0.746	0	0	0.476	0	0
	S ₀ →S ₃	0.369	0	0	0.072	0	0
	S ₀ →S ₄	-0.001	-0.269	0.127	0	-0.602	1.864
	S ₀ →S ₅	1.275	-0.001	0	-0.548	0	0.001
	S ₀ →S ₆	0.001	1.014	-0.744	0	0.439	-2.652
(M)-BN-[7]H	S ₀ →S ₁	-0.095	-1.551	-0.101	0.028	-0.010	-0.882
	S ₀ →S ₂	0.822	0.352	0.043	-0.383	0.232	0.528
	S ₀ →S ₃	0.095	0.065	0.252	-0.299	0.206	0.290
	S ₀ →S ₄	0.667	-0.193	0.585	-0.039	0.596	2.548

Table S9. Calculated transition dipole moments (μ , m , and θ) and g_{abs} values of model (M)-BN-[6]H and (M)-BN-[7]H.

compd	Excited States	$ \mu $ [10 ⁻²⁰ esu cm]	$ m $ [10 ⁻²⁰ erg G ⁻¹]	θ [°]	$\cos\theta$	g_{abs}^{cal}
(M)-BN-[6]H	S ₀ →S ₁	448.8	0.310	81	0.156	0.0004
	S ₀ →S ₂	189.6	0.441	180	-1.000	-0.009
	S ₀ →S ₃	93.7	0.067	0	1.000	0.003
	S ₀ →S ₄	75.5	1.816	47	0.682	0.066
	S ₀ →S ₅	324.1	0.509	180	-1.000	-0.006
	S ₀ →S ₆	319.6	2.493	44	0.719	0.022
(M)-BN-[7]H	S ₀ →S ₁	395.8	0.818	86	0.069	0.0006
	S ₀ →S ₂	227.5	0.642	110	-0.342	-0.004
	S ₀ →S ₃	70.4	0.431	63	0.454	0.011
	S ₀ →S ₄	230.7	2.427	55	0.574	0.024

Table S10. The nonplanarity values (NP) and NICS(1)_{zz} values.



Rings	BN-[5]H		BN-[6]H		BN-[7]H		E[6]H		E[4]H	
	NP ^[a]	NICS(1) _{zz} ^[b]								
Z	0.015	-23.7	0.015	-24.2	0.012	-23.1	0.019	-22.6	0.012	-22.7
A	0.014	-28.2	0.011	-28.8	0.028	-31.8	0.028	-31.5	0.004	-27.4
B	0.031	-23.3	0.020	-23.0	0.037	-22.5	0.028	--21.6	0.006	-17.2
C	0.075	-3.9	0.118	-4.0	0.062	-20.4	0.044	-22.8	0.005	-26.9
D	0.094	-2.6	0.118	-4.0	0.080	-1.7	0.084	-2.9	0.082	-1.3
E	0.024	-23.7	0.020	-23.0	0.107	-2.8	0.072	0.3	0.082	-1.3
F	-	-	0.011	-28.8	0.025	-23.0	0.018	-25.6	0.005	-26.9
G	-	-	-	-	0.022	-28.9	0.010	-17.7	0.006	-17.2
H	-	-	-	-	-	-	0.006	-27.5	0.004	-27.4

^[a] Based on X-ray single crystal structures. The average distance of the carbon atoms in a ring from a generated best-fit plane was used to evaluate the nonplanarity of a ring. ^[b] Calculated at the GIAO-B3LYP/6-311+G(d,p) level.

Table S11. The cartesian coordinates (\AA) of some optimized structures are listed as follows:Ground state of model **(P)-BN-[5]H**

N	2.99192700	-0.71196700	-0.53395200	C	3.60042300	1.65051700	-0.65160700	
N	-0.32894500	2.67158100	0.49078100	H	4.63307700	1.42035200	-0.88343800	
C	-2.36896800	-0.38697400	-0.26946400	C	-4.68559200	-1.92789000	-0.90933900	
C	0.18033000	-2.51698600	1.10418900	H	-5.56045600	-2.52741900	-1.14726700	
C	-1.20274100	0.40939000	0.05733800	C	3.21749000	2.98561700	-0.52567400	
C	-1.40221400	1.78270700	0.33639500	C	-2.72901600	2.30949800	0.45613600	
C	1.31190600	0.98621800	-0.07930400	H	-2.88963400	3.35875000	0.66937000	
C	0.85969600	-1.49120100	0.41031300	C	1.92512900	3.35864400	-0.16289500	
C	2.64793100	0.63902500	-0.42510100	H	1.67453100	4.41125200	-0.10759600	
C	2.22643600	-1.72057400	0.07481100	C	-0.56378400	3.99667200	1.06425100	
C	0.77590600	-3.73126400	1.42167300	H	0.35825500	4.35291100	1.52455600	
C	-3.38769300	-2.45087900	-1.11140400	H	-1.31603300	3.93082300	1.85222000	
H	-3.26723000	-3.44983800	-1.52385500	H	-0.89320300	4.73127700	0.31631000	
C	-3.68831900	0.15234000	-0.13195900	B	0.26088100	-0.09202200	0.11446200	
C	0.96850600	2.35337000	0.07592500	H	3.95616900	3.76234800	-0.70949500	
C	4.25381000	-1.06472100	-1.17672300	H	-0.84882600	-2.34103800	1.40357200	
H	4.45221900	-0.36348200	-1.98948900	H	0.22152600	-4.49502300	1.96056100	
H	4.17253600	-2.06104000	-1.61436300					
H	5.10546000	-1.05006100	-0.48111100	Ground state of model (P)-BN-[6]H				
C	2.10511200	-3.95345400	1.03857400	N	2.03742100	2.25969300	0.85955400	
H	2.59469400	-4.89443400	1.27858400	N	2.03983200	-2.25768700	-0.85960600	
C	-3.82370100	1.51120500	0.26020100	C	-1.36513900	-1.78206000	0.63273400	
H	-4.82156500	1.93459100	0.35566900	C	-1.36704400	1.78067800	-0.63284600	
C	-4.82596500	-0.64062000	-0.43562300	C	-0.08725700	-1.42556200	0.05366600	
H	-5.81449500	-0.20403400	-0.30614400	C	0.71541100	-2.47368400	-0.45303000	
C	-2.26771000	-1.70287300	-0.80340300	C	2.04629600	0.00102600	-0.00007900	
H	-1.28668800	-2.12013900	-0.99394500	C	-0.08876100	1.42542000	-0.05388300	
C	2.82561300	-2.96494100	0.37861300	C	-2.15840100	0.84352200	-1.35172100	
H	3.86887600	-3.14994700	0.15020300	H	-1.78780000	-0.16588400	-1.47986900	

C	2.76338300	1.14541700	0.42937000	H	4.74080200	-2.01725100	-0.70696400	
C	0.71281400	2.47431900	0.45292100	C	-3.87351400	2.50867000	-1.77498000	
C	-1.86750600	3.11869800	-0.54486900	H	-4.83350200	2.77258300	-2.21042700	
C	-3.37117000	-1.19802900	1.90476500	C	-3.37250100	1.19480300	-1.90494200	
H	-3.94668200	-0.45495000	2.45074700	H	-3.94724700	0.45122900	-2.45105800	
C	-1.86421400	-3.12060700	0.54499700	C	2.72471800	-3.25891700	-1.67251600	
C	2.76459500	-1.14264500	-0.42940400	H	3.49877400	-2.76585500	-2.26221700	
C	2.72109200	3.26165600	1.67258300	H	2.01856100	-3.71298900	-2.36959000	
H	3.49541600	2.76941700	2.26261600	H	3.19152600	-4.05287800	-1.07304300	
H	2.01424000	3.71513400	2.36934700	B	0.52600800	0.00024400	-0.00020500	
H	3.18732900	4.05600200	1.07317700	H	5.92986000	0.00300400	0.00008700	
C	-1.05784200	4.10226900	0.08170500					
H	-1.42890400	5.12256500	0.15026800	Ground state of model (P)-BN-[7]H				
C	-1.05354200	-4.10343200	-0.08144200	N	-0.18752646	2.02388502	-0.03141374	
H	-1.42353500	-5.12413000	-0.14980500	N	-0.06336446	6.75134702	1.02000026	
C	-3.12129900	-3.45621000	1.10876800	C	-3.67326246	6.08180902	0.29862226	
H	-3.47461300	-4.48127100	1.01809200	C	-2.29573846	5.77233002	0.59936326	
C	-2.15745500	-0.84558600	1.35143900	C	-4.25749846	7.27621002	0.80005926	
H	-1.78790900	0.16424100	1.47935300	C	-4.50791046	5.23436902	-0.54367374	
C	0.19487000	3.80462600	0.54241400	C	-5.66232246	7.51868202	0.67141526	
H	0.80621600	4.60627300	0.93756600	H	-6.07146546	8.42199802	1.11842626	
C	4.16917400	1.14395900	0.42748500	C	-1.46490946	6.84174702	1.03004526	
H	4.73869200	2.02202600	0.70706600	C	-2.21904946	2.96128202	0.98609526	
C	-3.87080900	-2.51244700	1.77507700	C	-3.42633846	8.20931602	1.46472226	
H	-4.83050500	-2.77728100	2.21060600	H	-3.87639246	9.09739102	1.90238226	
C	4.84265500	0.00244800	0.00005000	C	-2.06968646	8.03329702	1.53433426	
C	-3.12496400	3.45309000	-1.10852600	C	-3.98110946	4.20843002	-1.36521174	
H	-3.47934400	4.47776500	-1.01764900	H	-2.90971246	4.05742502	-1.40078774	
C	0.19883800	-3.80455600	-0.54225900	C	-3.43363146	2.67864502	1.72123826	
H	0.81099400	-4.60565600	-0.93724800	C	-5.91175946	5.49687302	-0.63910974	
C	4.17037600	-1.13975800	-0.42742000	C	0.62218854	5.57211702	0.70745826	

C	-5.30810446	3.40013502	3.11973426	C	-5.81730146	2.08428202	3.17031226	
H	-5.82658446	4.19896402	3.64373126	H	-6.73108146	1.87200502	3.71881326	
C	-4.15411846	3.68538602	2.41964826	C	1.96194854	3.17192602	0.05914026	
H	-3.77514946	4.69846802	2.41999026	H	2.50744254	2.25936502	-0.14797974	
C	-1.46279646	1.85872402	0.53187526	C	-5.12989146	1.07300002	2.53798926	
C	0.42642754	0.92889802	-0.77649174	H	-5.48485446	0.04571702	2.58846326	
H	-0.33848246	0.39600202	-1.34390074	B	-1.63416346	4.36934602	0.67250826	
H	1.13889854	1.34290002	-1.49143174	H	3.74974954	4.33576702	0.23160426	
H	0.95262854	0.21089402	-0.13184974	H	-1.47791746	8.78344402	2.04301226	
C	-1.97179846	0.52765402	0.64737926					
H	-1.39039246	-0.31551998	0.29595926	Transition state TS_BN-[5]H				
C	-6.46984346	6.63812102	0.02029326	C	-0.96825800	-2.32929800	-0.34561900	
H	-7.54009346	6.81360802	-0.05633374	C	1.38333800	-1.76140100	-0.08878100	
C	0.56248654	3.18194302	0.18544426	C	-1.30813200	-0.96391400	-0.13291800	
C	2.02737254	5.54468602	0.61288326	C	1.23433000	-0.35994900	-0.22402700	
H	2.63611954	6.41678302	0.80804326	C	2.55531500	-2.35241600	0.48625400	
C	-0.12181346	4.37878602	0.52094026	C	3.60389800	-1.58289100	0.88853500	
C	-3.93251046	1.34064802	1.82703426	C	3.62768100	-0.19780800	0.58086400	
C	-6.18750446	3.62594002	-2.17222274	C	2.48528700	0.38636100	-0.06373300	
H	-6.82602746	2.99786702	-2.78778174	H	2.56393700	-3.41489500	0.69930900	
C	-6.72842646	4.66065602	-1.43670374	H	4.44988600	-2.02983200	1.40532400	
H	-7.79575946	4.86589602	-1.47804074	C	4.79553200	0.56396000	0.83079600	
C	-4.79547246	3.41724002	-2.15316474	C	2.70590700	1.67523100	-0.60896700	
H	-4.35459646	2.64101202	-2.77277574	C	3.86821300	2.39343100	-0.40058800	
C	2.66421154	4.35029702	0.28907026	C	4.91414200	1.85830700	0.37425400	
C	0.73404654	7.97065402	1.15986726	H	5.61728400	0.08630800	1.36005700	
H	1.20854754	8.04396102	2.14658126	H	1.98288600	2.06884400	-1.29998200	
H	1.51239654	7.98713402	0.39424026	H	3.97977400	3.37134800	-0.86191100	
H	0.11562754	8.84837502	0.99382626	H	5.81686400	2.43362800	0.55938900	
C	-3.17748446	0.28883102	1.24639926	C	-2.66988900	-0.69079800	0.18227700	
H	-3.54692746	-0.73106598	1.32831926	C	-2.29026300	1.71455400	0.17211600	

C	-0.94047500	1.59005700	-0.29948100	C	4.23467600	1.21181500	-0.53401900
C	-2.93299400	2.97326900	0.22196900	C	4.89613600	0.00000100	-0.68563900
C	-2.29845600	4.12269300	-0.21641800	C	4.23466600	-1.21184700	-0.53401900
C	-1.00780200	4.03483300	-0.73528200	C	2.84858700	-1.20850700	-0.28745600
C	-0.37712900	2.79946500	-0.76758900	C	2.09487300	-0.00000700	-0.28399700
H	-3.96095600	3.04816400	0.55247400	B	0.55085500	-0.00000200	-0.33829700
H	-2.82422300	5.07358000	-0.18190800	C	-0.07134700	-1.44735500	-0.16131200
H	0.60590400	2.78421700	-1.19759300	C	0.82844200	-2.41989700	0.32981600
H	-0.49908800	4.91548800	-1.11715500	N	2.19502100	-2.38570200	0.04183300
C	-3.64836900	-1.69977300	0.13853100	C	2.95287700	-3.63522400	0.02949500
C	-3.27587000	-3.00144800	-0.17328100	C	0.38348400	-3.47037200	1.20305600
H	-4.69432400	-1.47101000	0.29981900	C	-0.94208100	-3.66905100	1.44701000
H	-4.03710600	-3.77627600	-0.21944100	C	-1.91002100	-2.96339900	0.68006400
C	-1.94858900	-3.33826500	-0.39999100	C	-1.45685500	-1.91527500	-0.18618600
H	-1.68663900	-4.37575000	-0.55948900	C	-2.37489400	-1.50131700	-1.17802100
C	0.73769300	-4.01904900	-0.84353100	C	-3.68261400	-1.94968400	-1.21385100
H	0.62725800	-4.74991300	-0.03060900	C	-4.15706000	-2.85016600	-0.24192600
H	0.09964800	-4.32701000	-1.67562000	C	-3.26715400	-3.36480800	0.67797600
H	1.76882300	-4.02952600	-1.19496900	C	0.82846000	2.41989000	0.32981700
C	-4.26647200	0.77988700	1.32180300	C	-0.07133500	1.44735500	-0.16131000
H	-4.14255200	1.60937100	2.02055800	C	-1.45684100	1.91528400	-0.18618400
H	-5.13965600	0.98228000	0.68559500	C	-1.90999800	2.96341100	0.68006700
H	-4.45969500	-0.12107600	1.90509300	C	-3.26712800	3.36483000	0.67797800
N	0.37349600	-2.66239800	-0.44208100	C	-4.15703800	2.85019600	-0.24192400
N	-3.03311000	0.59760700	0.56271600	C	-3.68259900	1.94971000	-1.21384900
B	-0.26451200	0.16107300	-0.27530800	C	-2.37488200	1.50133300	-1.17802000
				C	-0.94205300	3.66905500	1.44701400
Transition state TS_BN-[6]H				C	0.38351000	3.47036600	1.20306000
C	2.95290300	3.63520100	0.02948700	H	2.26893800	4.48054000	0.06216000
N	2.19504000	2.38568300	0.04183400	H	3.51937100	3.70867100	-0.90369200
C	2.84859200	1.20848300	-0.28745300	H	3.65544000	3.70331100	0.87018900

H	4.80675600	2.12916500	-0.55928600	C	0.99500800	-3.56851100	0.83938100
H	4.80675200	-2.12919100	-0.55927300	C	-1.15559600	-2.68847200	1.49275400
H	2.26890500	-4.48055900	0.06213800	C	-1.05881600	-1.73689500	0.44084600
H	3.51937200	-3.70868400	-0.90366700	C	-2.35173500	-2.76916800	2.28158500
H	3.65538900	-3.70334800	0.87021800	C	-3.47563800	-2.08514000	1.92969700
H	1.12058600	-4.05460200	1.74255900	C	-3.53018100	-1.44200700	0.64988700
H	-1.26617500	-4.41725700	2.16634000	C	-2.33029600	-1.31203500	-0.11800800
H	-2.00531000	-0.89023400	-1.98604900	H	-0.15383900	-4.34528900	2.46747000
H	-4.34180400	-1.61647700	-2.01134800	H	1.77921200	-4.31017300	0.94328100
H	-5.19256300	-3.17896200	-0.25429000	H	-2.33945100	-3.40282900	3.16569800
H	-3.58133900	-4.13243700	1.38196400	H	-4.37649300	-2.13533400	2.53599600
H	-3.58130800	4.13246200	1.38196600	C	-2.46127800	-1.05363900	-1.50204700
H	-5.19253800	3.17900000	-0.25428900	C	-4.76915600	-1.09842600	0.06178700
H	-4.34179100	1.61650800	-2.01134700	C	-1.59604300	1.77344400	-1.41573000
H	-2.00530200	0.89024800	-1.98604700	C	-2.51065200	3.92121400	0.10400300
H	-1.26614200	4.41726200	2.16634600	C	-3.69517000	-0.81662500	-2.07939500
H	1.12061600	4.05458900	1.74256500	C	-4.85442600	-0.78610000	-1.28209600
H	5.96760000	0.00000200	-0.86937700	C	-2.76799500	2.42135000	-1.75516000
				C	-3.25603900	3.48427800	-0.97011100
Transition state TS_BN-[7]H				H	-1.57205400	-1.11467800	-2.12074200
C	1.18130700	-2.46150000	-0.03743800	H	-3.76985700	-0.65885000	-3.15224900
C	0.24571300	-1.39737800	-0.10739800	H	-5.82024000	-0.57132400	-1.73191000
C	1.35666400	2.32253300	0.73016600	H	-5.66921700	-1.15937200	0.66938900
C	0.43866400	1.50922700	0.01314300	H	-1.21093400	0.99212300	-2.05563000
C	0.89217300	3.45746100	1.47581600	H	-3.31642300	2.10811500	-2.63875300
C	-0.82850700	2.15077800	-0.29030000	H	-4.18887700	3.97602900	-1.23237500
C	-1.27736500	3.30607800	0.42689600	H	-2.83237500	4.77960900	0.68996900
C	-0.39989400	3.88492200	1.38066000	N	2.72900100	2.07823800	0.72453100
H	1.56898000	4.00307700	2.11909900	N	2.39212000	-2.41110400	-0.75011700
H	-0.73591900	4.73790000	1.96581700	B	0.91915600	0.03962800	-0.26569500
C	-0.08387800	-3.59269800	1.68567300	C	3.62392900	2.90277700	1.53444200

H	3.75181500	3.91246000	1.12376500	C	6.89850627	3.45707100	-0.38500000
H	3.24150000	2.98403400	2.55533200	C	2.25250627	5.62107100	-0.57900000
H	4.59587400	2.41713200	1.59220300	C	-1.01049373	2.18507100	0.60500000
C	3.02369600	-3.65366400	-1.17260100	H	-1.23849373	2.88507100	1.40500000
H	3.43382000	-3.52738000	-2.17907600	H	-0.93349373	1.19507100	1.04500000
H	3.83842000	-3.96555200	-0.50339400	H	-1.83649373	2.19007100	-0.11300000
H	2.27300400	-4.44268600	-1.21622100	C	1.21750627	-0.67992900	-1.51200000
C	2.45202100	-0.04639400	-0.36765600	H	0.75050627	-1.62992900	-1.74200000
C	3.10440900	-1.22438600	-0.82447300	C	7.02750627	4.81207100	-0.77300000
C	3.28063700	1.05743800	-0.05066000	H	8.01950627	5.23507100	-0.87500000
C	4.44779400	-1.19973700	-1.23854700	C	8.03350627	2.66807100	-0.09300000
C	4.62957800	1.09091500	-0.45020600	H	9.01650627	3.10307100	-0.22900000
C	5.17608600	-0.02403600	-1.07670500	C	5.49150627	1.60907100	0.29500000
H	4.94035500	-2.08288000	-1.62519400	H	4.51450627	1.19607100	0.49200000
H	5.23715700	1.97681000	-0.30860800	C	0.47750627	0.29607100	-0.87300000
H	6.21183300	0.00734600	-1.40551800	H	-0.55849373	0.09407100	-0.64900000
				C	-0.36749373	4.89107100	0.11700000
Ground state of model (M)-BN-[5]H				H	-1.39449373	4.65007100	0.34000000
N	0.26150627	2.54707100	0.00000000	C	7.89750627	1.38707100	0.37600000
N	3.54450627	5.95307100	-0.97400000	H	8.76950627	0.78907100	0.60500000
C	5.58950627	2.91707100	-0.23900000	C	0.00150627	6.22307100	-0.00300000
C	3.10650627	0.78207100	-1.58100000	C	5.93550627	5.60307100	-0.95700000
C	4.42750627	3.70707100	-0.55600000	H	6.08950627	6.64807100	-1.17100000
C	4.61650627	5.07507100	-0.83100000	C	1.28650627	6.60907100	-0.35000000
C	1.92050627	4.25707100	-0.43100000	H	1.52450627	7.66007100	-0.40600000
C	2.40550627	1.79507100	-0.90600000	C	3.77350627	7.29007100	-1.51000000
C	0.59150627	3.89407100	-0.10100000	H	2.85750627	7.64807100	-1.97000000
C	1.04650627	1.55007100	-0.58200000	H	4.53350627	7.25007100	-2.28500000
C	2.53950627	-0.43892900	-1.88700000	H	4.08550627	8.00307100	-0.74300000
C	6.60750627	0.86607100	0.59000000	B	2.97850627	3.19507100	-0.61500000
H	6.49250627	-0.12892900	1.00200000	H	-0.74449373	6.98907100	0.17400000

H	4.13150627	0.97407100	-1.87000000	C	2.90384939	-0.71613401	-0.53700000
H	3.10750627	-1.19592900	-2.41200000	H	2.51284939	0.28086599	-0.66800000
				C	0.58784939	3.84986599	0.29600000
Ground state of model (<i>M</i>)-BN-[6]H				H	-0.01115061	4.66086599	-0.08500000
N	-1.27615061	2.33786599	0.00000000	C	-3.39815061	1.21286599	0.40000000
N	-1.27615061	-2.20913401	1.59000000	H	-3.96715061	2.09086599	0.13700000
C	2.12684939	-1.67013401	0.16200000	C	4.66184939	-2.33013401	-0.91900000
C	2.12684939	1.79986599	1.42800000	H	5.63484939	-2.56713401	-1.32900000
C	0.84184939	-1.34613401	0.72300000	C	-4.06715061	0.06386599	0.79500000
C	0.04884939	-2.40313401	1.20500000	C	3.92284939	3.42186599	1.86800000
C	-1.28615061	0.06486599	0.79500000	H	4.29884939	4.43386599	1.77300000
C	0.84184939	1.47586599	0.86700000	C	0.58784939	-3.72013401	1.29400000
C	2.90384939	0.84486599	2.12600000	H	-0.01015061	-4.53113401	1.67500000
H	2.51284939	-0.15113401	2.25800000	C	-3.39815061	-1.08513401	1.19000000
C	-1.99715061	1.21786599	0.39800000	H	-3.96715061	-1.96213401	1.45300000
C	0.04884939	2.53186599	0.38500000	C	4.66084939	2.45986599	2.50900000
C	2.64984939	3.12086599	1.33500000	H	5.63484939	2.69686599	2.91900000
C	4.13284939	-1.03313401	-1.05900000	C	4.13284939	1.16286599	2.64900000
H	4.70084939	-0.27813401	-1.58700000	H	4.70084939	0.40686599	3.17700000
C	2.64984939	-2.99113401	0.25500000	C	-1.97015061	-3.24413401	2.34500000
C	-1.99715061	-1.08913401	1.19200000	H	-2.75815061	-2.78313401	2.93300000
C	-1.97115061	3.37286599	-0.75500000	H	-1.28015061	-3.71913401	3.03700000
H	-2.75815061	2.91186599	-1.34300000	H	-2.41315061	-4.01113401	1.70300000
H	-1.28115061	3.84786599	-1.44700000	B	0.22484939	0.06486599	0.79500000
H	-2.41415061	4.13886599	-0.11300000	H	-5.15015061	0.06386599	0.79500000
C	1.84884939	4.11986599	0.73300000				
H	2.23684939	5.12886599	0.66000000	Ground state of model (<i>M</i>)-BN-[7]H			
C	1.84884939	-3.99013401	0.85700000	N	-1.09832634	2.41108774	0.00000000
H	2.23784939	-4.99913401	0.93000000	N	-0.59932634	7.15508774	0.74800000
C	3.92284939	-3.29213401	-0.27800000	C	-4.23332634	6.69208774	0.06900000
H	4.29884939	-4.30413401	-0.18300000	C	-2.88132634	6.32908774	0.36700000

C	-4.74132634	7.93908774	0.49600000	C	-0.26032634	3.50508774	0.18000000
C	-5.12832634	5.81808774	-0.66000000	C	1.38367366	5.75708774	0.49600000
C	-6.13832634	8.21608774	0.42200000	H	2.05667366	6.58408774	0.64400000
H	-6.49432634	9.16408774	0.80800000	C	-0.84032634	4.77208774	0.41400000
C	-1.98032634	7.35808774	0.72100000	C	-5.00032634	2.20408774	1.60200000
C	-3.05532634	3.57708774	0.88500000	C	-6.93132634	4.09308774	-1.97000000
C	-3.84132634	8.87408774	1.05100000	H	-7.61932634	3.41308774	-2.45500000
H	-4.22632634	9.81808774	1.41700000	C	-7.40432634	5.20208774	-1.31100000
C	-2.50132634	8.62308774	1.11300000	H	-8.46632634	5.41508774	-1.28600000
C	-4.67232634	4.72308774	-1.42100000	C	-5.54832634	3.87108774	-2.05100000
H	-3.61132634	4.55908774	-1.52400000	H	-5.16732634	3.03408774	-2.62200000
C	-4.32632634	3.45708774	1.54700000	C	1.92167366	4.49708774	0.28400000
C	-6.52332634	6.09908774	-0.67400000	C	0.28867366	8.30708774	0.86500000
C	-0.01032634	5.91008774	0.54200000	H	0.69367366	8.40908774	1.87500000
C	-6.17532634	4.42808774	2.79600000	H	1.11267366	8.20408774	0.16500000
H	-6.61932634	5.28708774	3.28200000	H	-0.23532634	9.21508774	0.59700000
C	-4.94432634	4.54808774	2.20100000	C	-4.34532634	1.06608774	1.07400000
H	-4.42932634	5.49408774	2.24300000	H	-4.84632634	0.10708774	1.11800000
C	-2.40632634	2.39708774	0.48600000	C	-6.86332634	3.20008774	2.78300000
C	-0.55232634	1.21908774	-0.63600000	H	-7.83832634	3.11908774	3.24500000
H	-1.32132634	0.73508774	-1.23200000	C	1.13167366	3.37108774	0.11000000
H	0.24767366	1.51308774	-1.30900000	H	1.60267366	2.41008774	-0.02200000
H	-0.15732634	0.49808774	0.08600000	C	-6.27232634	2.10508774	2.20600000
C	-3.08332634	1.14508774	0.57000000	H	-6.76832634	1.14208774	2.21700000
H	-2.59532634	0.23708774	0.25500000	B	-2.33832634	4.89808774	0.53400000
C	-7.00532634	7.30708774	-0.08800000	H	2.99867366	4.38808774	0.26600000
H	-8.07032634	7.50308774	-0.10500000	H	-1.85832634	9.38008774	1.53200000

7. NMR spectra and high-resolution mass spectrometry

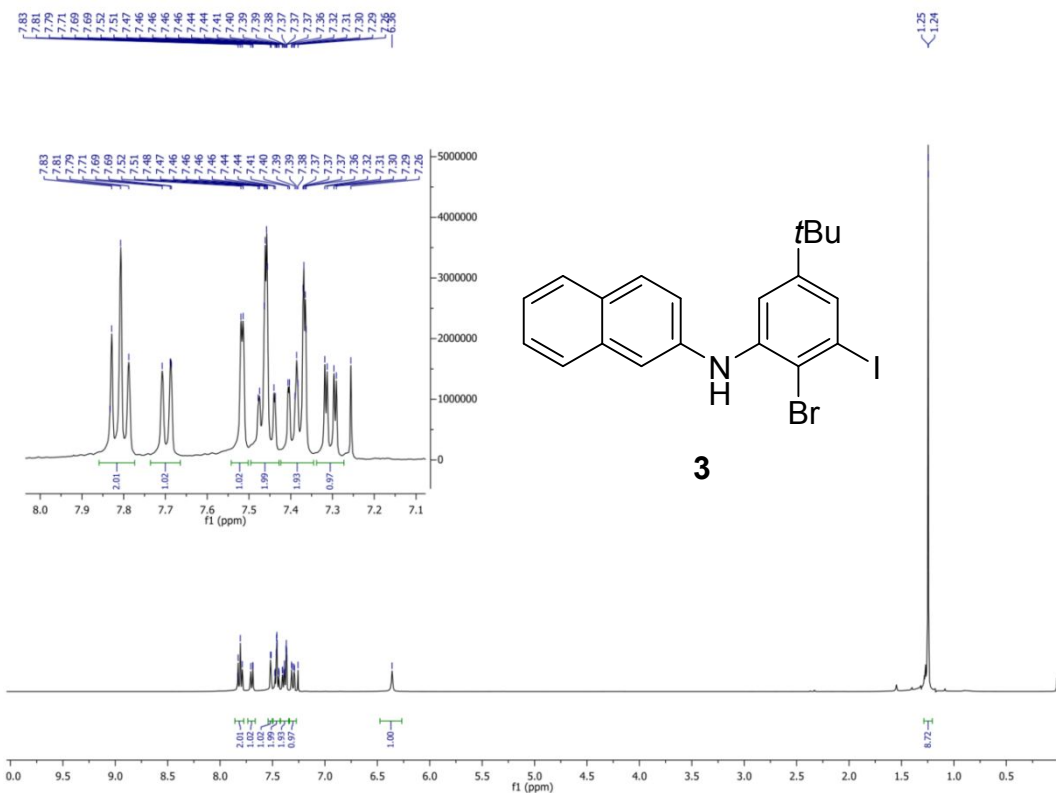


Figure S24 ^1H NMR spectrum of compound **3** in CDCl_3 (400 MHz, 298 K).

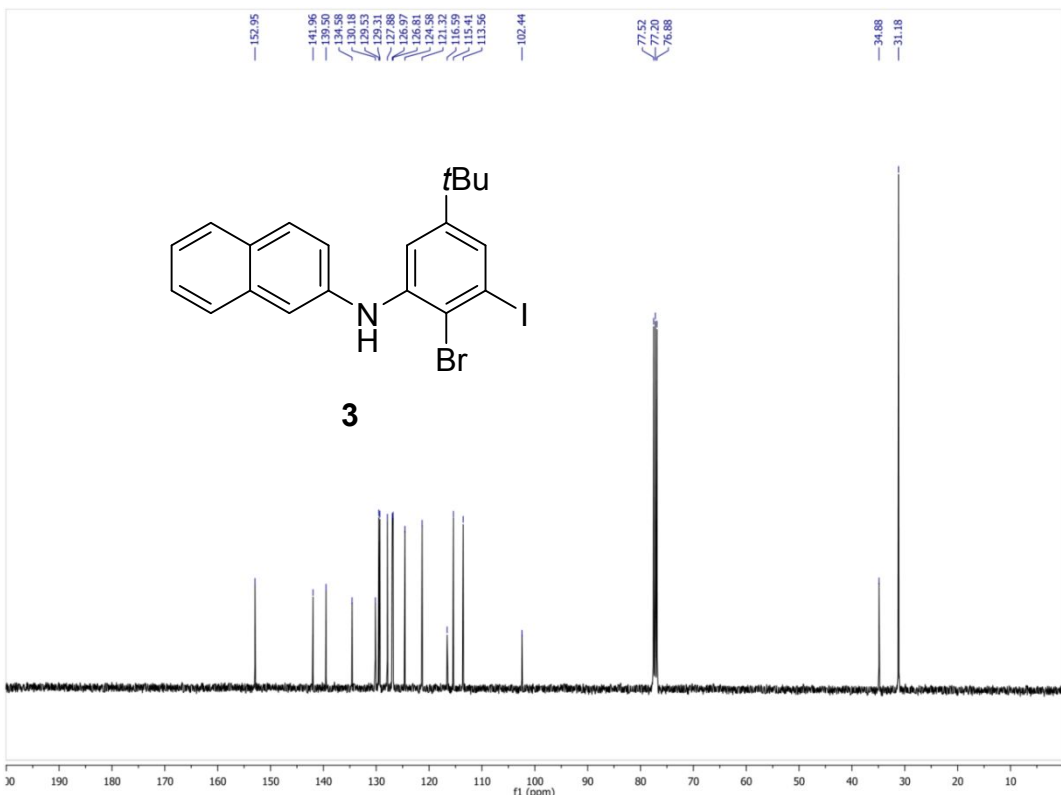


Figure S25 ^{13}C NMR spectrum of compound **3** in CDCl_3 (101 MHz, 298 K).

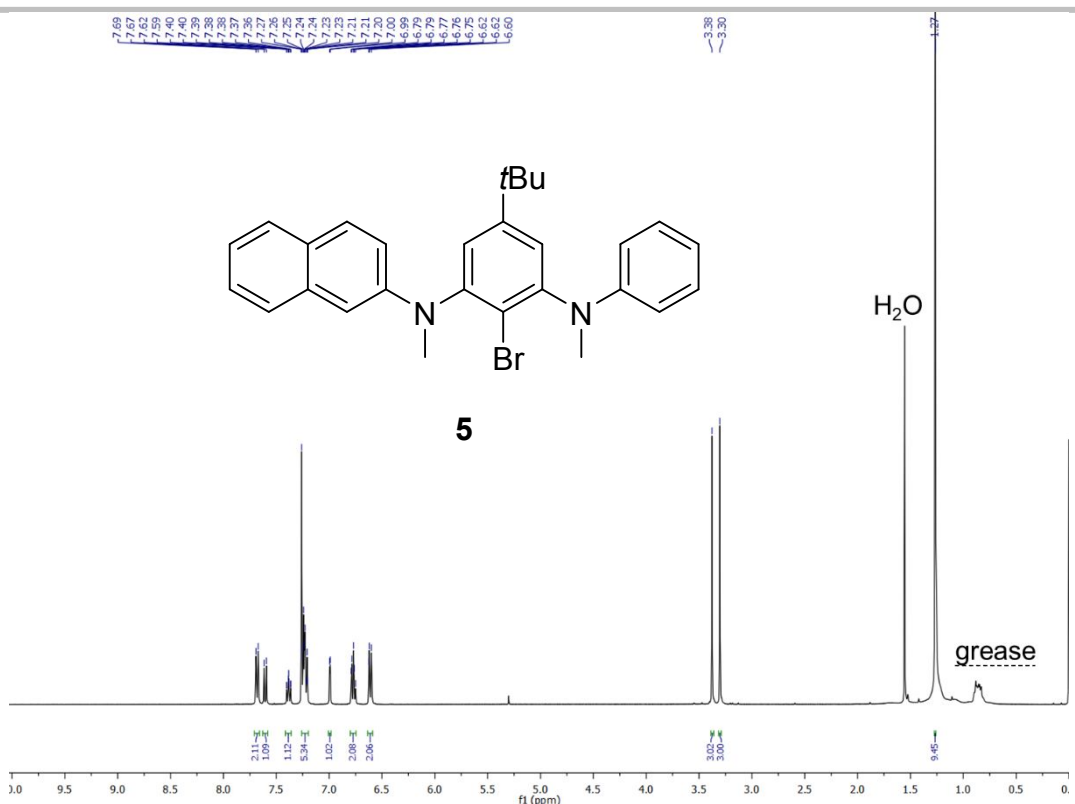


Figure S26 ^1H NMR spectrum of compound **5** in CDCl_3 (400 MHz, 298 K).

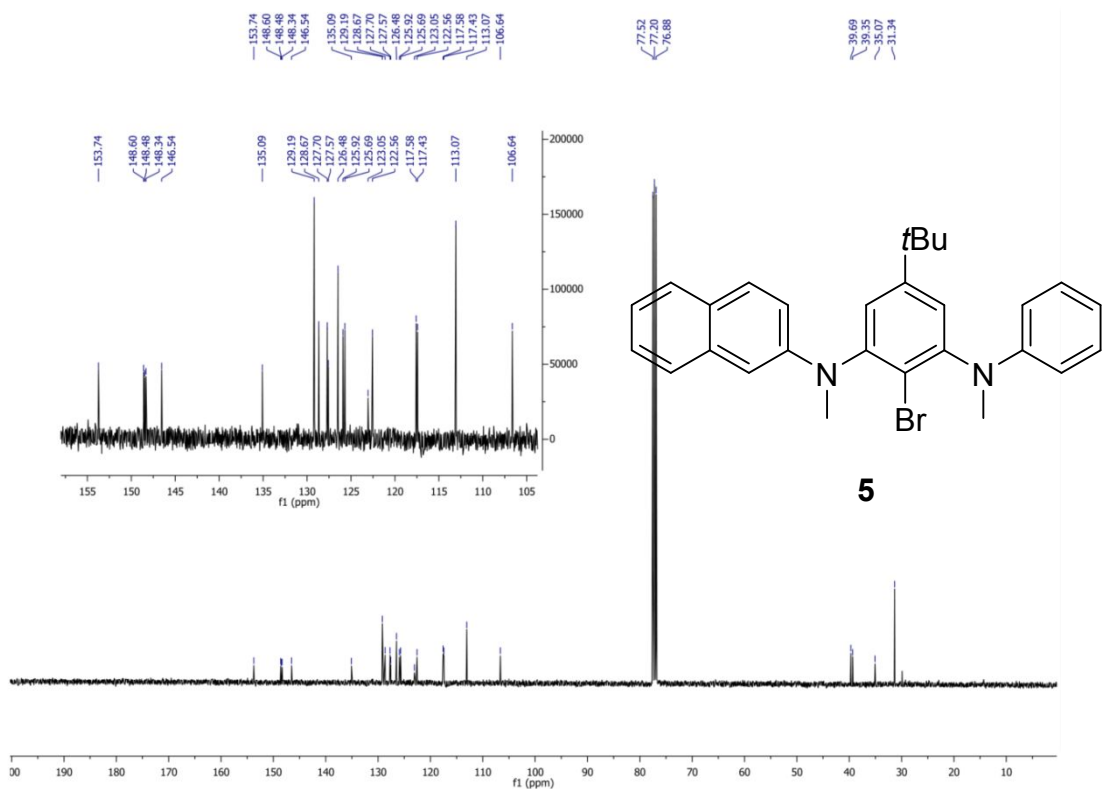


Figure S27 ^{13}C NMR spectrum of compound **5** in CDCl_3 (101 MHz, 298 K).

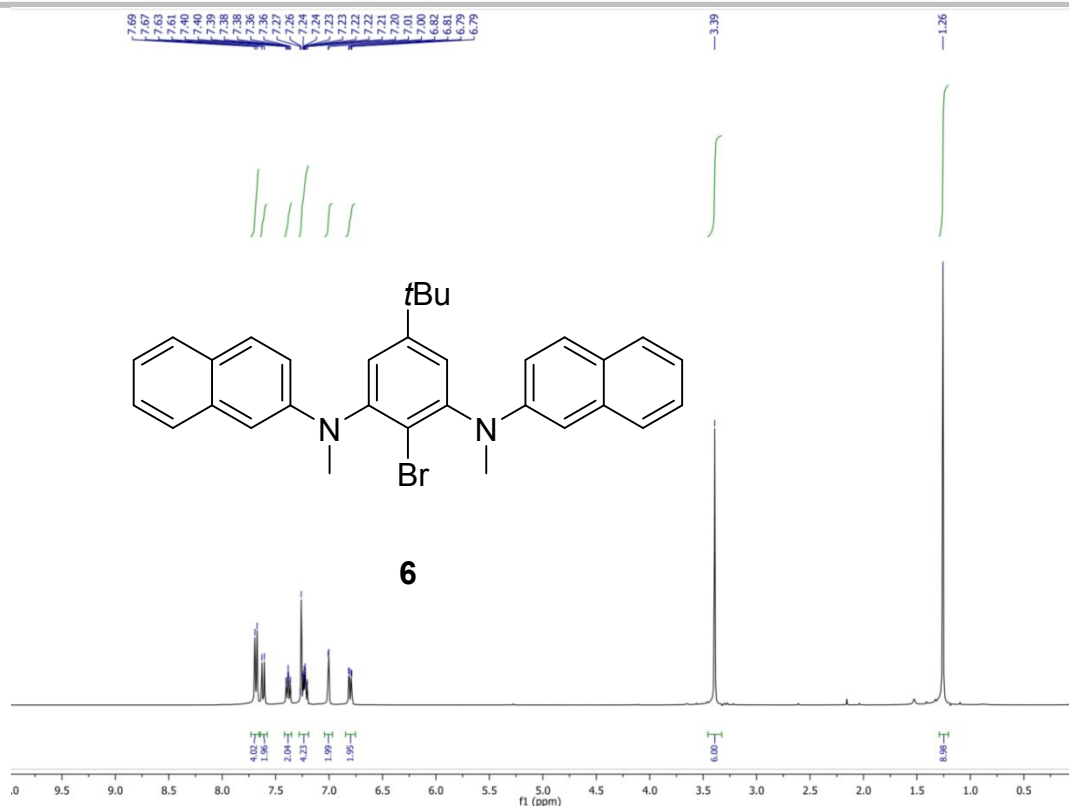


Figure S28 ^1H NMR spectrum of compound **6** in CDCl_3 (400 MHz, 298 K).

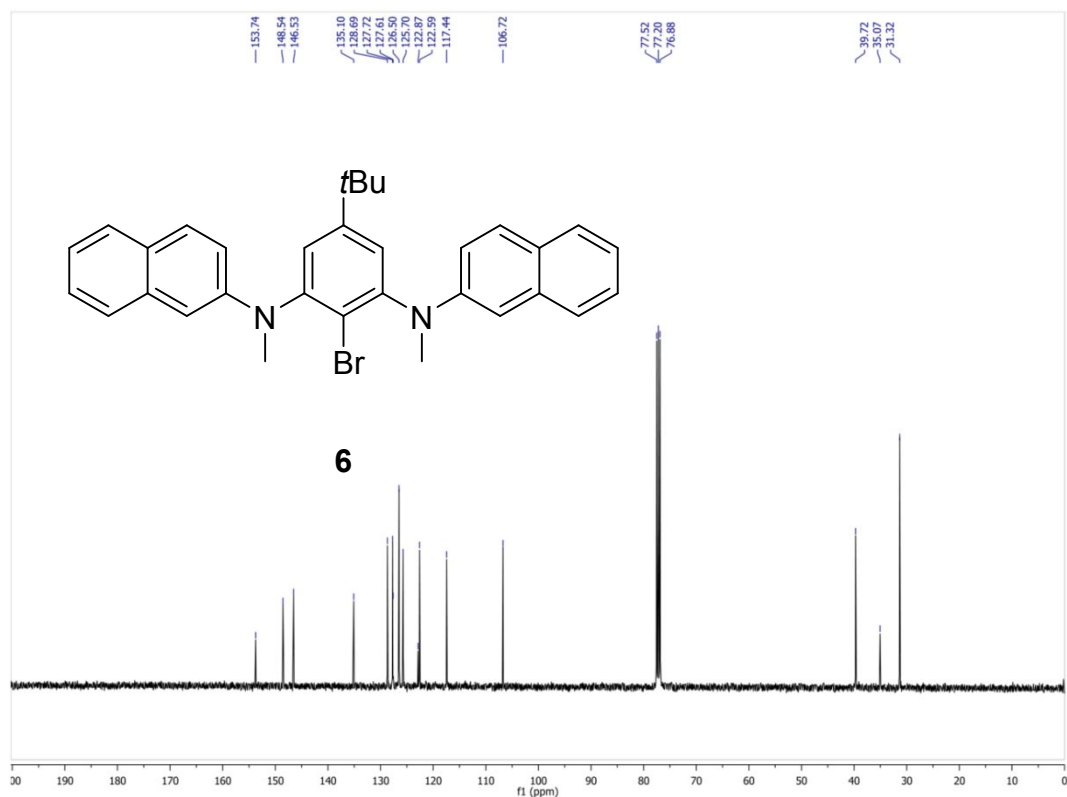


Figure S29 ^{13}C NMR spectrum of compound **6** in CDCl_3 (101 MHz, 298 K).

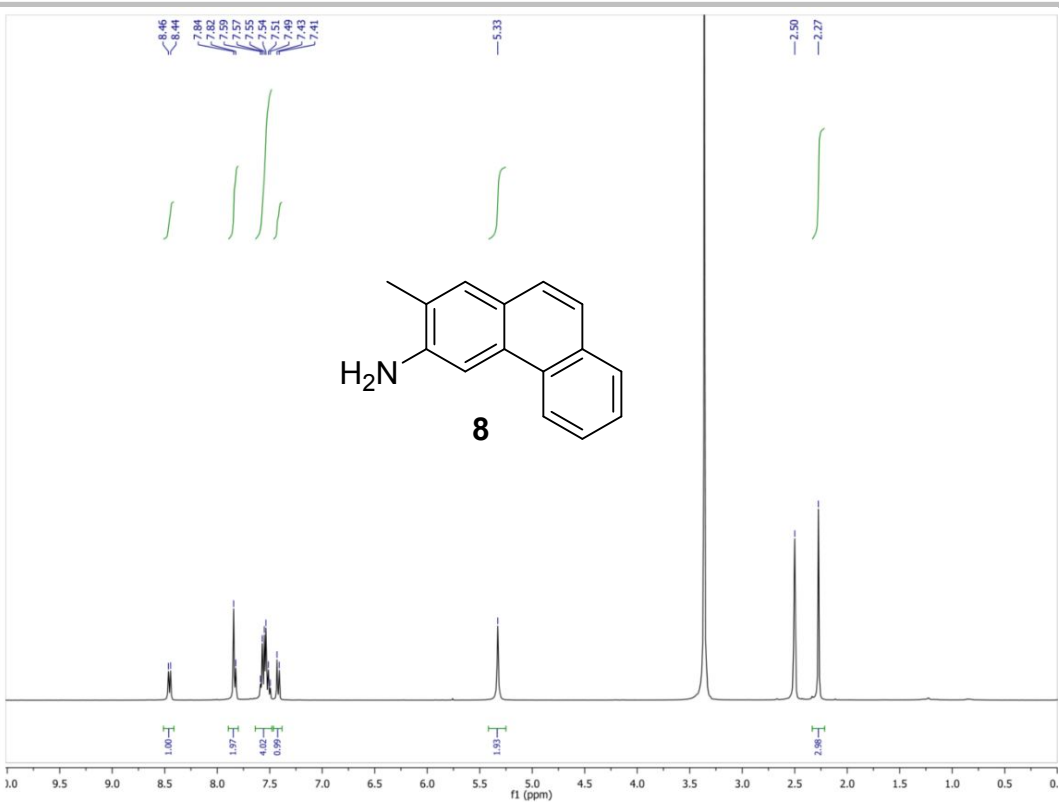


Figure S30 ^1H NMR spectrum of compound **8** in $\text{DMSO}-d_6$ (400 MHz, 298 K).

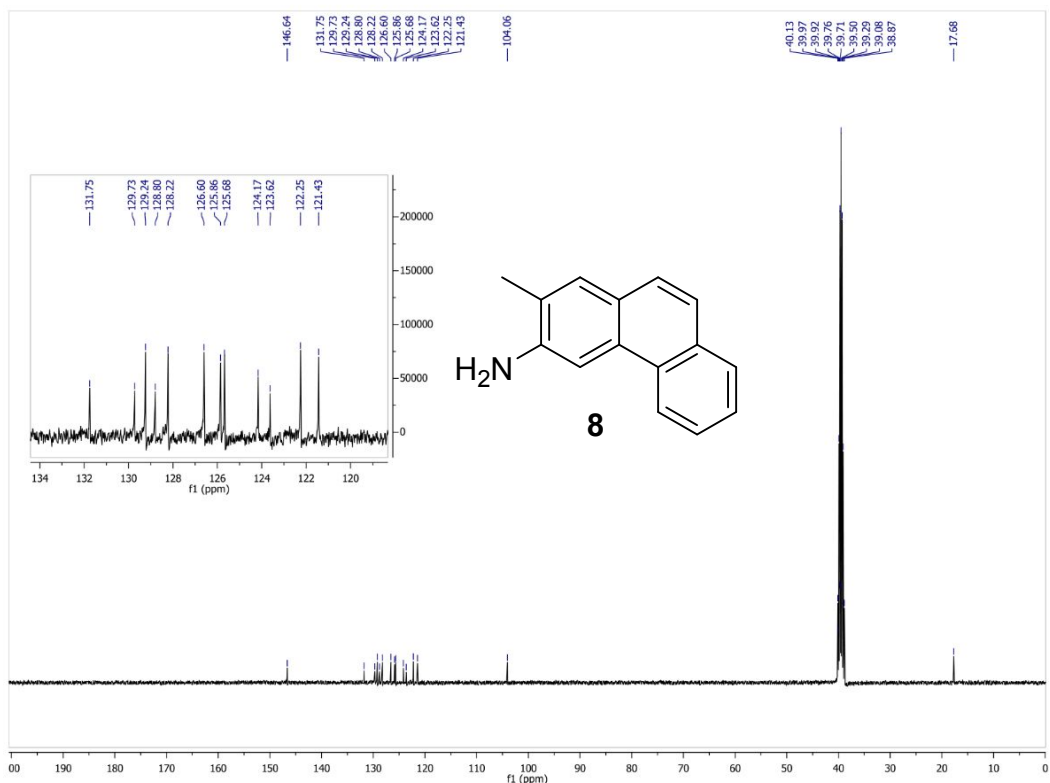
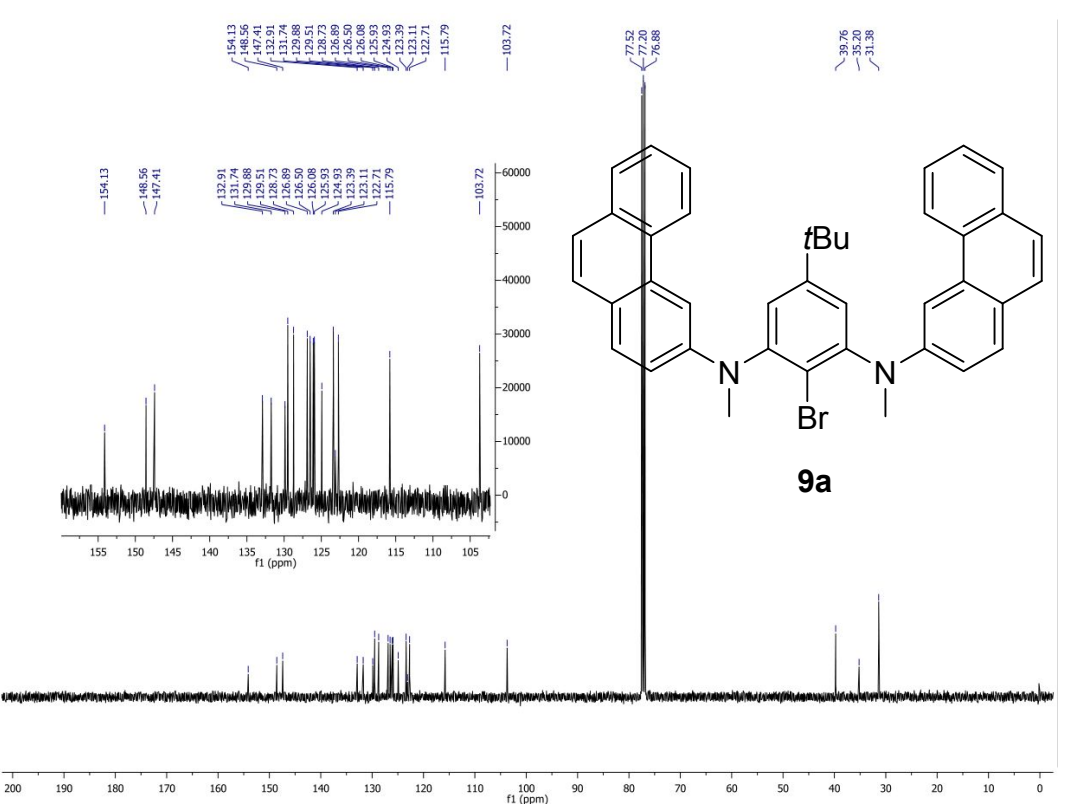
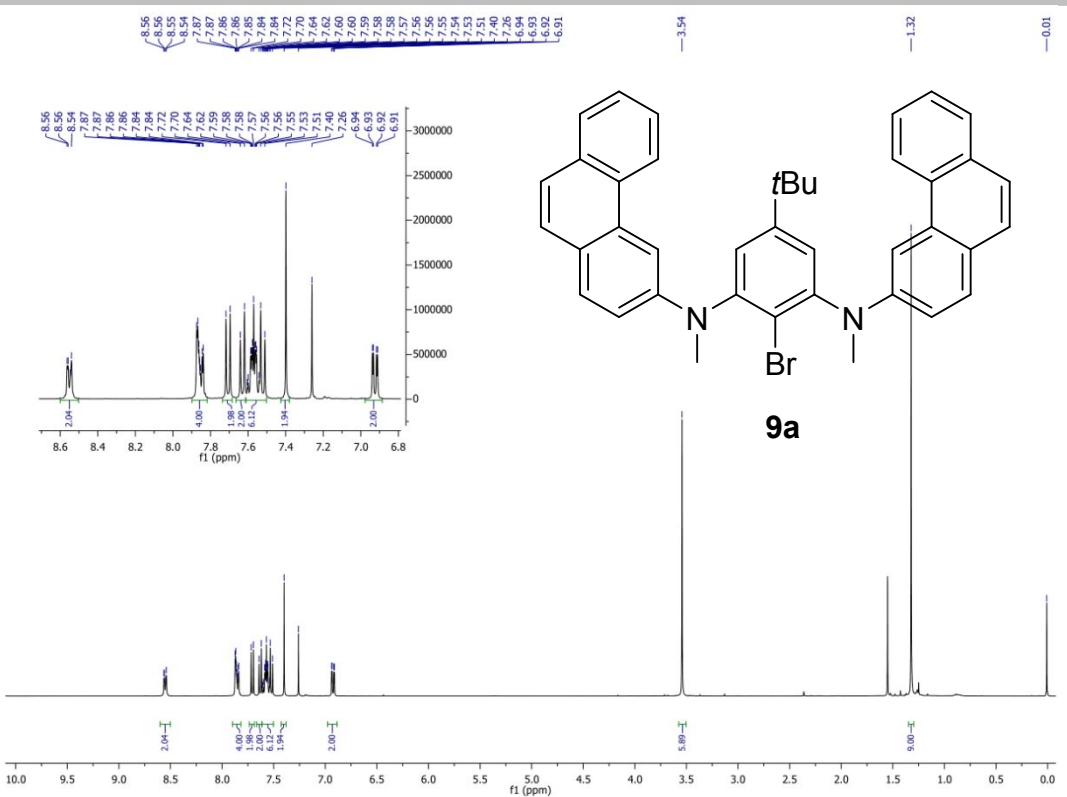


Figure S31 ^{13}C NMR spectrum of compound **8** in $\text{DMSO}-d_6$ (101 MHz, 298 K).



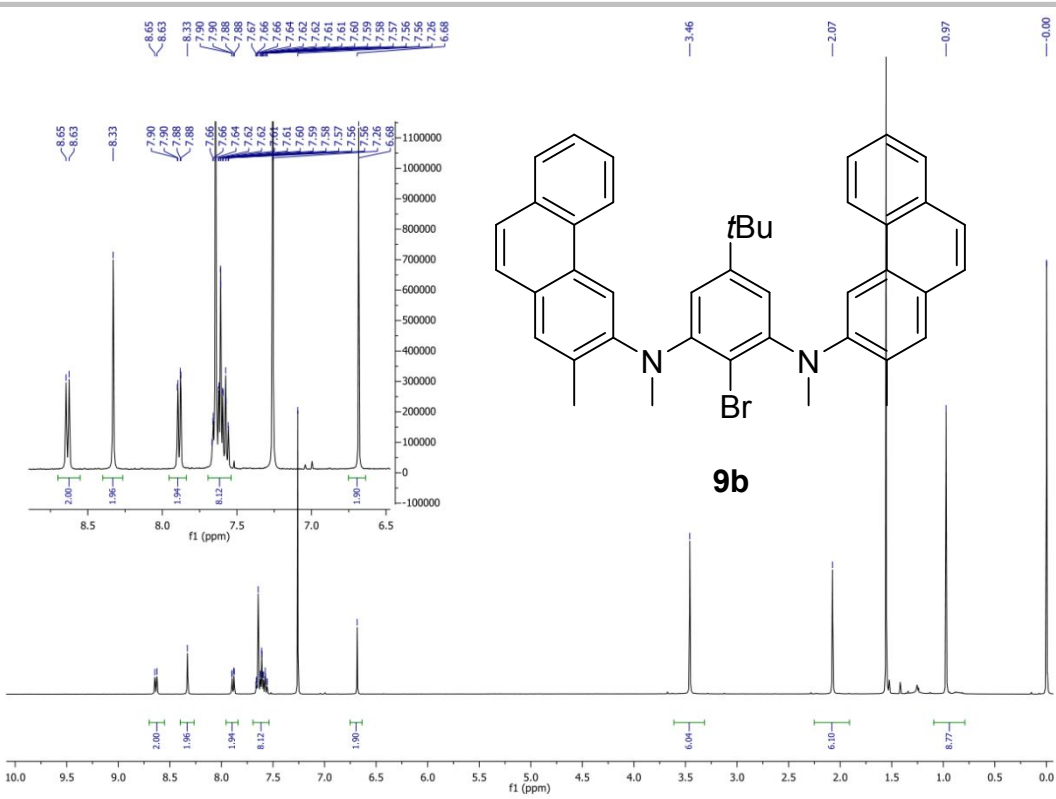


Figure S34 ^1H NMR spectrum of compound **9b** in CDCl_3 (400 MHz, 298 K).

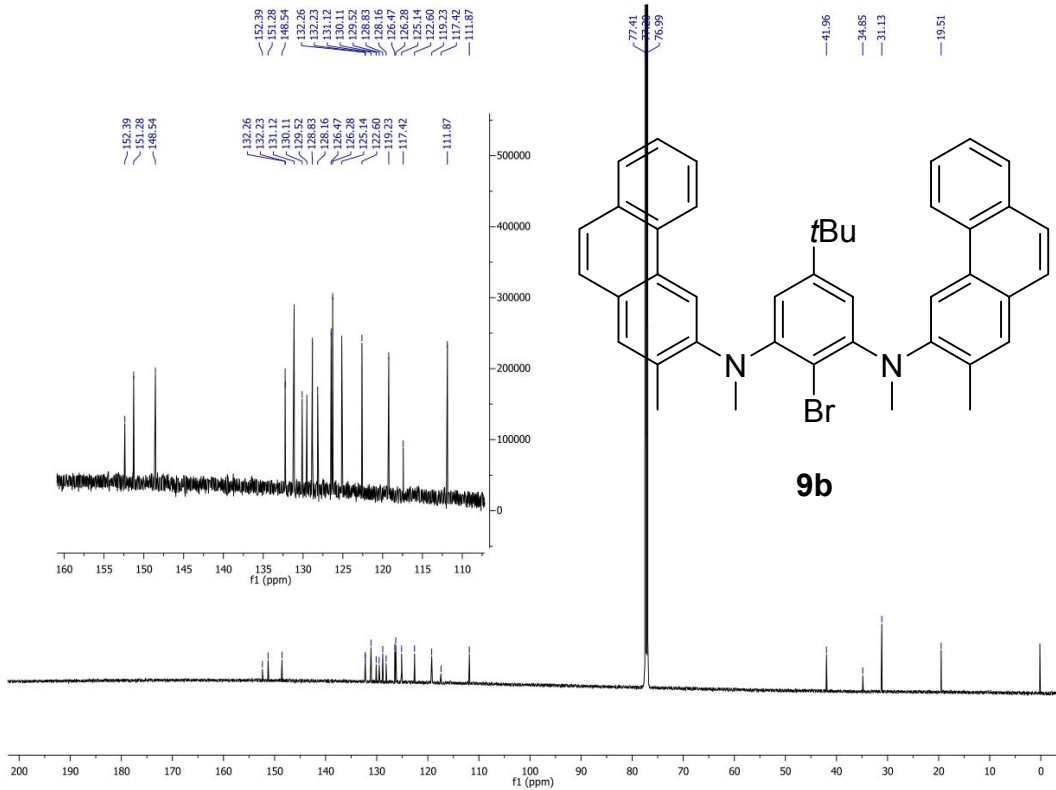


Figure S35 ^{13}C NMR spectrum of compound **9b** in CDCl_3 (151 MHz, 298 K).

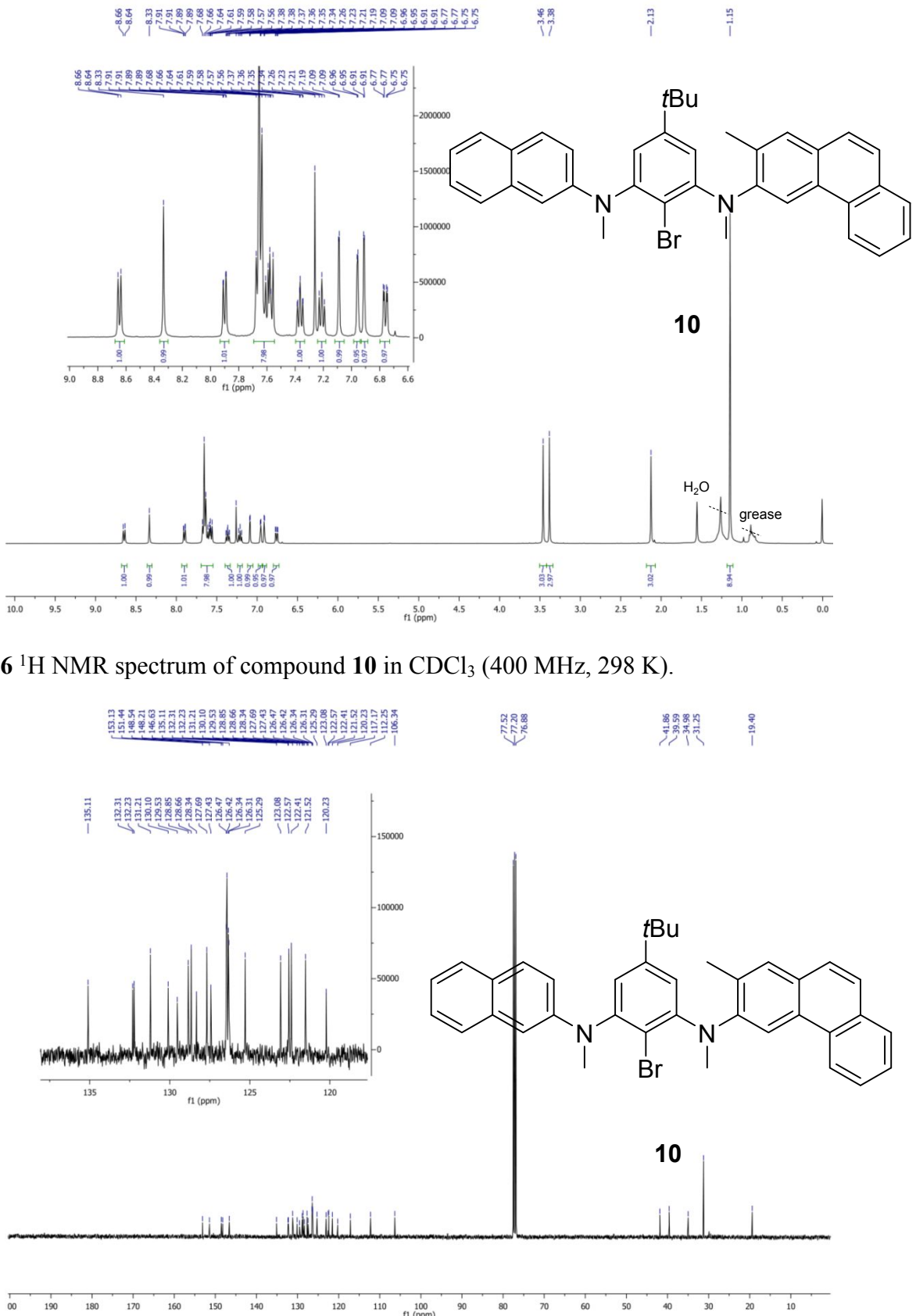


Figure S37 ^{13}C NMR spectrum of compound **10** in CDCl_3 (101 MHz, 298 K).

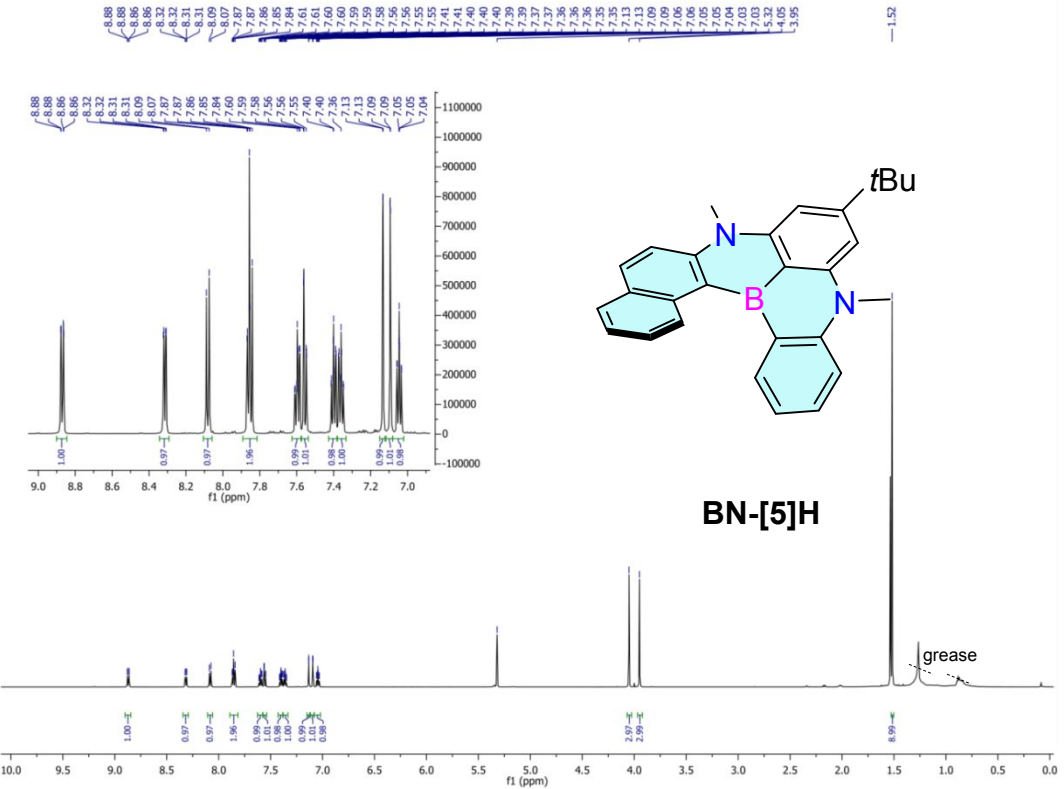


Figure S38 ^1H NMR spectrum of BN-[5]H in CD_2Cl_2 (600 MHz, 298 K).

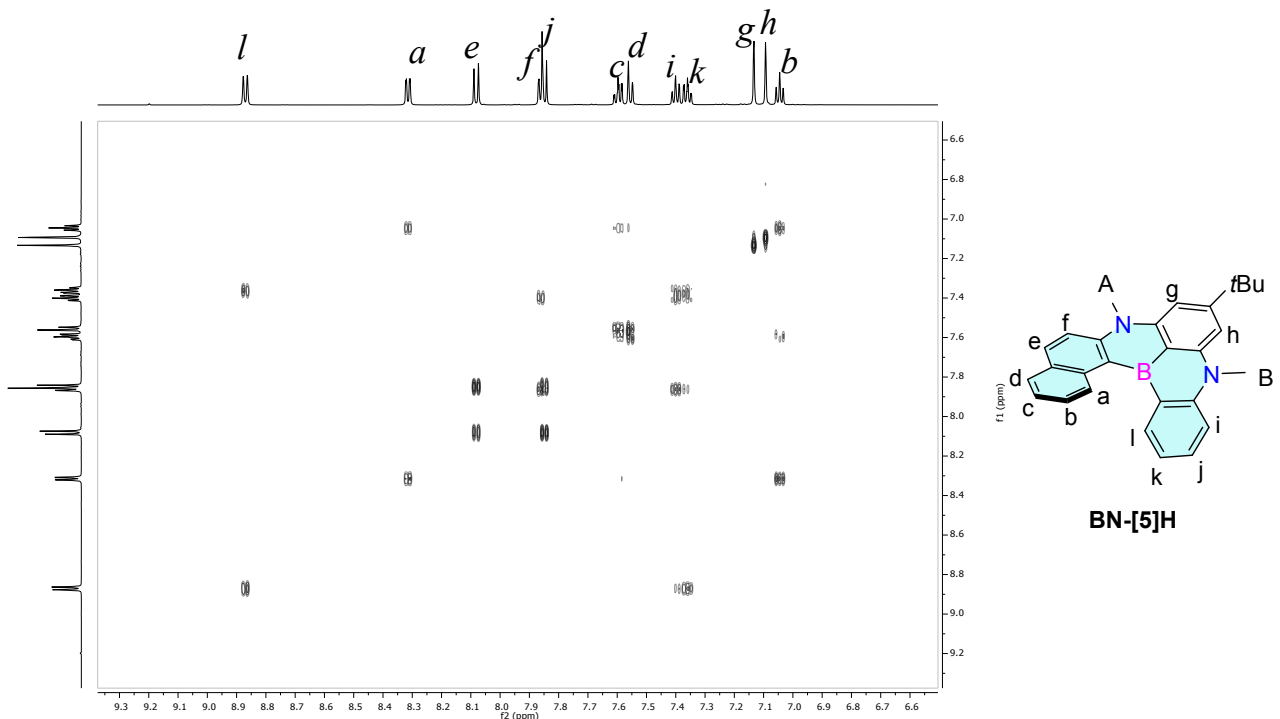


Figure S39 $^1\text{H}-^1\text{H}$ COSY spectrum of BN-[5]H in CD_2Cl_2 (298 K).

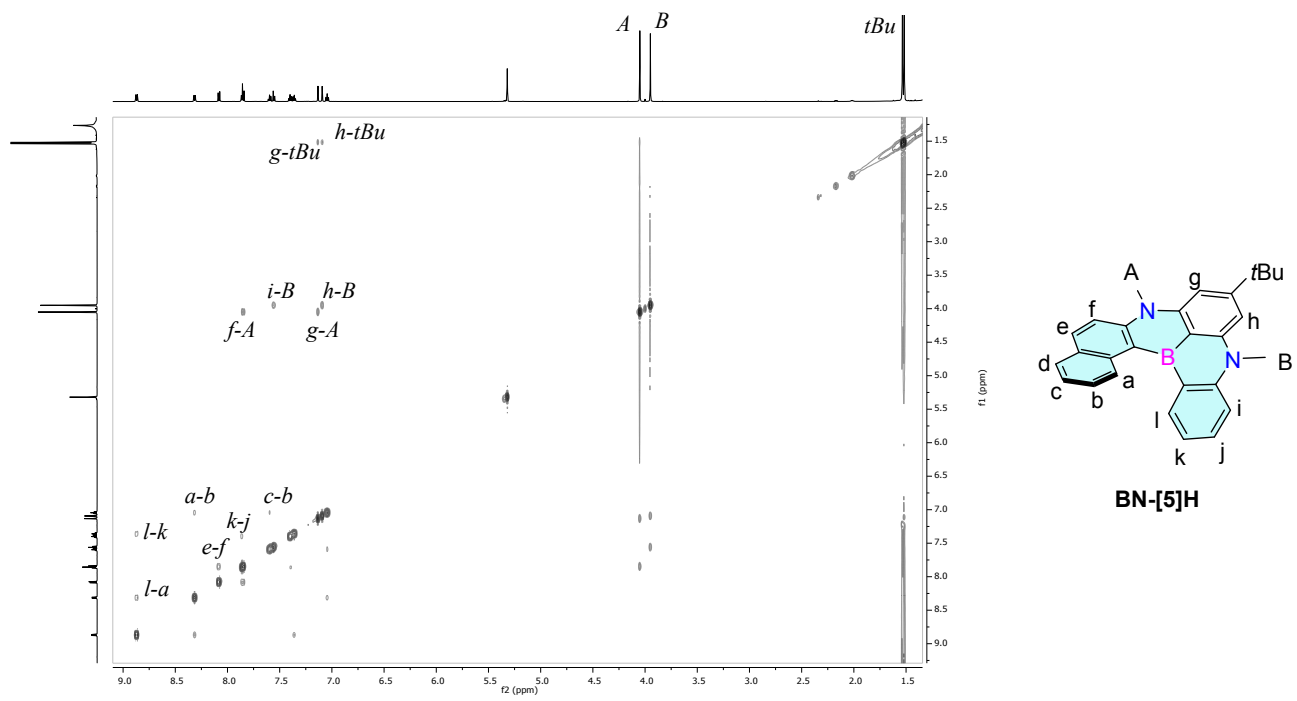


Figure S40 2D-Noesy spectrum of BN-[5]H in CD_2Cl_2 (298 K).

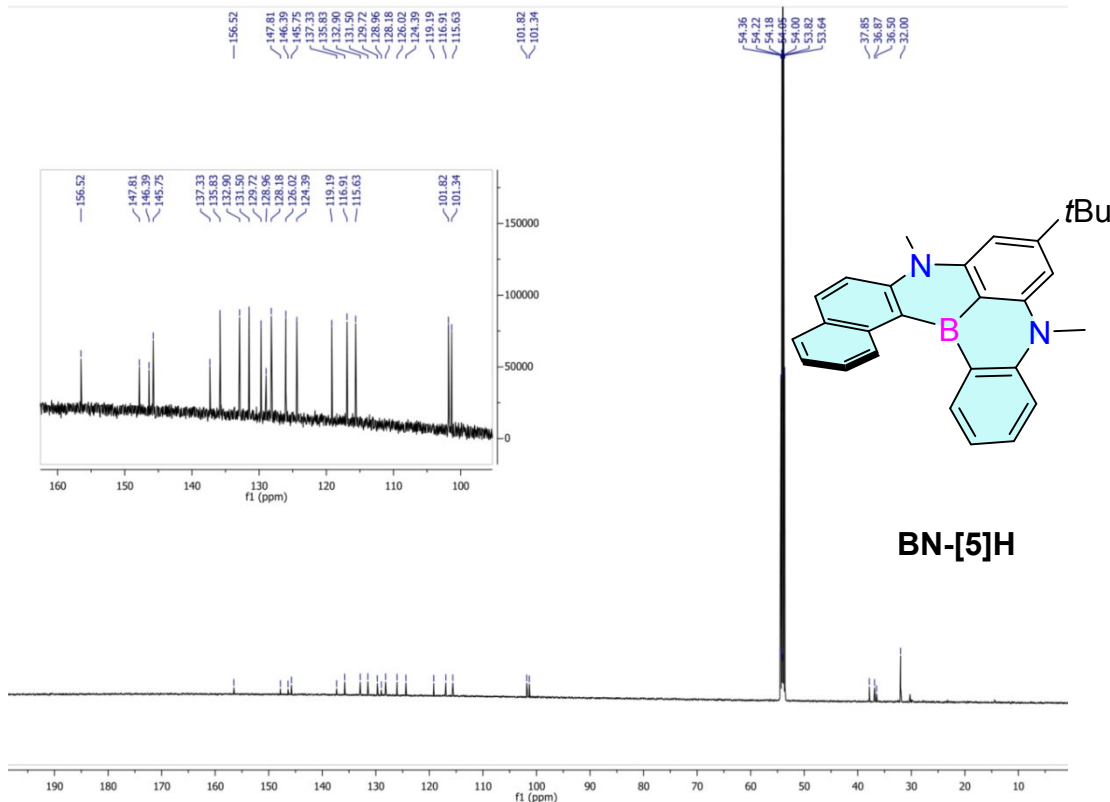


Figure S41 ^{13}C NMR spectrum of BN-[5]H in CD_2Cl_2 (151 MHz, 298 K).

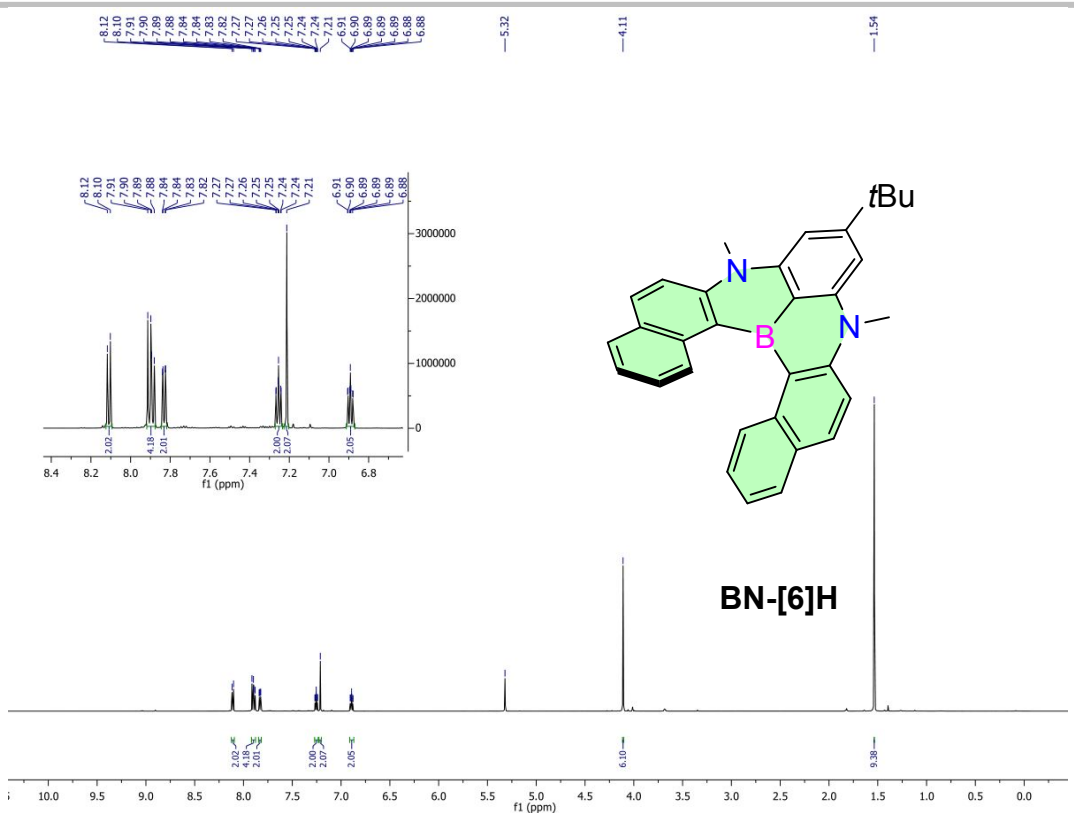


Figure S42 ^1H NMR spectrum of BN-[6]H in CD_2Cl_2 (600 MHz, 298 K).

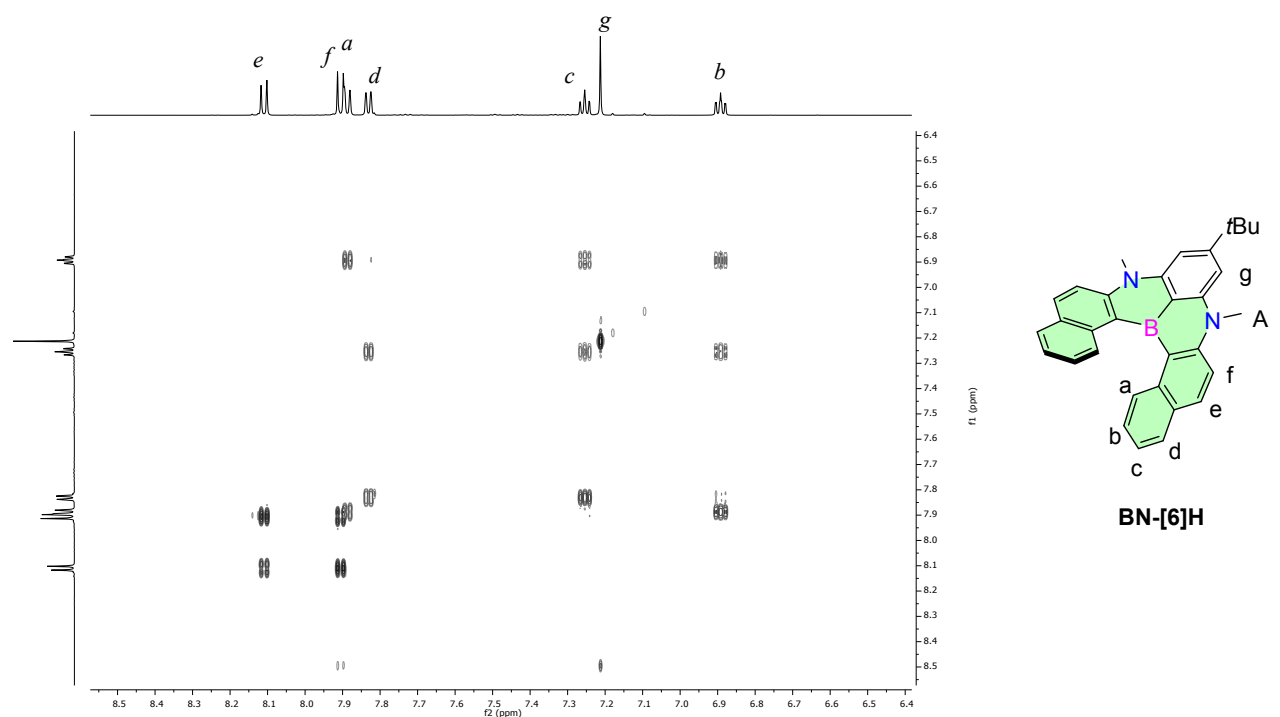


Figure S43 $^1\text{H}-^1\text{H}$ COSY spectrum of BN-[6]H in CD_2Cl_2 (298 K).

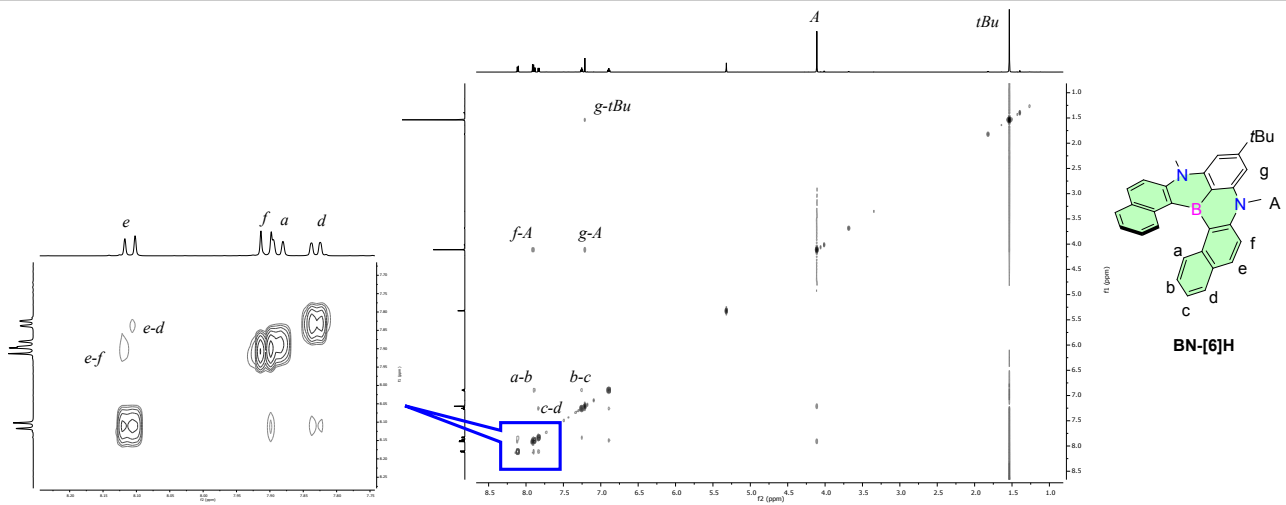


Figure S44 2D-Noesy spectrum of BN-[6]H in CD_2Cl_2 (298 K).

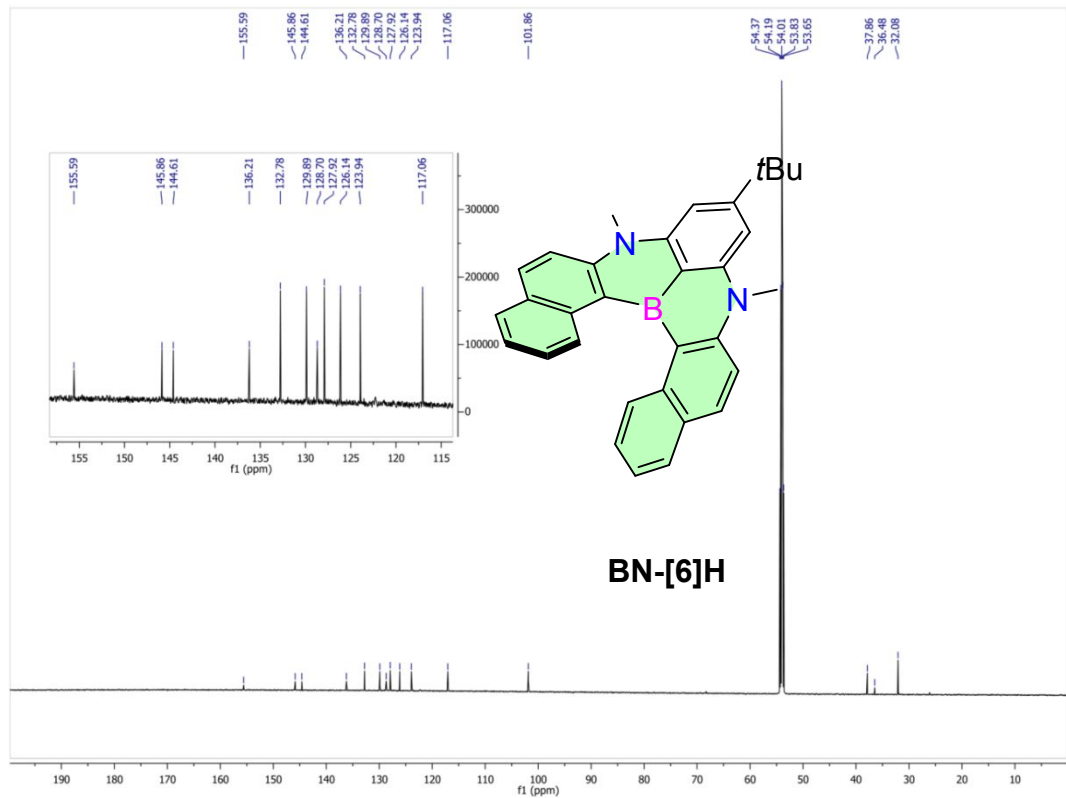


Figure S45 ^{13}C NMR spectrum of BN-[6]H in CD_2Cl_2 (151 MHz, 298 K).

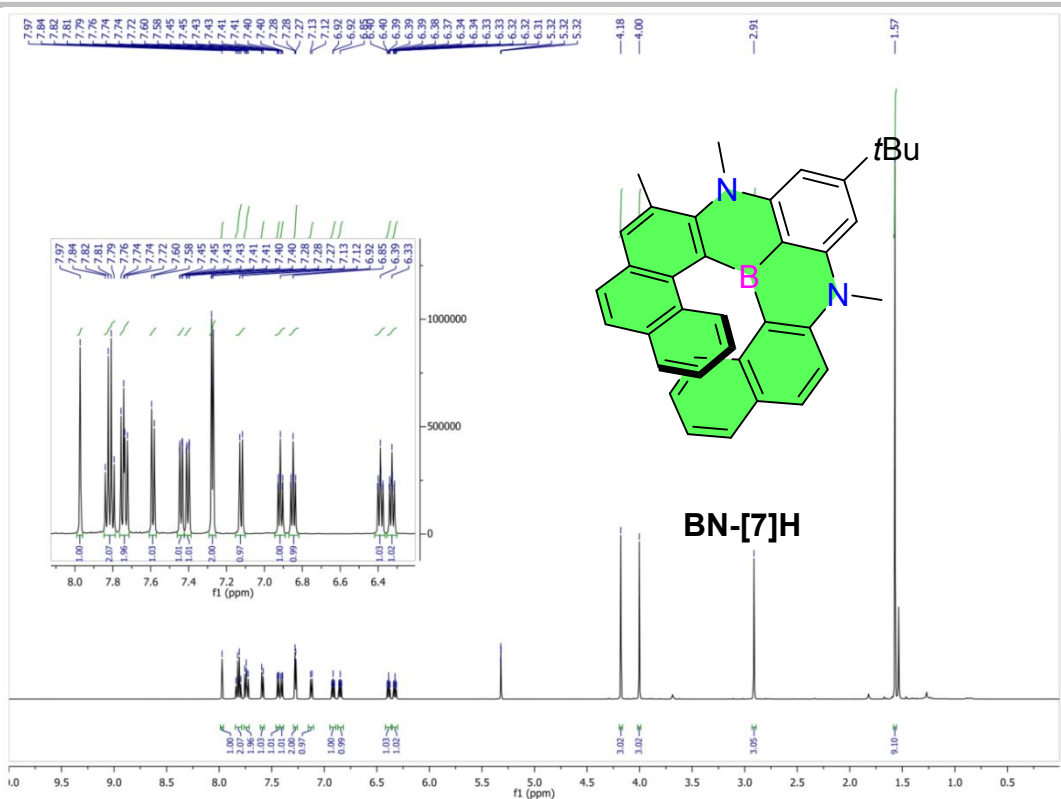


Figure S46 ^1H NMR spectrum of BN-[7]H in CD_2Cl_2 (600 MHz, 298 K).

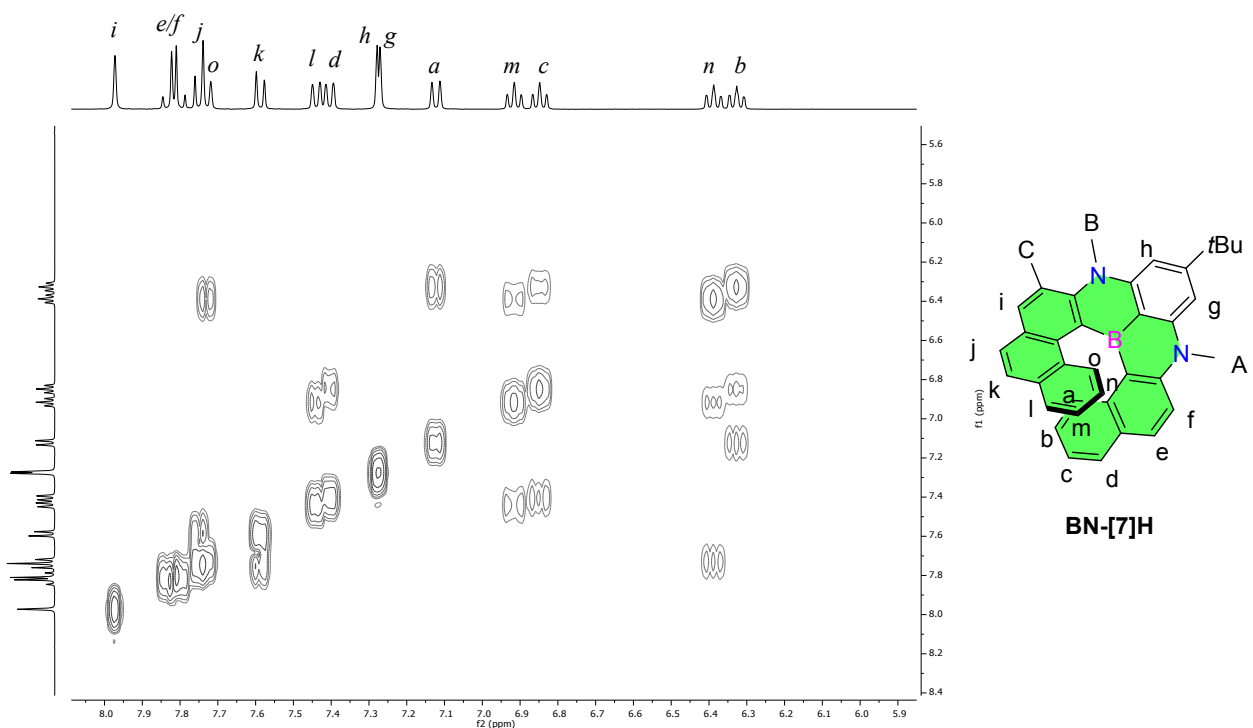


Figure S47 $^1\text{H}-^1\text{H}$ COSY spectrum of BN-[7]H in CD_2Cl_2 (298 K).

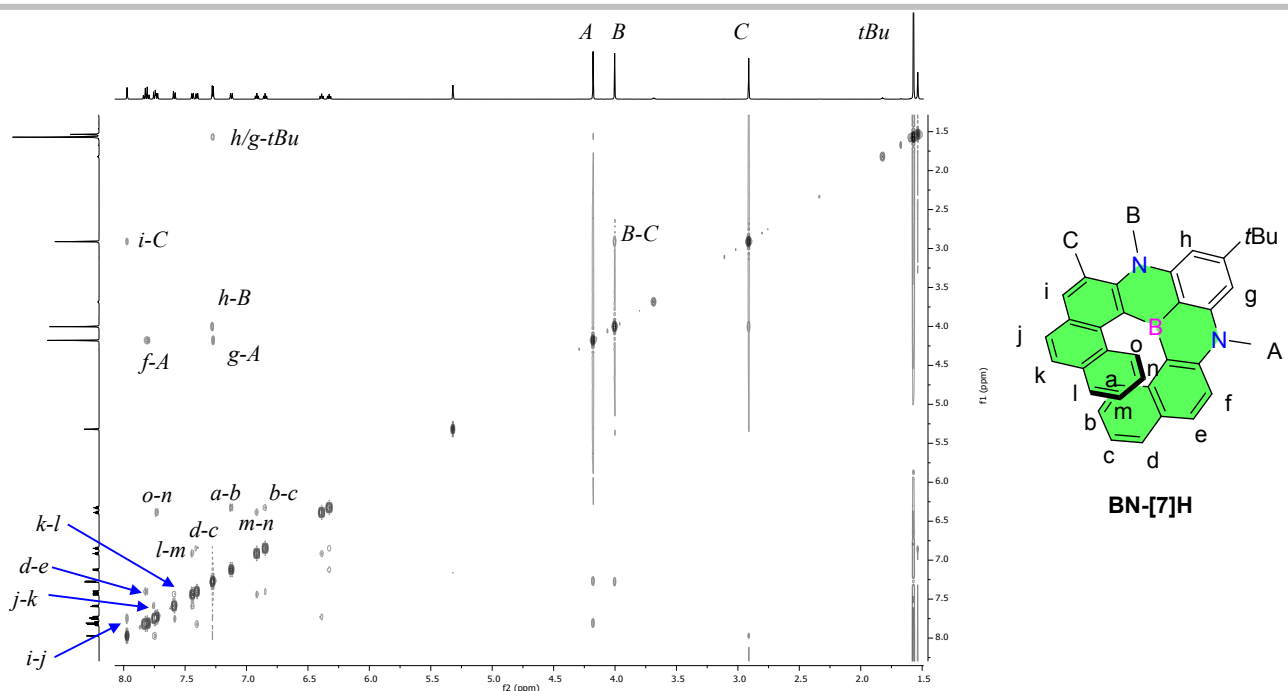


Figure S48 2D-NOESY spectrum of BN-[7]H in CD_2Cl_2 (298 K).

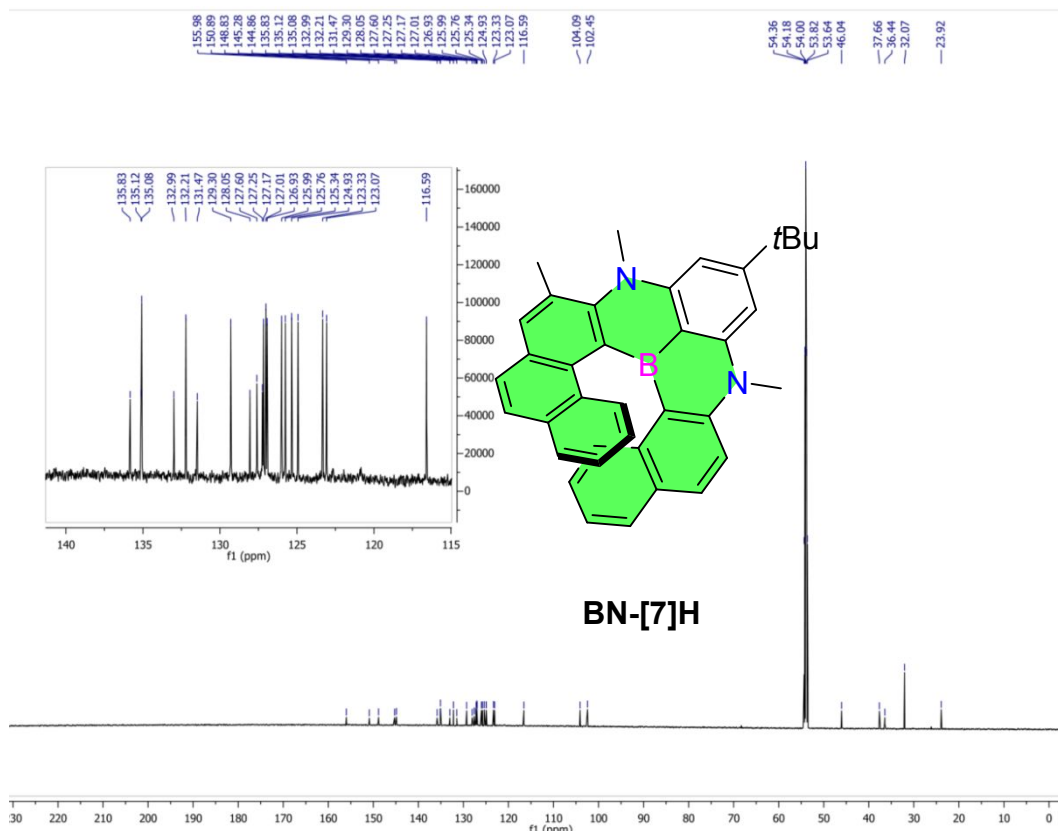


Figure S49 ^{13}C NMR spectrum of BN-[7]H in CD_2Cl_2 (151 MHz, 298 K).

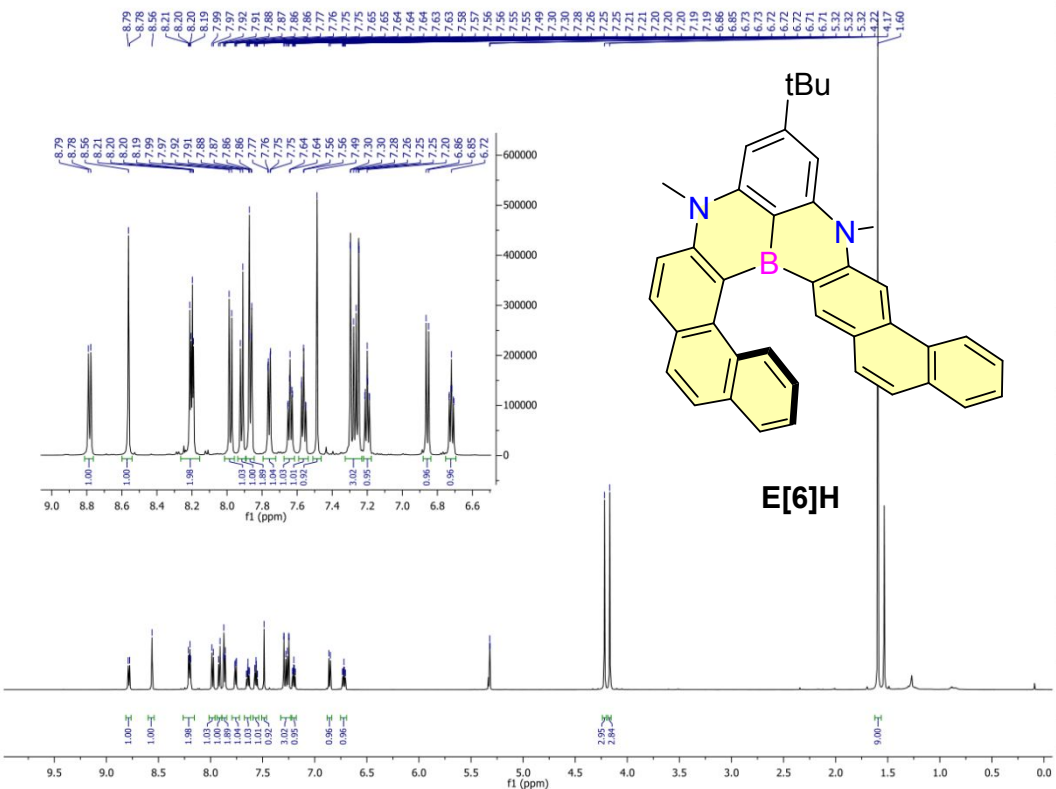


Figure S50 ^1H NMR spectrum of **E[6]H** in CD_2Cl_2 (600 MHz, 298 K).

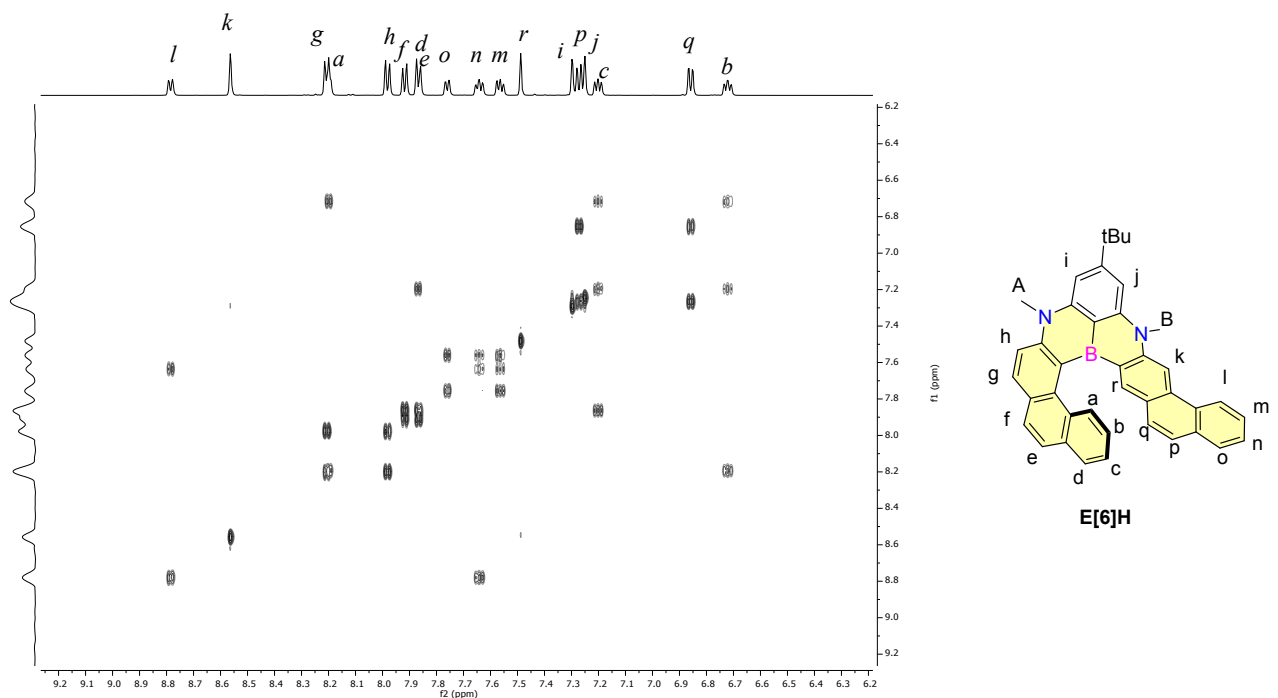


Figure S51 $^1\text{H}-^1\text{H}$ COSY spectrum of **E[6]H** in CD_2Cl_2 (298 K).

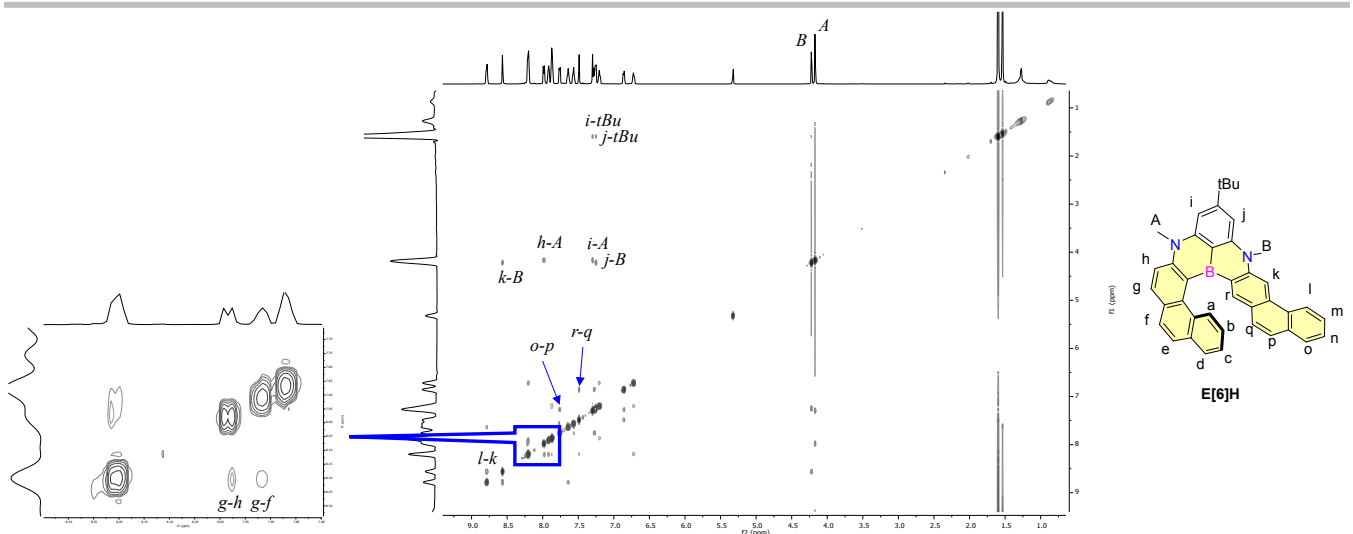


Figure S52 2D-NOESY spectrum of E[6]H in CD_2Cl_2 (298 K).

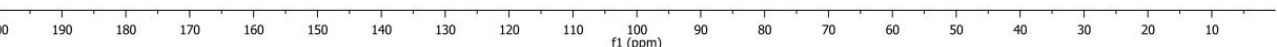
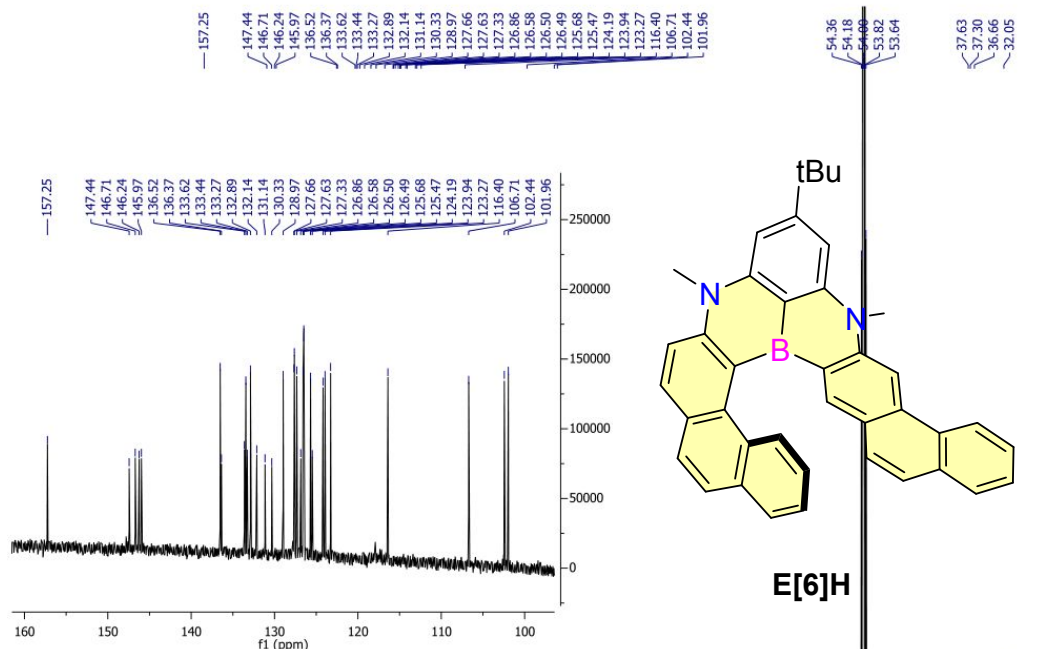


Figure S53 ^{13}C NMR spectrum of E[6]H in CD_2Cl_2 (151 MHz, 298 K).

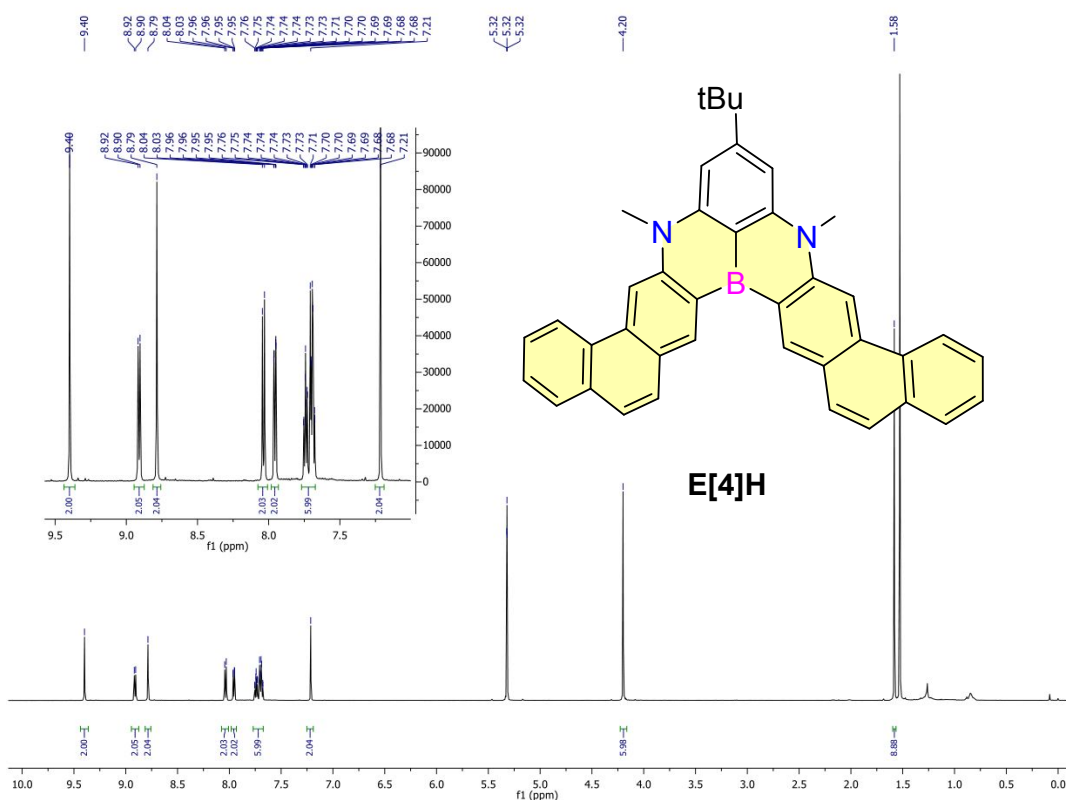


Figure S54 ^1H NMR spectrum of E[4]H in CD_2Cl_2 (600 MHz, 298 K).

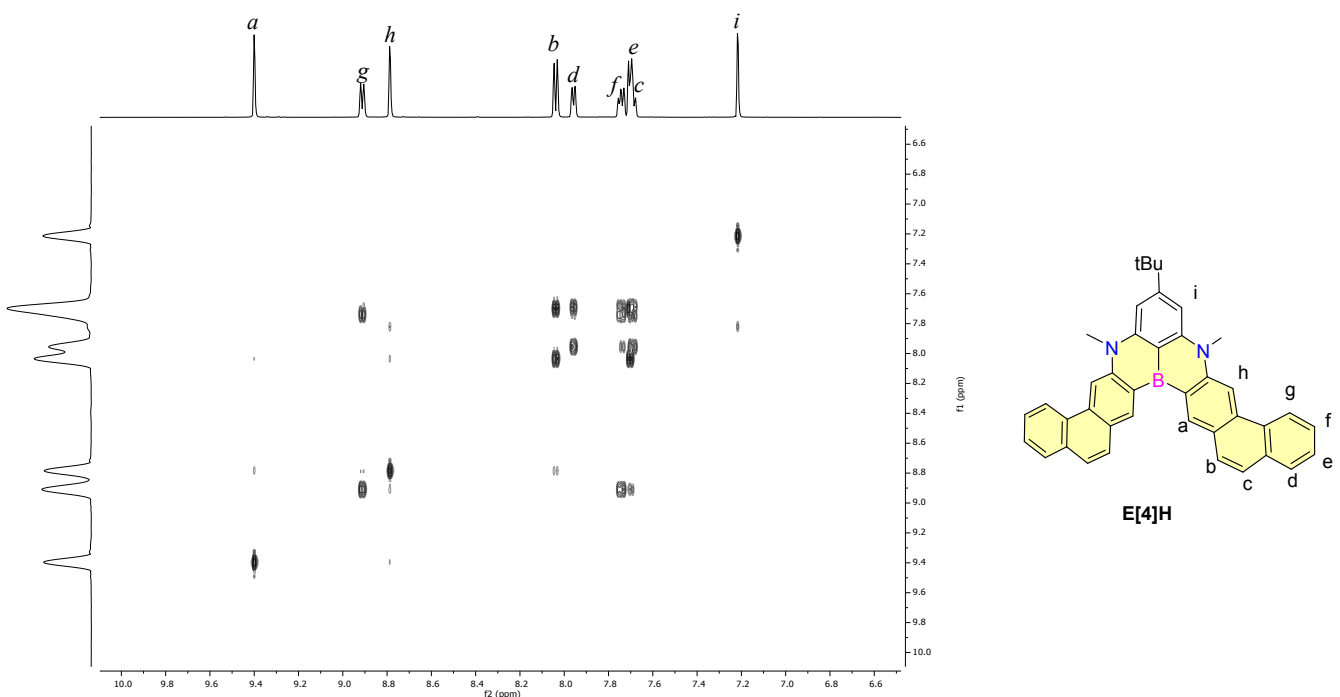


Figure S55 ^1H - ^1H COSY spectrum of E[4]H in CD_2Cl_2 (298 K).

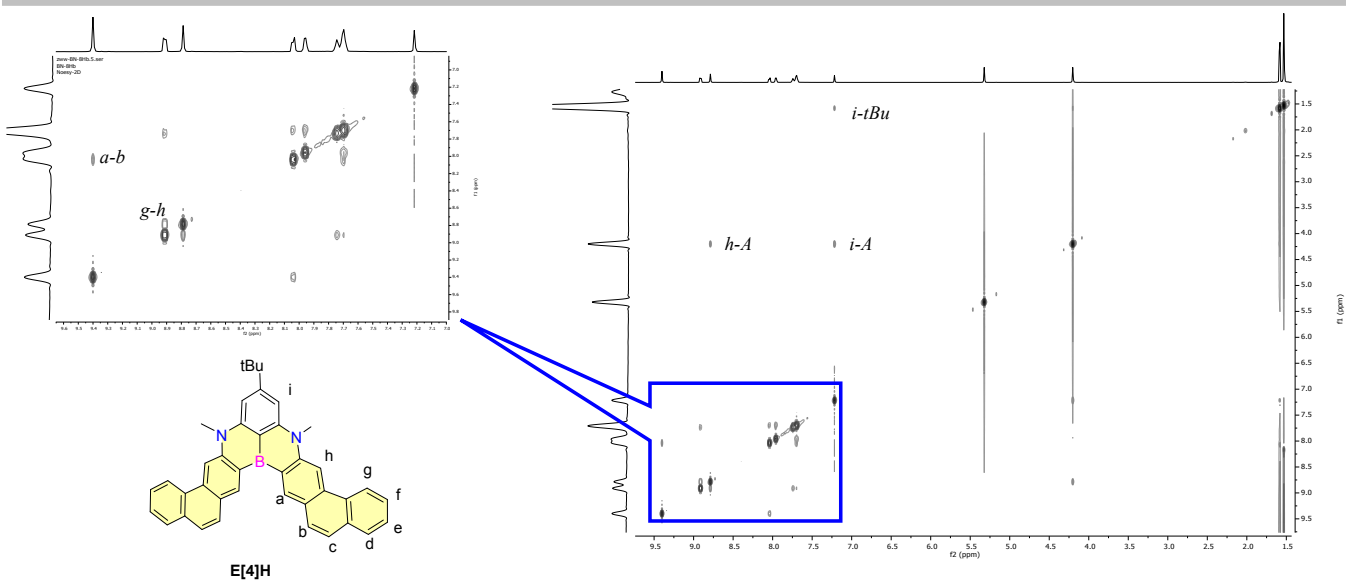


Figure S56 2D-Noesy spectrum of E[4]H in CD₂Cl₂ (298 K).

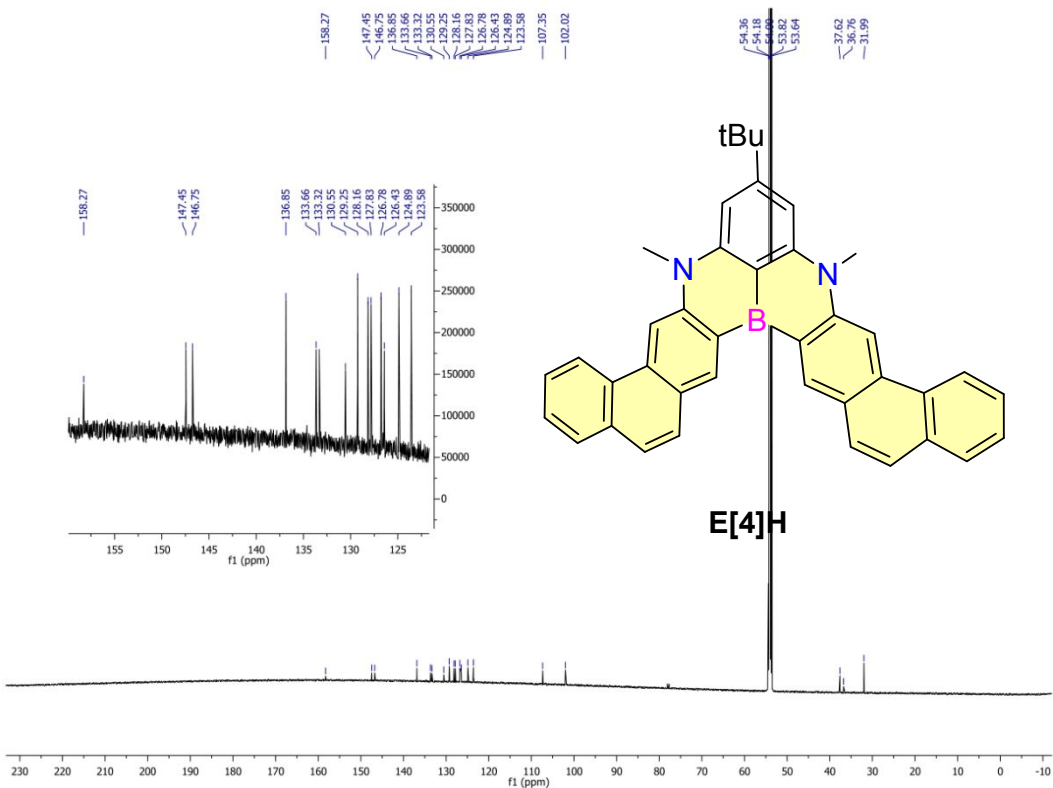


Figure S57 ^{13}C NMR spectrum of E[4]H in CD_2Cl_2 (151 MHz, 298 K).

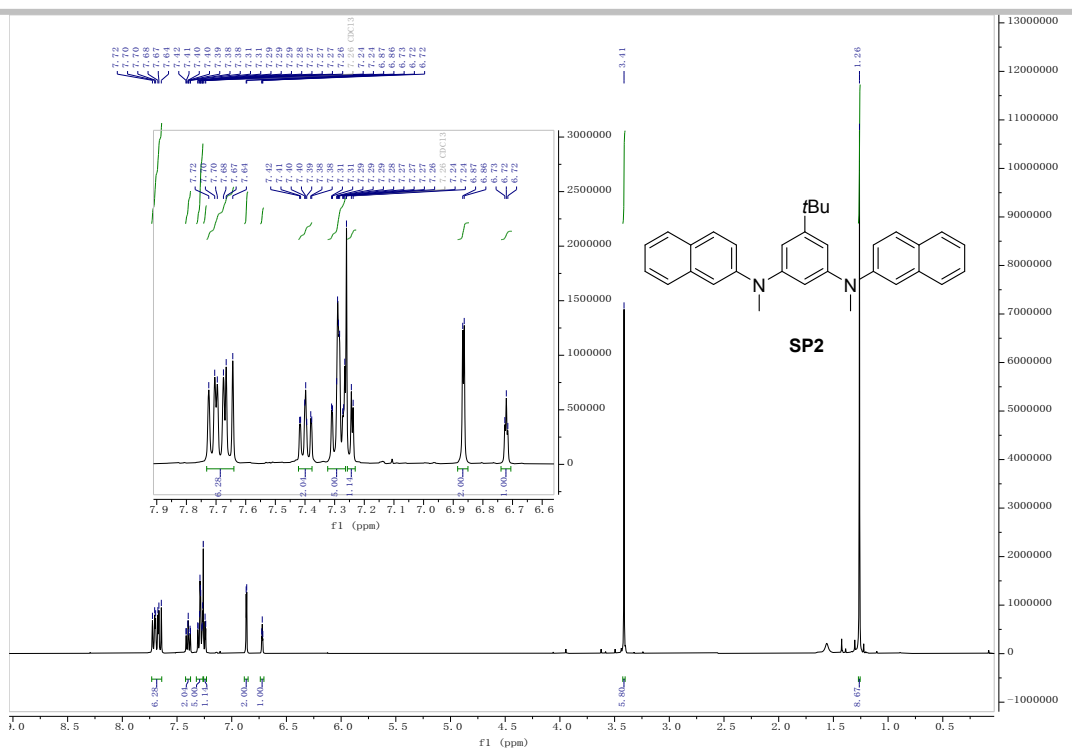


Figure S58 ^1H NMR spectrum of compound **SP2** in CDCl_3 (400 MHz, 298 K).

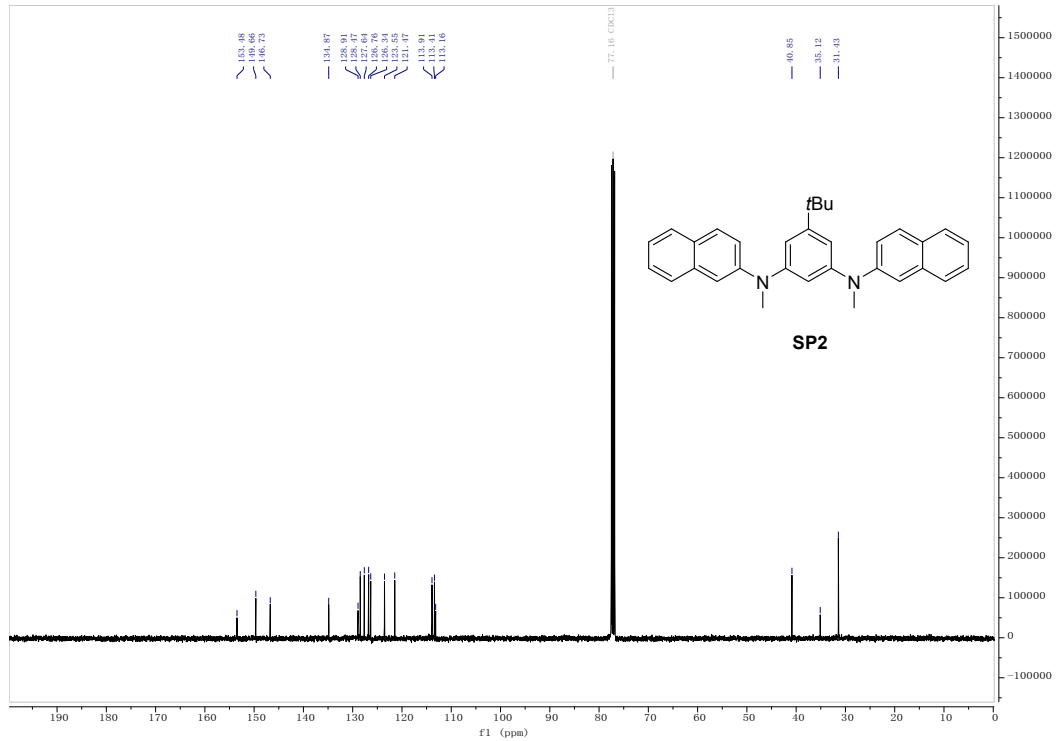


Figure S59 ^{13}C NMR spectrum of compound **SP2** in CDCl_3 (101 MHz, 298 K).

High-resolution mass spectra

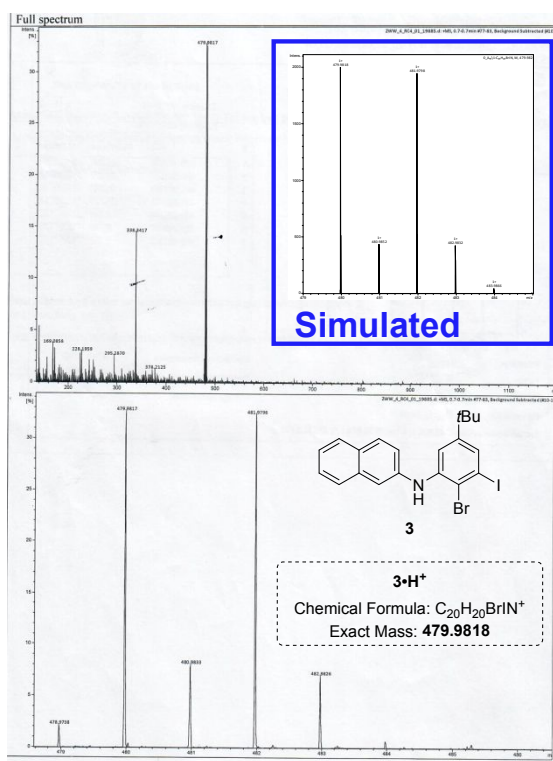


Figure S60 HR-ESI mass spectrum of compound 3.

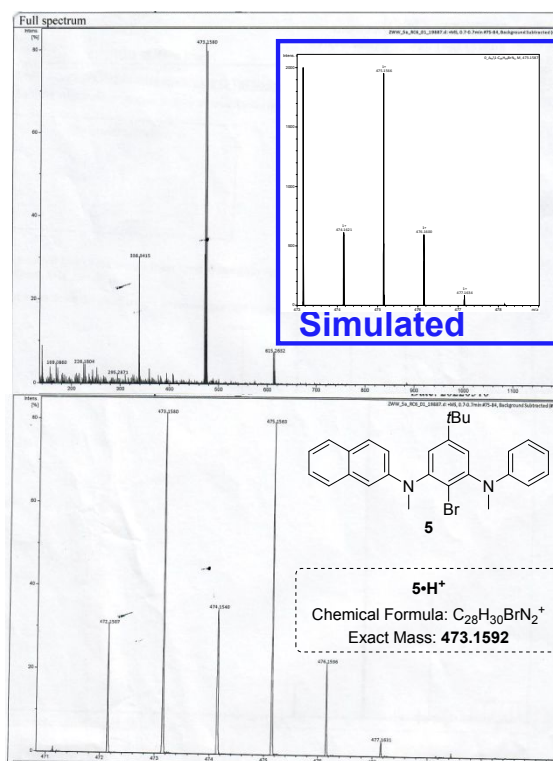


Figure S61 HR-ESI mass spectrum of compound 5.

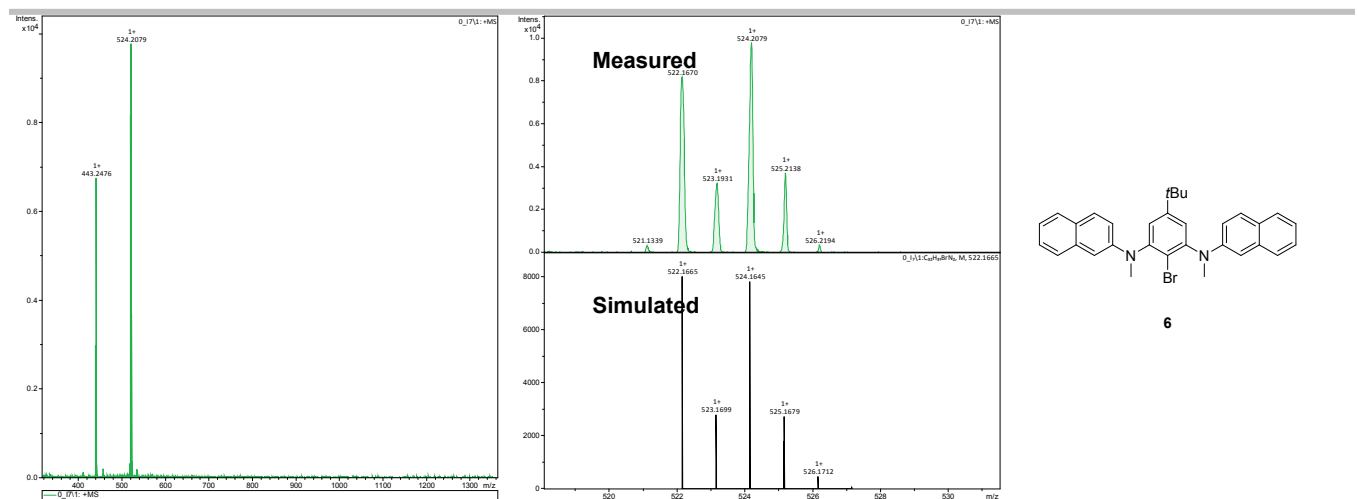


Figure S62 HR-MALDI-TOF mass spectrum of compound **6**.

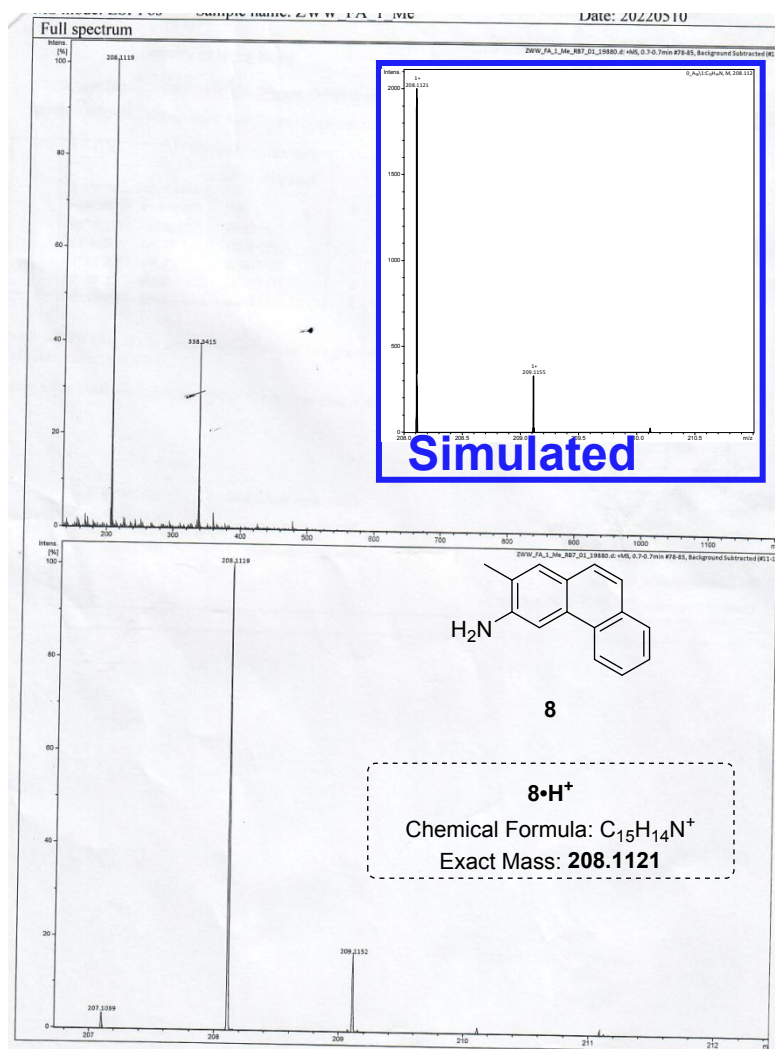


Figure S63 HR-ESI mass spectrum of compound **8**.

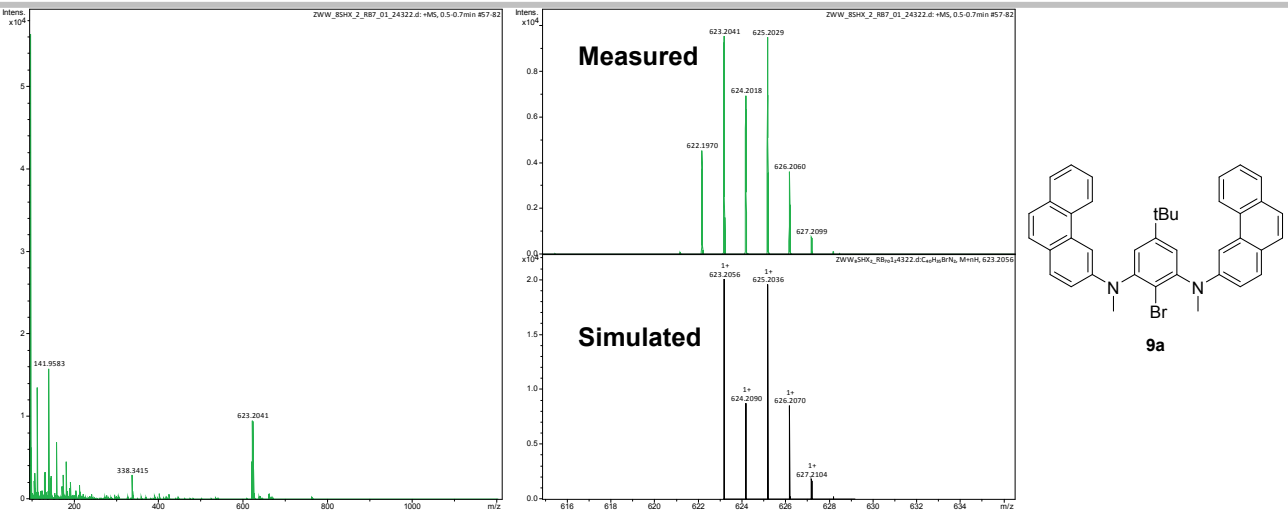


Figure S64 HR-ESI mass spectrum of compound **9a**.

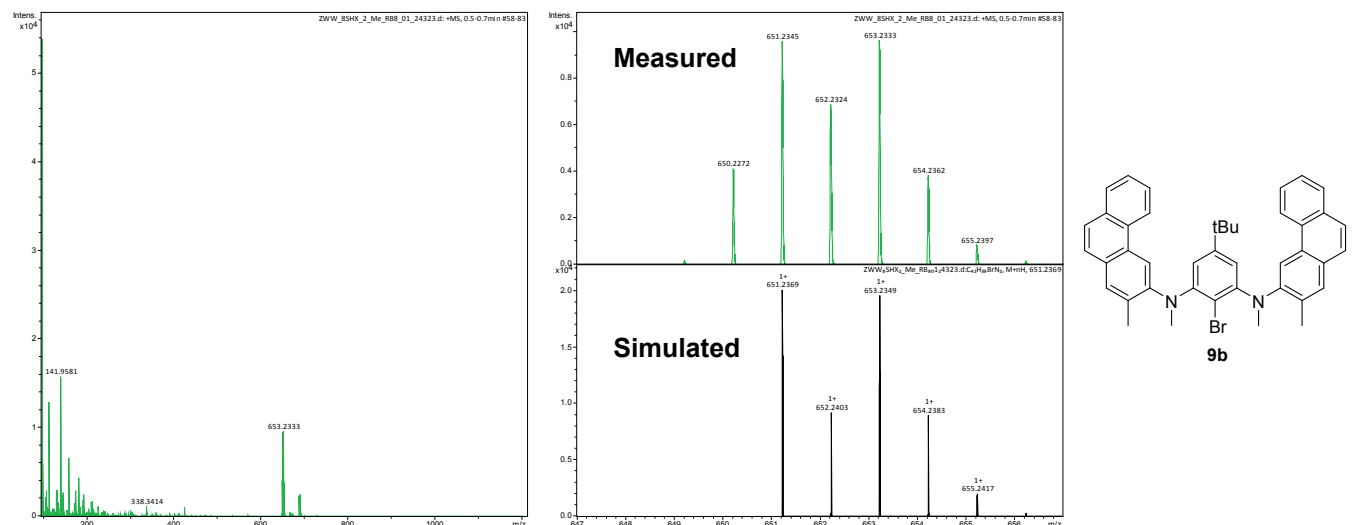


Figure S65 HR-ESI mass spectrum of compound **9b**.

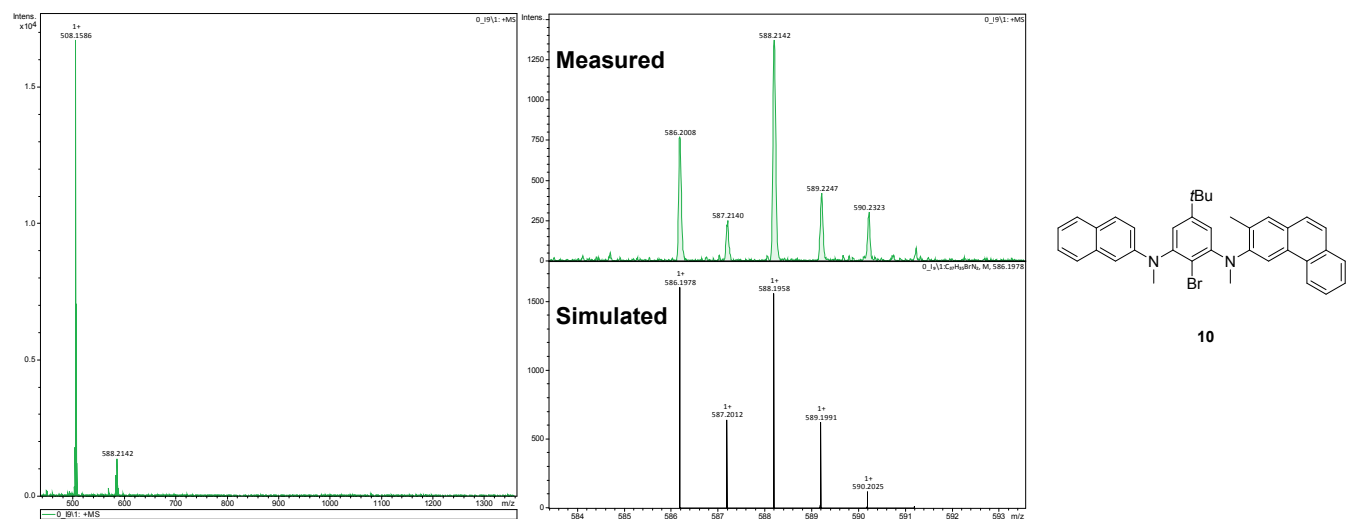


Figure S66 HR-MALDI-TOF mass spectrum of compound **10**.

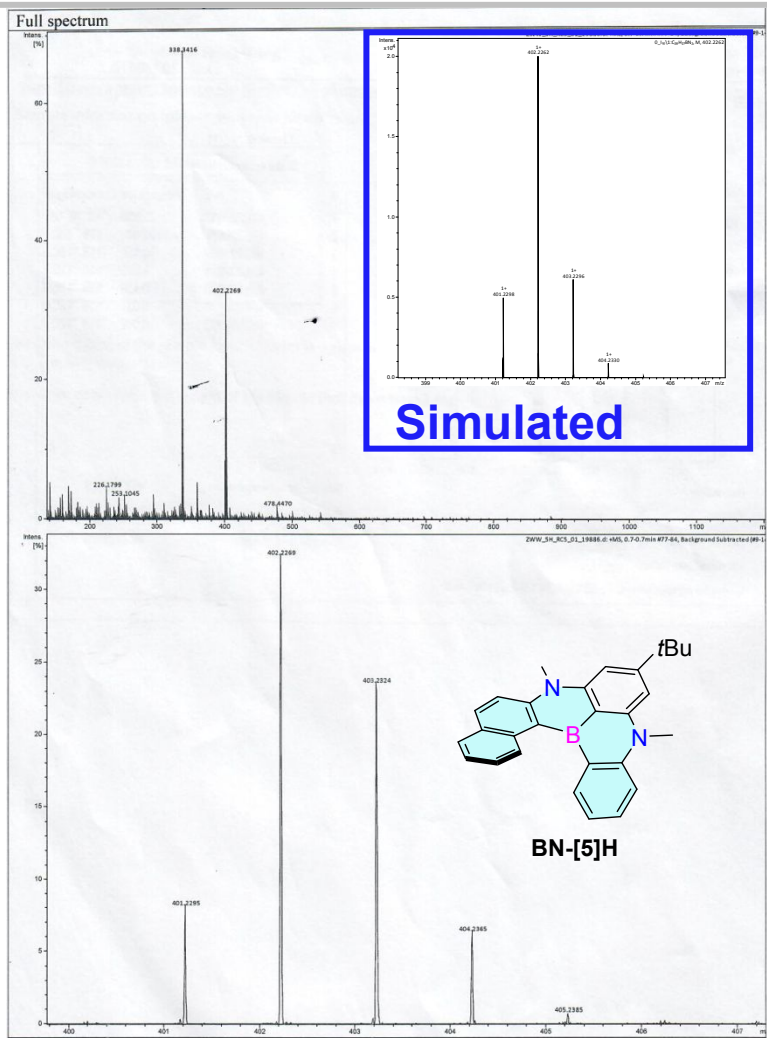


Figure S67 HR-ESI mass spectrum of BN-[5]H.

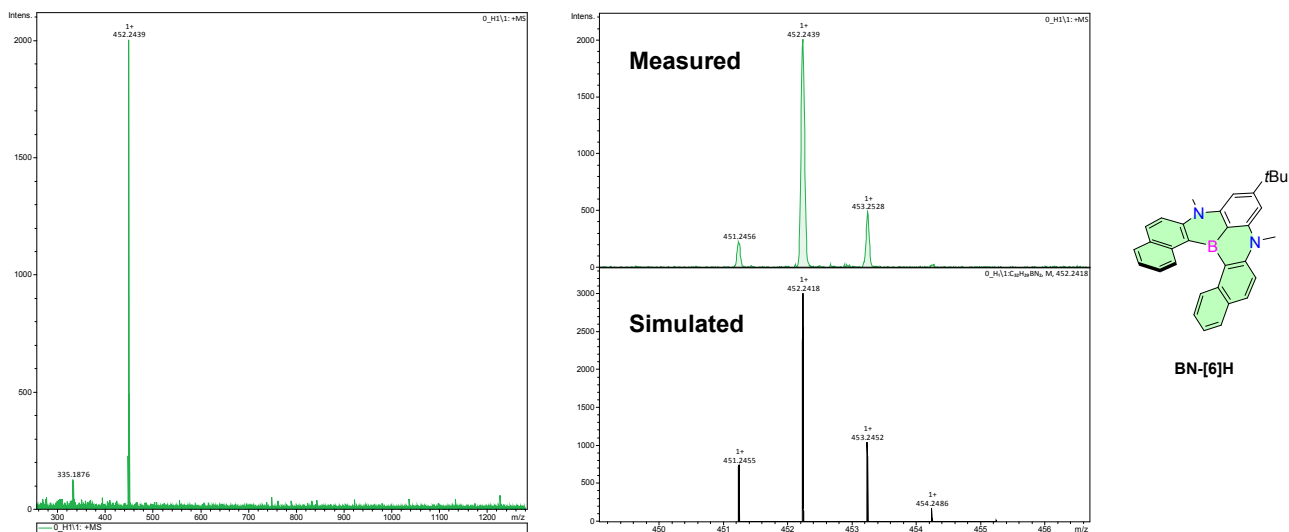


Figure S68 HR-MALDI-TOF mass spectrum of BN-[6]H.

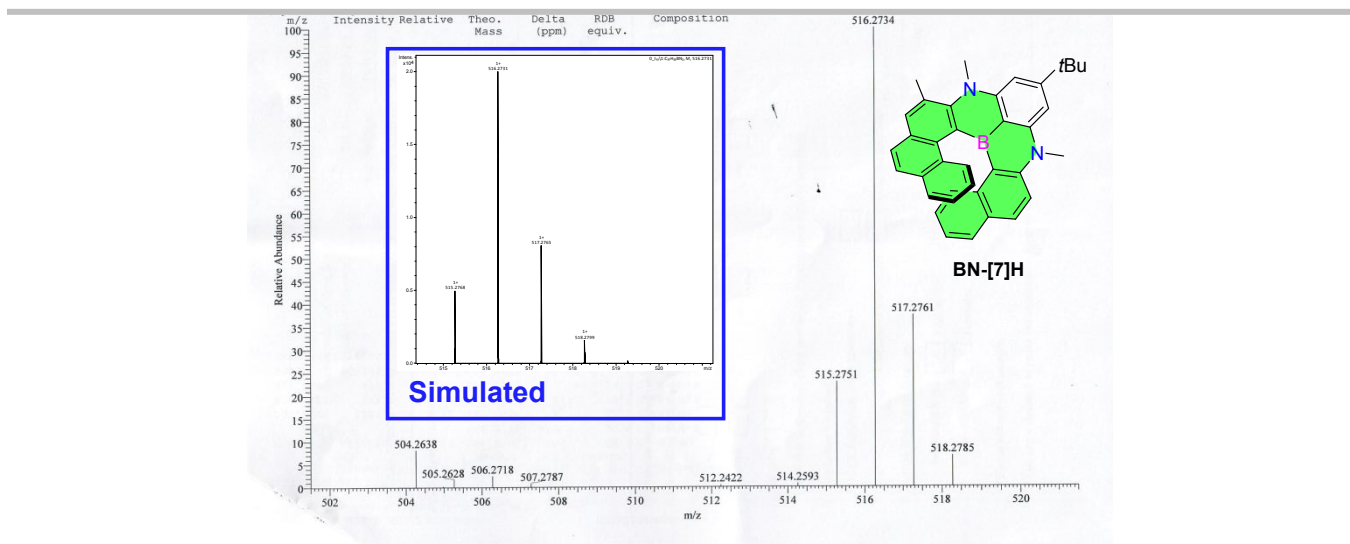


Figure S69 HR-EI mass spectrum of BN-[7]H.

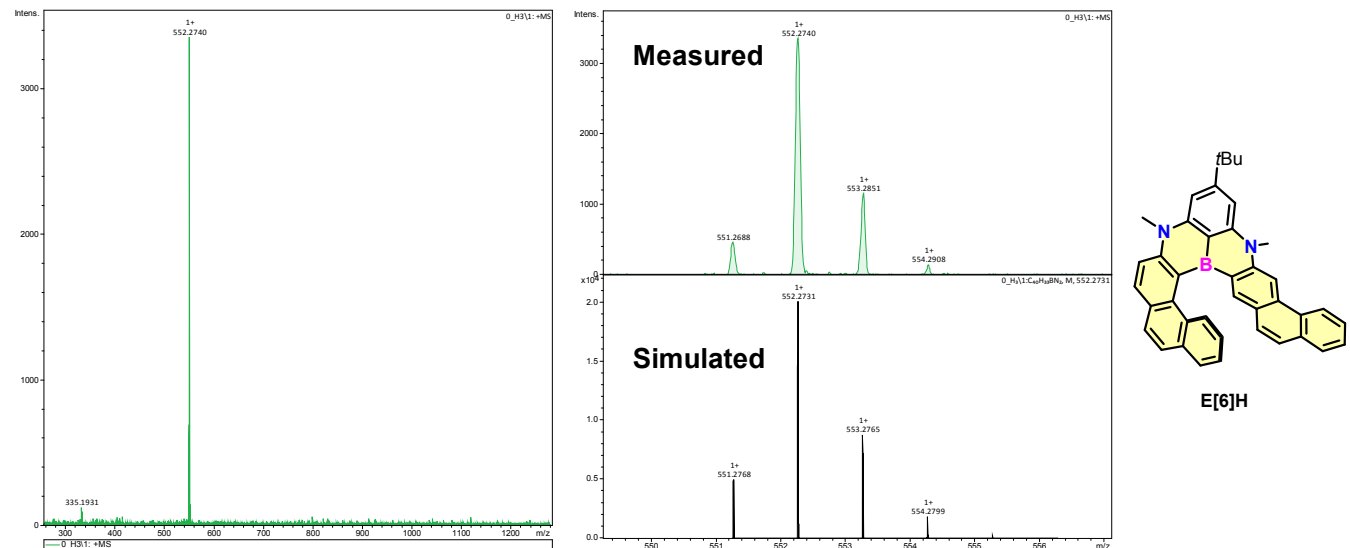


Figure S70 HR-MALDI-TOF mass spectrum of compound E[6]H.

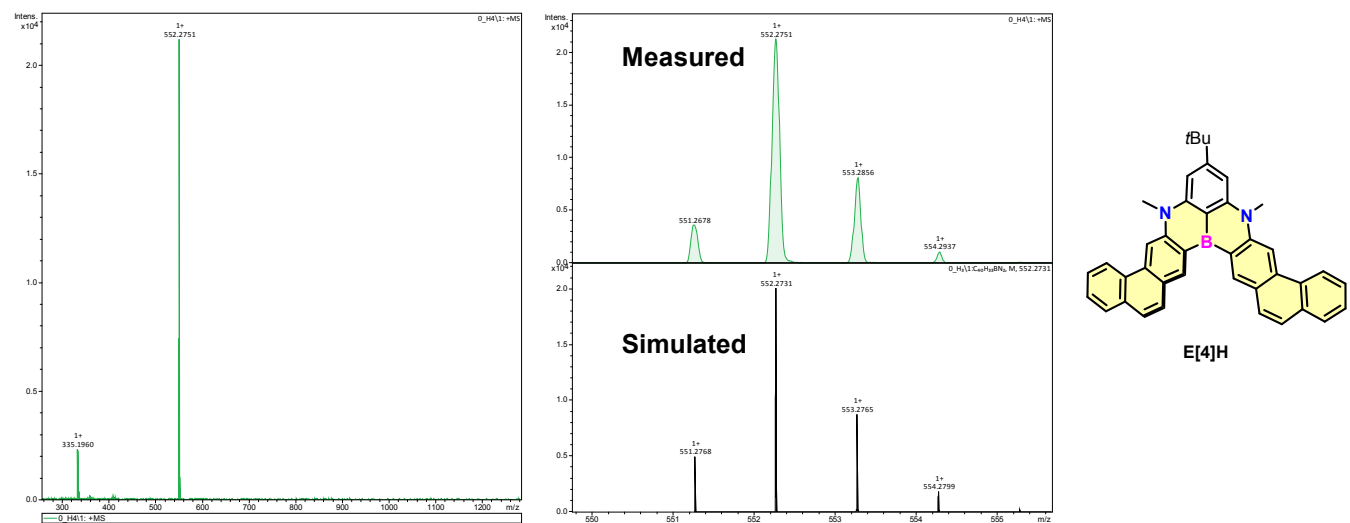


Figure S71 HR-MALDI-TOF mass spectrum of compound E[4]H.

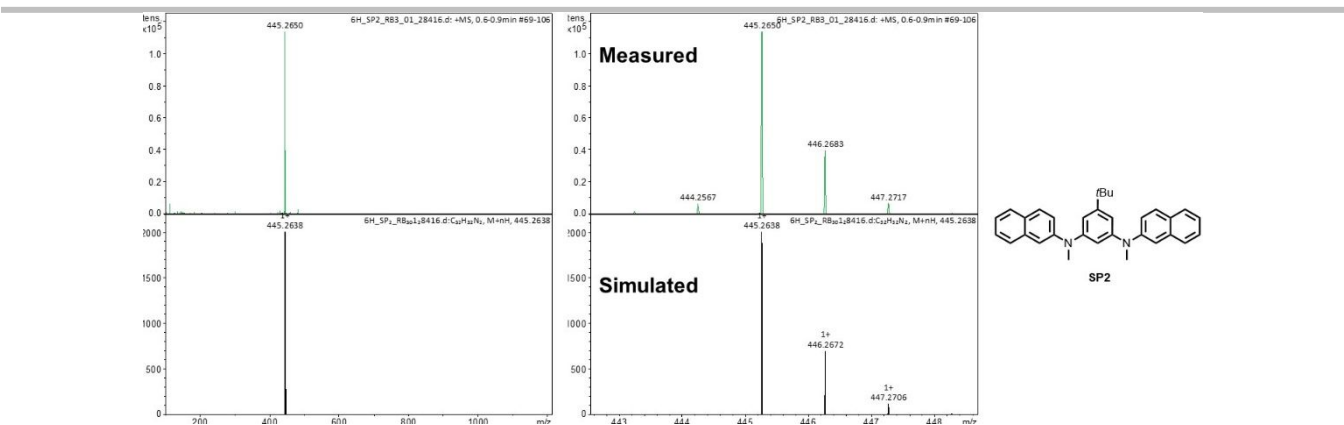


Figure S72 HR-ESI mass spectrum of compound **SP2**.

8. References

- [S1] W. Yang, J. H. K. S. Monteiro, A. de Bettencourt-Dias, V. J. Catalano, W. A. Chalifoux, *Angew. Chem. Int. Ed.* **2016**, *55*, 10427-10430; *Angew. Chem.* **2016**, *128*, 10583-10586.
- [S2] X. Chang, Q. Zhang, C. Guo, *Org. Lett.* **2019**, *21*, 4915-4918.
- [S3] D. L. Fields, *J. Org. Chem.* **1971**, *36*, 3002-3005.
- [S4] J. E. Field, G. Muller, J. P. Riehl, D. Venkataraman, *J. Am. Chem. Soc.* **2003**, *125*, 11808-11809.
- [S5] H. Tanaka, M. Ikenosako, Y. Kato, M. Fujiki, Y. Inoue, T. Mori, *Commun. Chem.* **2018**, *1*, 38.
- [S6] K. Yuan, D. Volland, S. Kirschner, M. Uzelac, G. S. Nichol, A. Nowak-Król, M. J. Ingleson, *Chem. Sci.* **2022**, *13*, 1136-1145.
- [S7] H. Kubo, T. Hirose, T. Nakashima, T. Kawai, J.-Y. Hasegawa, K. Matsuda, *J. Phys. Chem. Lett.* **2021**, *12*, 686-695.
- [S8] J. Full, S. P. Panchal, J. Götz, A. M. Krause, A. Nowak-Król, *Angew. Chem. Int. Ed.* **2021**, *60*, 4350-4357; *Angew. Chem.* **2021**, *133*, 4396-4403.
- [S9] F. Saal, F. Zhang, M. Holzapfel, M. Stolte, E. Michail, M. Moos, A. Schmiedel, A. M. Krause, C. Lambert, F. Würthner, P. Ravat, *J. Am. Chem. Soc.* **2020**, *142*, 21298-21303.
- [S10] T. Yanagi, T. Tanaka, H. Yorimitsu, *Chem. Sci.* **2021**, *12*, 2784-2793.
- [S11] Y. Yamamoto, H. Sakai, J. Yuasa, Y. Araki, T. Wada, T. Sakanoue, T. Takenobu, T. Kawai, T. Hasobe, *J. Phys. Chem. C* **2016**, *120*, 7421-7427.
- [S12] M. J. Frisch, G. W. Trucks, H. B. Schlegel, G. E. Scuseria, M. A. Robb, J. R. Cheeseman, G. Scalmani, V. Barone, G. A. Petersson, H. Nakatsuji, X. Li, M. Caricato, A. V. Marenich, J. Bloino, B. G. Janesko, R. Gomperts, B. Mennucci, H. P. Hratchian, J. V. Ortiz, A. F. Izmaylov, J. L. Sonnenberg, D. Williams-Young, F. Ding, F. Lipparini, F. Egidi, J. Goings, B. Peng, A. Petrone, T. Henderson, D. Ranasinghe, V. G. Zakrzewski, J. Gao, N. Rega, G. Zheng, W. Liang, M. Hada, M. Ehara, K. Toyota, R. Fukuda, J. Hasegawa, M. Ishida, T. Nakajima, Y. Honda, O. Kitao, H. Nakai, T. Vreven, K. Throssell, J. A. Montgomery, Jr., J. E. Peralta, F. Ogliaro, M. J. Bearpark, J. J. Heyd, E. N. Brothers, K. N. Kudin, V. N. Staroverov, T. A. Keith, R. Kobayashi, J. Normand, K. Raghavachari, A. P. Rendell, J. C. Burant, S. S. Iyengar, J. Tomasi, M. Cossi, J. M. Millam, M. Klene, C. Adamo, R. Cammi, J. W. Ochterski, R. L. Martin, K. Morokuma, O. Farkas, J. B. Foresman, and D. J. Fox, Gaussian, Inc., Wallingford CT, **2016**.
- [S13] C. Adamo, V. Barone, *J. Chem. Phys.* **1999**, *110*, 6158-6170.
- [S14] a) A. D. Becke, *J. Chem. Phys.* **1993**, *98*, 5648. b) C. Lee, W. Yang, R. G. Parr, *Phys. Rev. B* **1988**, *37*, 785.
- [S15] W. J. Hehre, L. Radom, P. v. R. Schleyer, J. A. Pople, *Ab Initio Molecular Orbital Theory*; John Wiley & Sons: New York, 1986 and references cited therein.

-
- [S16] a) A. Schäfer, C. Huber, R. Ahlrichs, *J. Chem. Phys.* **1994**, *100*, 5829-5835; b) F. Weigend, R. Ahlrichs, *Phys. Chem. Chem. Phys.* **2005**, *7*, 3297-3305; c) F. Weigend, *Phys. Chem. Chem. Phys.* **2006**, *8*, 1057-1065.
- [S17] a) M. E. Casida, C. Jamorski, K. C. Casida, D. R. Salahub, *J. Chem. Phys.* **1998**, *108*, 4439-4449.
b) R. E. Stratmann, G. E. Scuseria, M. J. Frisch, *J. Chem. Phys.* **1998**, *109*, 8218-8224.
- [S18] J. Tomasi, B. Mennucci, R. Cammi, *Chem. Rev.* **2005**, *105*, 2999-3093.
- [S19] S. Grimme, S. Ehrlich, L. Goerigk, *J. Comput. Chem.* **2011**, *32*, 1456-1465.
- [S20] a) Z. Chen, C. S. Wannere, C. Corminboeuf, R. Puchta, P. V. R. Schleyer, *Chem. Rev.* **2005**, *105*, 3842-3888. b) P. V. R. Schleyer, C. Maerker, A. Dransfeld, H. Jiao, N. J. R. van Eikema Hommes, *J. Am. Chem. Soc.* **1996**, *118*, 6317-6318.
- [S21] a) T. Lu, Q. Chen, *J. Comput. Chem.* **2022**, *43*, 539-555; b) T. Lu, F. Chen, *J. Comput. Chem.* **2012**, *33*, 580-592.